NUMERICAL SIMULATION OF BI-DIRECTIONAL OSTERBERG LOAD TESTS PERFORMED IN LIMESTONE BY USING FINITE ELEMENT ANALYSIS

by

Nejla Yıldız

B.S., Civil Engineering, Middle East Technical University, 2011

Submitted to the Institute for Graduate Studies in
Science and Engineering in partial fulfillment of
the requirements for the degree of
Master of Science

Graduate Program in Civil Engineering
Boğaziçi University
2017

ACKNOWLEDGEMENTS

I would like to thank to Prof. Erol Güler for his understanding and patience during the long process of my thesis writing. I would like to thank him for his support, guidance and smiling face all the time I spoke with him. During writing of my thesis I have faced a lot of difficulties. There were times that I lost my faith to fulfil my graduate study, but his expertise in geotechnical engineering has improved my research skills and prepared me for challenges.

I wish to express sincere thanks to all my co-workers for their support and facilities that gave me. Rasin Düzceer being in the first place, Mr. Alp Gökalp and Mr. Şenol Adatepe always encourage me to study on my thesis and finish it. They shared their valuable knowledge with me for my studies.

I would like to express my gratitude to my instructor in Middle East Technical University during my undergraduate geotechnical studies, Asst. Prof. Nejan Huvaj who never ceased to believe in me and to support me all the time. It's my chance to be a student of her and to know her.

I am grateful to my parents and brother who have always stayed behind me, stayed sleepless with me but never complained about it. I cannot succeed without their love and support. They have been always in the centre of my life. They were willing more than me for my graduation.

Last but not least, I would also thank you my fiancée for his love, patience and support all the time and to all my friends believing and encouraging me to finish my studies.

ABSTRACT

NUMERICAL SIMULATION OF BI-DIRECTIONAL OSTERBERG LOAD TESTS PERFORMED IN LIMESTONE BY USING FINITE ELEMENT ANALYSIS

Pile load tests are one of the most important geotechnical field tests. Piles are loaded in practise by the structure from the top. However especially for piles with large load capacities, it is very difficult to simulate this loading method. To overcome this difficulty, bi-directional pile load test which is also called Osterberg Cell load test has been developed. Within the scope of this thesis, the theory which is used for converting load-settlement behaviour obtained during bi-directional pile load test into equivalent load-settlement behaviour in ideal top-down load test has been verified. To compare the pile behaviour during these two tests; test results of three large-diameter instrumented piles socketed in limestone and performed in Moscow are back-analysed by using finite element analysis. Until load-displacement behaviour obtained during the field test is simulated and unit shaft frictions measured via strain gauges are obtained, soil parameters of analysis model are calibrated and ideal top loaded pile behaviour generated by these parameters is investigated. As a result of the analyses, it is seen that if the strain gauges are not placed in the correct position, incorrect data can be measured during pile load test and participating this data in the evaluation could lead to miscalculation of the unit shaft friction and consequently the end bearing resistance. Comparing O-cell load test with the ideal top loading test, it is observed that the unit shaft friction values are the same but the locations where they are observed are different. It is also observed that the pile bearing capacity and pile behaviour could not be predicted correctly when the applied test load is much smaller than the pile bearing capacity and thus the settlements measured during the test are very small.

ÖZET

KİREÇTAŞINDA YAPILAN ÇİFT YÖNLÜ OSTERBERG KAZIK YÜKLEME DENEYLERİNİN SONLU ELEMANLAR YÖNTEMİ İLE SAYİSAL SİMÜLASYONU

Geoteknik saha deneylerinin başında gelen kazık yükleme deneylerinde, kazıklar üstten yüklenir. Ancak özellikle yüksek taşıma gücüne sahip kazıklarda bu kuvvetin uygulanmasındaki güçlükler sebebiyle, statik basınç yükleme deneyi uygulama tekniklerinden biri olan ve Osterberg Cell yükleme testi olarak da adlandırılan çift yönlü kazık yükleme deneyi geliştirilmiştir. Bu tez kapsamında çift yönlü kazık yükleme testleri sonucu elde edilen yük-oturma davranışının, ideal üstten yüklenen kazık yük-oturma davranışına dönüştürülmesi sırasında kullanılan teorinin doğruluğunu ve iki yöntem arasındaki kazık davranışı farklılığını incelemek için Moskova'da kireçtaşına soketli büyük çaplı kazıklarda gerçekleştirilen üç adet çift yönlü kazık yükleme deneyi, sonlu elemanlar yöntemi ile geri analiz edilmiştir. Deney sırasında elde edilen yük-deplasman davranışı simule edilene ve gerinim ölçerler ile ölçülen birim çevre sürtünmeleri gözlemlenene kadar analiz modelindeki zemin parametreleri kalibre edilmiş ve bu parametrelerle oluşturulan ideal üstten yüklenen kazık hareketi incelenmiştir. Yapılan analizler sonucunda, gerinim ölçerlerin doğru konuma yerleştirilmemesi durumunda yükleme testinde yanlış verilerin ölçülebildiği ve değerlendirmeye katılması durumunda birim çevre sürtünmesi ve dolayısıyla uç direncinin yanlış hesaplanabileceği görülmüş; iki deney yöntemi karşılaştırıldığında birim çevre sürtünme değerlerinin büyüklüklerinin aynı; ancak oluştukları yerlerin farklı olduğu da gözlemlenmiştir. Analizler sonucunda kazık yükleme deneylerinde uygulanan yükün kazık kapasitesinin çok altında olduğu, dolayısıyla ölçülen deformasyonların da az bulunduğu durumlarda kazık taşıma kapasitesinin ve kazık davranışının doğru tahmin edilemeyeceği de görülmüştür.

TABLE OF CONTENTS

LIST OF FIGURES

LIST OF TABLES

LIST OF SYMBOLS

A	Area of pile
c	Cohesion
$C1$	Slope of straight line in Chin's Method
D	Diameter of pile
E	Young's Modulus
E_{ref}^{50}	Secant Stiffness in standard drained triaxial test
L	Length of pile
Q	Applied load
Q_{ult}	Ultimate load
s	Total settlement of pile
ϕ	Internal Friction Angle
υ	Poisson ratio
ψ	Angle of dilatancy

LIST OF ACRONYMS/ABBREVIATIONS

API	American Petroleum Institute
ASTM	American Society of Testing Materials
BS	British Standards
BSI	British Standards Institution
CFA	Continuous Flight Auger
ECT	Enclosed Compression Telltale
FPDS	Foundation Pile Diagnostic Systems
O-CELL	Osterberg Cell
OD	Outer Diameter
OLT	Osterberg Load Test
PDA	Pile Dynamic Analysis
PPL	Pile Platform Level
PVC	Polyvinyl Chloride
SG	Strain Gauge
TLT	Top Load Test
UNESCO	United Nations Educational, Scientific and Cultural Organization

1. INTRODUCTION

1.1. General

Civil Engineering profession has a long historical background dating back to the existence of humankind. The words themselves include the meaning of this profession as being the engineering principle of civilization. From this point of view, it is well agreed that civil engineering solves problems of society by applying physics and scientific principals into life itself with the integration of new requirements and new demands of people who are changing as the world is changing. Since this profession is directly related with the human life, these requirements and demands include a lot of essential applications and principles about civilization; in other words about life of people. It deals with materials, structures, hydrology, geology, environment, water resources etc. With the change in time and education system, some of these subdivisions become major principles and separated from this major; some of them on the other hand become more dominant and prerequisite for most of the civil engineering applications.

Foundation engineering is one of these major principles because all kinds of structures have to be built on soils whether it is a skyscraper or a culvert. Foundation engineering principle mainly focuses on design of substructures for various soil conditions under different environmental issues. Prior to design processes, the designer should have clearly known the engineering properties of soil. Therefore soil investigation works and preliminary pile tests are essential for a good design.

Increase in population and decrease in settlement areas day by day in developing brings a great deal of problems together with to meet the rising needs and requirements. It is not wrong to say that solution of these problems sets ground for new approaches and new methods for the engineering applications in all areas. Construction sector is by far the clearest example of this situation. In order to meet the demand of people by occupying the least surface area makes engineers and designers design extraordinary and mega structures more than past. On the other hand, in today's modern and

developing world, mega structures such as high rise skyscrapers or very long bridges are seem to be indicators of wealth, power and level of development of that country. These elements can be claimed as being the back-stage of developments to find new approaches and methods in construction engineering world.

Construction of mega structures makes the design and construction of a feasible foundation system more sophisticated and more essential compared to ordinary structures. In order to get an economical, safe and realistic solution related with foundation problems, site investigation tests are needed to be executed and evaluated for both soil properties and the behavior of piles. The ones executed for piles are mainly named as pile load tests.

There are several types of pile load tests with different purposes and different applications. Osterberg Cell Tests are one of these pile load tests which are mainly dealt with in this thesis scope. They are performed for piles especially under excess loads to determine capacity and to examine the soil-pile behavior by confidently and trustable.

Within the scope of this thesis, O-cell tests are discussed by evaluating and comparing the results of them for different soil types and for different projects. It is planned to obtain Equivalent Top Load-Settlement Curves given in O-cell test reports by interpreting data recorded during test in theoretically and also planned to find this curve by numerically with finite element analysis. In other words, the soil model which gives corresponding side friction and tip resistance will be calibrated by using finite element software Plaxis. On this finite element model, a force will be applied on top of pile and load- settlement graph is examined by comparing the one given in O-cell test report. As a result, theoretical and numerical results will have been compared and evaluated.

2. BRIEF HISTORY OF PILES

Issue of sheltering has always taken place an important role in human's life throughout history to continue their lives safely by accessing essential sources easily such as water, food and even the transportation. This makes sense to imagine that in ancient times the most valuable good was the water which was including both food and transportation facilities within its constitution. That's the evidence why in different parts of the world such as Switzerland, Italy, Scotland, most people chose to settle on lake shores or near lakes about 4000 years ago (Keller, 1866).

Building a shelter on such a location brought some challenges as might be expected in terms of soil conditions. The evidences and archaeological studies have shown that people from different part of the worlds were used piled foundations in order to eliminate settlement problems on soft, marshy soils. Various nations and countries adopted piling techniques and used for different purposes such as shoring facilities and housing. Mostly timber piles were used having an average length of 3m. The timber was selected mainly from oak and birch and cedar. The cedar timber had a different background than the other timbers. It was believed that Egyptians who were known to be the excellent sailors and builders did not have an appropriate timber to process like cedar. Therefore, they exported cedars from Lebanon and used them in the construction of sheet piles. However; when the demand became so excessive that big cedar forests were reduced significantly (Keller, 1866).

As mentioned previously ancient settlements near lakes used timber piles to make shore facilities and to support their houses which they build on lakes or lake shores in order not to face with the effects of water level changes. For Alpine Region history of lake dwellings goes back to prehistoric ages from 5000 to 500 BC. This region is special because it gives a unique clue about life in earliest agricultural settlements. It includes 111 dwellings in Austria (5), France (11), Germany (18), Italy (19), Switzerland (56) and Slovenia (2). Although these structured are under water and some of them were buried in sands of lake shores, UNESCO defined them as one of the cultural heritage

of humanity and called as “pile-dwelling sites”. 111 no’s of villages were reported to be the most important archeological evidence which shows how the life and community had changed ranging from Neolithic Age to Bronz Age (Keller, 1866).

There are also evidences and findings from other parts of the world. For example in 1863, 30,000 timber piles were explored in Ireland. Another example was found from Herodotus records. He mentioned in his records that a Thracian tribe named as Paeonions had dwellings on lake which were supported by timber piles in 4th century BC. It was explained that the tribe had implemented laws in order to regulate life of the community. One of their law was that if a man wanted to marry a women, he had to drive 3 piles. If their adoption of polygamy was taken into account, one should think the great number of piles (Fleming *et al.*, 2009).

In the beginning of nineteenth century more attention was given to the durability of piles especially for the ones not fully under water. The main reason was the fluctuation of water level creating wet-dry cycles repeatedly. In order to prevent this damage on piles, coating with tar was being executed for the parts below water unless pile was fully submerged; now in modern approaches giving its place to galvanization with zinc. In the middles of nineteenth century metal piles were began to be used. When it was discovered that durability of metal piles was much more than the timber ones, they were especially preferred for important structures by considering their long lasting lives. In same years screw piles were added to the geotechnical inventions by Alexander Mitchell. These piles were known to have first used for Maplin Sands Lighthouse located in Thames Estuary in 1838 (Fleming *et al.*, 2009).

It was in 1824 that Joseph Aspdin planted the seeds of Portland cements by having taken patents of hydraulic cement. It attracted a lot of people from different parts of the world which made it become widely available by the end of century. Furthermore, A.A. Raymond was known to be the first person who took advantage of Portland cement and used it in production of economical cast in place concrete pile in 1897. Following these advancements, another method emerged in 1903 by R.J. Beale which utilized driving a close-ended steel pipe, filling inside with concrete; and then

removing of pipe. There were also developments in steel piles at about same years. For a highway bridge in Nebraska, United States, I beam piles were produced and used. Later on, with the beginning of twentieth century Bethlehem Steel Co. fabricated rolled H-sections and made it available worldwide (Fleming *et al.*, 2009).

By following these advancements in piling engineering, in early 1930's bored piles executed by boring tools came into the stage in United Kingdom. Indeed, the history of foundation piles with boring method dates back earlier than this century when issue of concreting was omitted. The technique was called "well foundation" and similar to open caissons. It was a widely-used method by Indians especially for support of important structures during Moghol period; i.e. Taj Mahal. Since this method depended on ability of workers to go down the wells for bottom to top construction, diameters and lengths of piles were limited to the man's capacity. It was very obvious that bored piling technique brought a breath of fresh air into foundation engineering practices. Method made top to bottom construction possible since concrete could be mixed on the ground and then poured to the hole. It also paved the way for construction of piles with smaller diameters and longer in lengths. Although it had advantages over piling with casings (steel pipes), the system had a deficiency when ground water existed in the media, since water was penetrating into the hole while concreting. This problem later overcome by using steel lining tubes with air locks on them which has given its place to tremie pipes now in modern use (Fleming *et al.*, 2009).

Today, there are great number of methods being applied for piling works in geotechnical engineering era and increasing parallel to the developments in machinery and equipments. Selection of construction technique is done by analyzing soil investigation results, type of superstructure, loads coming from superstructure and existing underground facilities. In order to verify the selection and design of the system quality control/quality assurance tests are conducted. As a result, the most durable and sound design and construction technique is designated regarding both of the issues mentioned above.

3. CLASSIFICATION OF PILES

Piles are structural members used for multiple purposes with different functions. They are mainly used for the purpose of transferring loads coming from the superstructure to relatively stiffer soil stratum or through soil layers. As Bowles, 1997 listed in his book, there are different areas and purposes for use of piles which are listed below:

- Piles can be used to resist overturning moment and uplift forces such occurs on the foundation of a tall building, in a basement mat under water level, or a tower leg exposed to intense wind forces,
- Piles can be used for a compaction process of a loose cohesionless fill or an embankment by driving them with vibration,
- Piles can be executed under a mat or spread foundation over a compressible soil in order to control settlements,
- Piles can be used in offshore structures such as jetties or berths for lateral and dynamic loads,
- Piles can be used in retaining walls or for slope stability purposes.

Piles are classified in different ways according to different classification systems or standards. Literature studies show that classification of piles can be grouped as follow (Prakash and Sharma, 1990):

- Pile material,
- Method of pile fabrication,
- Amount of ground disturbance through pile installation,
- Method of pile installation into ground,
- Method of load transfer.

Moreover, in British Standard Code of Practice for foundations (BS8004: 2015) piles are classified into three categories with respect to ground disturbance caused by installation these categories are provided as given below:

- High displacement piles,
- Low displacement piles,
- Replacement piles.

Within the scope of this thesis classification of piles will be conducted according to the previously done literature studies.

3.1. Classification of Piles with respect to Pile Materials

Piles can be divided into four major groups as timber, concrete, steel and composite piles.

3.1.1. Timber Piles

As indicated on Timber Pile Design and Construction Manual (2002), timber piles are known to have been used for more than 6000 years (see Figure 3.1 and 3.2). Timber piles are frequently used in United Kingdom, Scandinavian countries and Australia for low loads especially up to 500 kN due to their smaller cross sections and thus lower compressive strengths. Timber piles are generally produced in square cross sections but, circular cross sections are also available in markets (Fleming, *et al.*, 2009). Both softwood and hardwood timbers are used as piles. Commercially available timbers for piling purposes are pitch, Douglas fire, pine, larch and western red cedar in soft wood class and greenheart, jarrah opepe, teak and European oak in hardwood class.

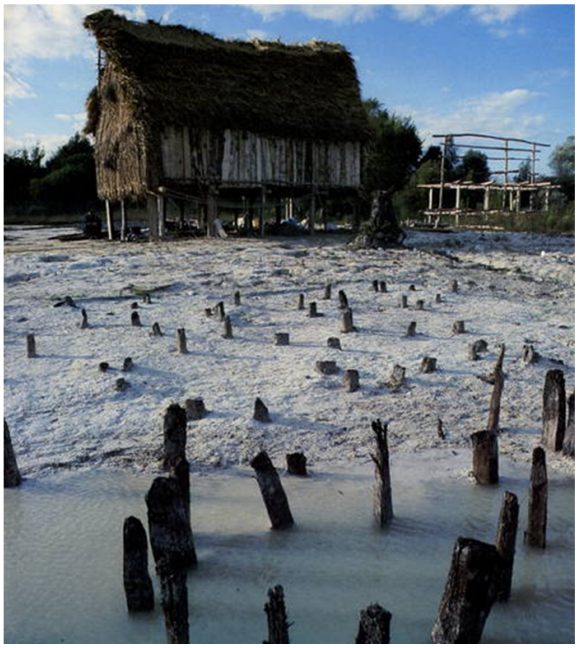

Figure 3.1. Original piles in Neolithic dwelling around the Alps.

Figure 3.2. The remains of 20 prehistoric villages in Switzerland.

Since the material is timber which is prone to decay when exposed to oxygen and moisture in time; using a material to extend its lifetime as a structural member

becomes inevitable. In ancient times, in order to preserve timber and maintain a long service time, animal or vegetable oils were applied on piles. Piles found as the foundation system of ancient structures after several years that they were constructed show how these preservatives served their purpose by protecting piles from many effects and contributing them to reach the present day.

In 1902, a church located in Venice and named as St. Mark was demolished because of its structural vulnerability. The church was lying on timber piles which were driven AD. 900. After demolishment of church, these piles were found to be is good condition and they were reused for the new structure to be built instead of church. As it is well known, the ground water level in Venice is always in high level and these piles have been under water for centuries (Rajapakse, 2008).

They are especially preferred in marine construction works generally selected for small jetties owing to their good energy-absorbing properties. However there are regulations and restrictions that the codes and standards such as; British Standards EN 12699, (BSI, 2001) and in the United States, the American Wood Preservers stipulate if the timber piles are used in contact with water. Part of the pile above ground water level is prone to decay due to oxygen and moisture in the air; therefore this part is cut-off up to lowest water level and extended with concrete cap to the design level. Another option for preservation of timber from decay is using chemical protectives such as creosote or arsenates if it is permitted. These chemicals are also used for increasing resistance of the part of timber pile which is under water against attack of marine organisms and borers for both hardwood and softwood types (Tomlinson and Woodward, 2007). If appropriate precautions are taken and effective preservative methods are applied, durability of timber piles can be several decades. Untreated timber piles have been graded by Building Research Establishment according to their durability and resistance to fungal attack as given in following table:

Table 3.1. Durability and resistance to fungal attack of timber piles.

Specie of **timber pile**	**Durability**	**Average life when in contact with ground**	**Resistance to fungal attack**
Douglas fir	Non-durable	5 to 10 years	Resistant
Pitch pine	Durable	15 to 25 years	Moderately resistant
Larch	Moderately durable	10 to 15 years	Resistant
Western red cedar	Durable	15 to 25 years	Resistant
Greenheart	Very durable	More than 25 years	Extremely resistant
Jarrah	Very durable	More than 25 years	Extremely resistant
Opepe	Very durable	More than 25 years	Moderately resistant
Teak	Very durable	More than 25 years	Extremely resistant

Timber piles have been used both in very soft soil and gravelly soils with different tip geometry. Generally in soft soil large tip is selected to improve bearing capacity by resting on a firm soil layer; whereas in gravelly soils square or pointed tips is selected (Bowles, 1997).

Table 3.2. Typical pile characteristics and uses (Bowles, 1997).

Pile Characteristics	**Pile Property**
Maximum Length	35m
Optimum Length	9-20m
Applicable Material Specification	ASTM-D25, Standards of American Wood Preservers Association
Recommended Maximum Stress	4-6 MPa for Softwood Piles; 5-8 MPa for Hardwood Piles
Maximum Load for Usual Conditions	45 tons
Optimum Load Range	8-24 tons
Disadvantages	Splicing difficulty Vulnerable to damage in hard driving Vulnerable to decay unless treated Difficult to pull and replace when broken during driving
Advantages	Comparatively low initial cost Permanently submerged piles are resistant to decay Best suited for friction pile in granular material

3.1.2. Concrete Piles

Concrete piles are divided into 3 groups owing to their construction methods. These are as followings;

(i) Precast concrete piles: Precast piles are prepared and produced in a casting yard before they are installed. They can be casted in circular, octagonal or squared shape. Practically precast piles are designed up to 300 tons. In precast piles, generally end bearing is the major component for bearing capacity but they are also used as friction piles when driven in sand, gravel or clay.

Precast piles are produced either as reinforced or prestressed. Lengths of reinforced precast concrete piles are 12m to 15m and maximum allowable stress is taken as 33% of 28 day strength (Prakash and Sharma, 1990). During installation of pile minor cracking may occur through the pile .These cracks are accepted up to 0.25mm and may give damage to pile especially in freeze-thaw act in and under marine environment.

In addition to reinforced precast piles; prestressed concrete piles are constructed. In this type of pile, steel rods or wires are used instead of longitudinal steel bars in reinforced concrete as a tensile member. Prestressed piles are further subdivided into two groups as pretensioned and posttensioned piles. Pretensioned concrete piles are produced in full length; whereas posttension piles are usually produced in segments which can be jointed in situ or in the fabrication yard. Prestressed piles have higher capacities, lighter and longer than the conventional reinforced piled. They are more durable to aggressive environmental conditions; since the concrete is subjected to compressive forces continuously.

(ii) Cast in place concrete piles: Cast in place concrete piles are produced either by replacing soil or by compressing it. They have advantages over precast piles, since they do not need a casting or a storage yard and they are only designed for the service load, not for driving and lifting stresses. Moreover, pile lengths can be changed according to field condition is situ.

Cast in place concrete piles can be classified according to their method of construction as followings:

- Driven cast in place concrete piles: Driven cast in place piles are used in variable sites and wide range of working loads. In this type of pile construction, the driven component is the casing which can be either temporary or permanent. In permanent casing type, firstly a tube with an end plate (expandable shoe) is driven with the help of a hammer till to the design level of pile. Then reinforcement cage is lowered and concrete is poured and vibrated in while the tube is withdrawn. It is important to note that end plate is remains at the base while the tube is withdrawn.

  Previously a slightly different method has been used. In this method soil is mixed with concrete or gravel to form a plug as a base material under the tube. Tube is driven with this plug down to design level and if there exist aggressive ground condition or down-drag forces are desired to be eliminated then permanent casing is used by applying suitable preservative material on the tube.
- Screw cast-in place concrete piles: Different from the bored piling technique this type of pile installation is based on compaction of the soil instead of remaining it from the drilled hole. While screwing through the soil performed

  Reinforcement cage is lowered at the same time. Since the machinery itself has the ability to maintain the stability of drilling hole, there is no need to use extra casing. After drilling and cage lowering are completed, concreting is performed through tube of the machine while unscrewing and withdrawal of the drilling component. When pile size and diameter are kept same for both this method and traditional method, it is true that pile constructed with this method has higher resistance to bending stress and greater pile capacity. Main disadvantage of this method may be the restricted pile diameter due to drilling machinery.
- Vibrated concrete columns: This is newly established method which is similar to vibro displacement stone column. With the help of vibroflot stem concrete is injected until the design depth is reached. Then reinforcement cage is lowered into wet concrete. This method is suitable especially for weak soils. Diameters are generally between 400mm-750mmand load capacities are similar to traditional concrete piles.
- Bored cast-in place piles: Bored cast in place piles are the most commonly used

pile productions. In this method a hole is drilled by using a casing or supporting fluid where the soil around the hole is instable. Pile capacities are considerable due to various applicable pile diameters and lengths. Up to diameter of 600mm bored piles are called as small diameter piles; larger than 600mm piles are called as large diameter piles. This type of pile construction has special methods under its name as followings:

- Micro piles: According to BS EN 14199, micro piles are the general name of piles the diameter of which is less than or equal to 300mm for bored piles and 150mm for driven piles. They are used as bearing piles for lightly loaded structures, for reducing differential settlements between an old and existing building for underpinning a foundation to increase strength of structures. They are also used for retaining and shoring purposes in slope stabilization projects and excavation projects.
- Continuous flight auger piles (CFA): Continuous flight auger piles are available up to 1200mm diameter. Contrary to traditional bored piles; places where high ground water table is observed there is no need to use casing or supporting fluid for borehole stability and no need to use tremie method for concreting. It is applicable in sandy, gravelly, clayey soils.

  First the hole is bored with continuous flight auger until design depth is reached. After completion of drilling, concreting or injection (depending on the project) is executed simultaneously slowly withdrawing of auger during which spoil of boring is also extracted. When concreting process is finished and the auger is completely withdrawn from the borehole; reinforcement cage is lowered into the wet concrete.

  Depth of application is restricted to approximately 30m due to capacity of Continues flight auger machinery. Concrete slump is generally selected as 150mm considering workability conditions and 28 days-strength of should not be less than 30 MPa (Fleming *et al.*, 2009)

3.1.3. Composite Piles

Piles which are formed from more than one material are named as composite piles. Composite piles can be in various forms for different purposes. Composite piles are not economical as one-material piles. Generally used composite piles are listed below:

- Timber-concrete piles and timber- steel pipe piles: Concrete or steel pipe piles are used together with timber piles as the extending part of them above ground water table to prevent decaying of timber. It is also practical to use steel pipe piles as the casing to install timber piles.
- Precast concrete piles-Steel H Pile: When precast piles are to be longer than 15-18m, they become uneconomical and also difficult to drive into hard soils. That is why steel H sections are attached to the end of precast concrete piles. However, skin friction capacity will be higher in concrete part owing to its larger perimeter.
- Steel pipe-concrete piles: In marine structures, jetties are constructed on top of steel pipe piles. These piles are driven into bearing strata first and to form the connection between piles and jetty to work together, top part of piles are constructed as reinforced concrete piles inside this pipe piles.

3.1.4. Steel Piles

Steel piles are produced in different geometrical shapes for different purposes. They can be in plane tubes, box sections, box piles built up from sheet piles, H sections, and hollow section. Steel piles are light to handle and if they are driven into hard soil, they are capable of carrying high compressive loads. When compared to precast concrete piles, they have the advantage of being shaped (cut or extended) according to the site condition; but more expensive than the precast piles. They need to be protected against corrosion via cathodic protection, bituminous or resin coatings or other newly improved methods. For higher compressive loads hollow piles with close end are preferred in order to account the resistance from the end bearing component. Open ends are more preferred for longer lengths.

In order to avoid considerable ground heave and lateral displacement H section piles are used since they have small volume-displacement. However they have the disadvantage of carrying low loads owing to their small cross sections. If they are demanded to be used for high loads, then cross section of H piles are increased by welding additional H sections to the toe part of piles to form a winged shape piles. It is important to note that they should be used properly according to the direction of forces acting on it since they have a tendency to bend about their weak axes while driven into soil. For the capacity of H section piles for carrying proposed loads, Bjerrum (Tomlinson and Woodward, 2007) recommends a method. In this method, after driving of pile, radius of curvature is measured with the help of inclinometer by the deviation from the axis of pile and if the curvature is found to be less than 366m.

For tubular, box and H section piles BS8004 and BS4360 states that compressive working stress is limited to 30% of yield strength providing that factor of safety for driving resistance is not greater than 2.0. For jacked piles and end bearing piles driven in sound rock or dense granular soils limit is 50% of yield strength. Selection of steel piles depend both on environmental condition and design working stress. BSEN12699 states that peak calculated shear stress during driving should be limited to 0.9 of characteristic yield strength of steel. On the other hand API states that dynamic stress during driving should not exceed 80/90% of yield strength.

3.1.5. Classification of Piles with respect to Pile Fabrication Methods

Piles can be categorized according to the method of their fabrication process as precast-prefabricated or cast in place. Prefabricated piles are produced in a fabrication yard, transported to the construction site and driven into the soil. Timber and steel piles are always produced as prefabricated; on the other hand, concrete piles can be produced either precast or cast in place.

3.1.6. Classification of Piles with respect to Ground Disturbance

Piles are grouped into 3 main categories according to ground disturbance during their installation. These are provided below:

- Large displacement piles can be both driven piles and cast-in-place piles. They are large diameter piles which displace the soil rather than removing it. Timber piles, precast concrete piles, prestressed piles, screw piles, close ended steel tube and box type piles are the example of large displacement piles.
- Small displacement piles are similar to large displacement piles but have small cross sections which give less disturbance to soil. They can be H section or I section steel piles or open ended pipe or box sections. If these type of piles encounter with a plug during driving, then they can be called as large displacement piles.
- Replacement (Non-displacement) piles are constructed by removing soil from the drilled hole and then placing the concrete or precast pile into the hole. This is performed also by placing precast concrete piles into drilled hole.

3.1.7. Classification of Piles with respect to Installation Methods

Pile types according to installation method are categorized into two major groups as driven and bored piles. There also exist piles which are combination of both types. Timber piles, steel piles and precast concrete piles are example of driven type of piles whereas cast-in-place concrete piles are example of bored piles.

3.1.8. Classification of Piles with respect to Load Transfer Method

Piles are grouped as four groups according to their load transfer mechanisms (Prakash and Sharma, 1990):

- End bearing piles: They rest on a stiff stratum through soft and loose soil. This stiff stratum can be dense sand, hard rock or gravel.
- Friction piles: They use their entire shaft perimeter to transfer load through all

the soil layers which in contact with. Friction piles are used for both compressive and tension loads.

- Combining end bearing and friction piles: In this type of load transfer mechanism, both skin friction and end bearing contribute to the pile capacity. Part of the load is transferred to the skin friction whereas the remaining portion is transferred to end bearing.
- Laterally loaded piles: These piles are used to transfer lateral loads to the soil through piles.

4. PILE LOAD TESTS

Prior to application of piles in a project, pile load tests are performed in order to make proper and efficient design and to observe the behavior of pile in actual site conditions. Eurocode 7 clause 7.5 states that pile tests have to be performed if:

- There is not any comparable experience about the type of pile or type of installation method within the project area,
- There are not any piles tested under similar conditions,
- There are some uncertainties in design due to insufficient data or lack of theory and practice,
- There are differences during installations between the observed behavior of pile and expected pile behavior (Tomlinson and Woodward, 2007).

Pile load tests are divided into different categories according to two criteria provided below:

(i) According to type of execution they can be divided into two groups as:
- Preliminary pile load tests: This type of pile tests are performed prior to designed project piles in order to check,
- Working pile load tests: They are performed after construction of pile head.

(ii) Alternatively, according to loading type they can be divided into three main groups as:
- Static Load Tests,
- Dynamic Load Tests,
- Rapid Load Tests, Statnamic, Pseudo static.

4.1. Static Load Tests

Static load tests are the ones used most commonly in order to assess the behavior of pile both prior to construction and after the construction. According to the working

principle of pile three type of pile load tests are available:

Prior to performing each type of load tests, following sequence of works which can be divided into two headlines, shall be done as a preparation stage. It should be noted that sequence of works will be common for both of compression and test loads except minor differences.

(i) Headline I (Piling Works)
- Setting out of pilot pile's location / working pile's location,
- Setting out of piles' locations,
- Boring of reaction piles
- Installation of steel reinforcing cage in splices for reaction piles,
- Concreting of reaction piles
- Boring for pilot pile / working pile,
- Installation of steel reinforcing cage in splices for pilot pile / working pile,
- Concreting of pilot pile / working pile,
- Capping of pilot pile / working pile.

(ii) Headline II (Assembling of Test System with Required Equipment)
- Installation of bearing plate(s) on pilot pile's cap / working pile's cap,
- Installation of hydraulic jack on bearing plate(s),
- Installation of bearing plate(s) on hydraulic jack
- Installation of test beam(s) over connectors
- Welding of longitudinal rebars of anchor piles to connectors,
- Installation of reference beams,
- Connection of hydraulic hoses from the hydraulic power pack to the jack,
- Installation of dial gauges.

There are two types of measurement for pile movement which are butt axial movement measurement and incremental strain measurements (Sharma, 1990). Butt axial movement measurement is applied in all pile load tests and it is the measurement of pile head movement both in compression and tension tests. For this purposes, dial gauges are mainly used together with surveying measurements.

The movement of the pile head under load is measured from two independent reference beams by minimum 2 nos of dial gauges fixed to the pile head. Practically, dial gauges, which has an accuracy of 0.25 mm and stem level of minimum 50mm of pile diameter is placed diametrically opposed positions and equidistant from the pilot pile's or working pile's center. The reference beam and measuring gauges is protected against sun and wind (ASTM D1143). It is also possible to use different measurement tools instead of dial gauges which is wire mirror and scale arrangement. This system is composed of two parallel wires in each side of the test pile A mirror and a scale is placed on the face of test pile. Displacements are taken and recorded from the scale with the wire and its image in the mirror. In addition to these measurement tools, readings are also taken by a surveyor's level system. This is practically performed to check and verify the other measurements.

Telltales or in other words strain rods are used especially when pile head is not on the working platform level or displacements at different depths of pile are needed to be known. These rods are placed inside a steel or PVC tube which is bonded to the reinforcement cage during preparation of it. It is important to note that telltales or strain rods should be left freely inside the tubes since their movement with respect to pile top level or working platform level during pile testing is recorded. With the help of telltales it is possible to find elastic shortening of pile.

Strain gauges are another tools for determination of pile displacements. There exist electric strain gauges and vibrating wire strain gauges and they can be placed wherever it is asked to the reinforcement cage. It is applicable both on bored piles and driven piles. They measure local strains and these strains are transferred to either stresses or to loads. If a long term monitoring process is necessary for the project in question then, it is a most common practice to use vibrating wire strain gauges since they are not influenced by the changes in voltage, corrosion and temperature.

4.1.1. Compression Load Tests

Load is applied to the pile axially to observe the load-time-settlement behavior under compression. Application of load to the pile can be done in different ways as listed below:

(i) Kentledge type of loading: In this loading arrangement, concrete blocks, pigs of cast iron, bricks, steel piles are used as kentledge. Hydraulic jack, load cell and reaction beam is placed at top of pile. Reaction beam must be strong enough to bear the bending and shear moment due to loading. This whole weight together with reaction beams should be placed on a support which can be timber, concrete or other cribbage elements (see Figure 4.1). These support elements should be spaced minimum 1.5m clear distance to each other regarding ASTM D1143 Clause 6.4.1. It is also important to consider the bearing capacity of the soil while the cribbage is designed to be placed.

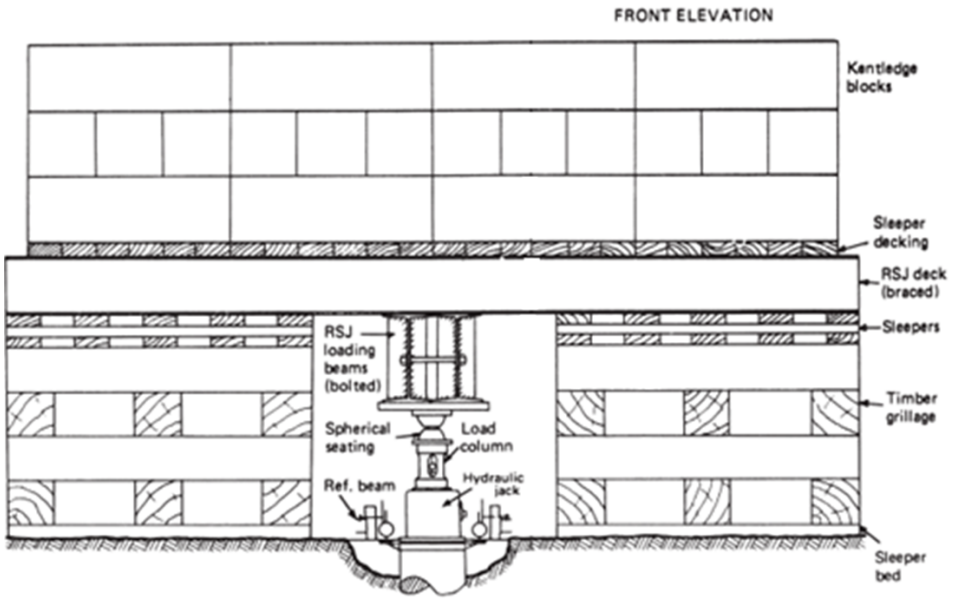

Figure 4.1. Test arrangement by using kentledge (Fleming *et al.*, 2009, Figure 4.9).

(ii) Tension piles and ground anchors: They are also used as reaction system with sufficient pull out capacity. The length of these piles may be larger than tested compression pile. Clear spacing between piles should be minimum 5 times the

diameter of largest pile and not less than 2.5m according to ASTM D1143 Clause 6.3.1. However, if the site or layout of the piles is not appropriate or the length of beam is limited, then 3 to 4 times pile diameter between center to center of piles is used in practically. In this case, some corrections should be made to minimize the effect of pile interaction.

This system of loading usually called as conventional system and it is the most preferred loading type. In this system reaction piles are constructed by maintaining extra reinforcement length to allow welding between pile reinforcement and connection elements. Load is applied with a hydraulic jack to the pile and thus to the steel beams placed on top of both tension piles and test piles (see Figure 4.2). Instead of tension piles it is also possible to use ground or rock anchors for the reaction system (see Figure 4.3). In both systems readings are taken via dial gauges replaced properly around test pile and reaction system (see Figure 4.4).

Figure 4.2. Test arrangement by using reaction piles (year of photo: 2016).

Figure 4.3. Test arrangement by using ground anchors.

Figure 4.4. Measurement of movements.

(iii) Osterberg Cells: This is a new system compared to others and different than traditional methods. Since this is the topic of this thesis, it will be focused more detailed in next chapters.

Compression tests are also separated into following groups according to the procedure of the test according to ASTM (D1143):

- Quick test,
- Maintained test,
- Loading in excess of maintained test,
- Constant time interval test,
- Constant rate of penetration test,
- Constant rate of movement increment test,

- Cyclic loading test.

4.1.2. Pull-out (Tension) Load Tests

Pull out tests or tension tests are very similar to compression load tests. In this type of test setup the hydraulic jack is either put onto test pile (see Figure 4.5) or on top of each reaction pile according to the application of load and test arrangement. In either ways pile is pulled out to a predetermined tension load and upward movements of pile are recorded. Conventionally load applied by hydraulic jacks is verified by pressure gauge and/or load cells. All these equipment should be calibrated by third reliable parties and presented before the test.

Figure 4.5. An example of pull-out test setup.

4.1.3. Lateral Load Test

Lateral load test is used in order to determine behavior of pile under design lateral loads which are quite smaller than axial loads in general. In most cases there is no need to construct a reaction pile since the adjacent pile can be used as reaction. Steel plates are placed against side of pile where load is applied. Plate dimensions should not be less than or more than one half of the diameter and side dimension of pile.

There should be at least 5 times the maximum diameter of largest test or reaction pile and it should not be less than 2.5m. According to type of soil, reaction pile length and test setup conditions, this distance can be decreased or increased.

Figure 4.6. An example of lateral load test setup.

4.2. Dynamic Load Test

Dynamic Pile Testing is executed to assess driving efficiency as well as confirmation of the findings of the preliminary testing phase with regard to the required bearing

capacity.

Strain (or force) and acceleration (or velocity, displacement) data is collected via transducers installed diametrically opposite to each other, upon impact by an impact hammer on the test pile. From the gathered data, information can be extracted based on one-dimensional wave theory, on the bearing capacity, the hammer performance and the pile stresses (as well as some other quantities). The method does not replace with static testing, but is very useful in combination with Static Load Testing. The following data acquisition system is generally used:

- Foundation Pile Diagnostic Systems (FPDS),
- Cable for pile monitoring with a total length of 40 m,
- two sets of strain and accelerometer transducer (see figure 2).

During installation of the pile section monitoring can be performed continuously (PDA). With depth (or time or blow number) quantities like “driving resistance”, “energy level” and “pile stress2 can be presented. From the results statements can be formulated with regard to driving circumstances and hammer efficiency. At the end of driving the signal of one blow can be used for further analysis, i.e. Signal Matching. This analysis will result in an estimation of the (mobilized) bearing capacity. In general the estimation becomes more accurate (and higher) when a certain setup time is considered. This phenomenon occurs mainly due to the existence and sometimes persistence of excess pore pressures.

After the setup period ends, the pile is subjected to a re-drive (DLT) where monitoring is continued until the engineer decides a successful and useful signal is recorded. It is also important that in order to mobilize the entire capacity displacement of the pile must occur. One of the recorded signals can be used for further analysis, i.e. Signal Matching (see Figure 4.7).

When static and dynamic components of the soil resistance along the pile (shaft friction) and underneath the pile (toe resistance) have been determined from signal

matching, static bearing capacity of the pile can be calculated. Total (static) bearing capacity of the pile is the sum of all static contributions of the soil to the pile since the dynamic soil resistance occurs during driving only.

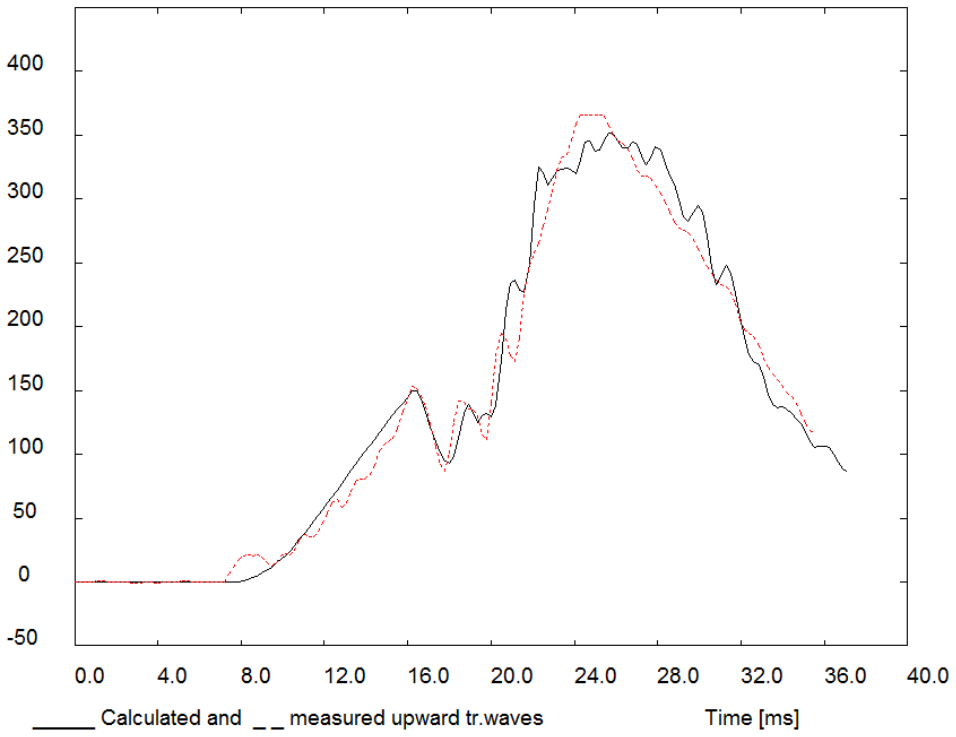

Figure 4.7. An example of signal matching.

4.3. Rapid Load Test

Rapid load tests are the general term used for impulse or push-load on a pile. Rapid lod tests measure load and displacement directly. When compared to static load tests rapid load tests do not need a reaction system setup, so they have quick setup time, less expensive and need less space than static tests. Contrary to static pile tests; in rapid load tests displacements are measured by an optical displacement transducer and loads are measured by a load cell. Although they have several advantages, they are not as widely preferred as static tests since it is too fast to investigate change of movement with respect to time and to distinguish shaft friction and end bearing if strain gauges are not installed to the test pile. Moreover, this type of testing may overestimate capacity f pile in clayey soils.

4.3.1. Statnamic Pile Load Test

Statnamic test is first used by Berminghammer Foundation Equipment in Canada at the end of 1980's. The idea emerged from testing of piles with a high capacity by not constructing an expansive reaction system. Test methodology is based on the momentum principle which is force equals to mass times acceleration. The force applied on pile is created by a combustion chamber which burns solid fuel propellant and generate high pressure gases to energize the mass upward by 10 to 20g (Fleming *et al.*, 2009). This upward pressure creates a downward reaction and thus test load on pile. Schematic sketch of test setup is provided in Figure 4.8 below.

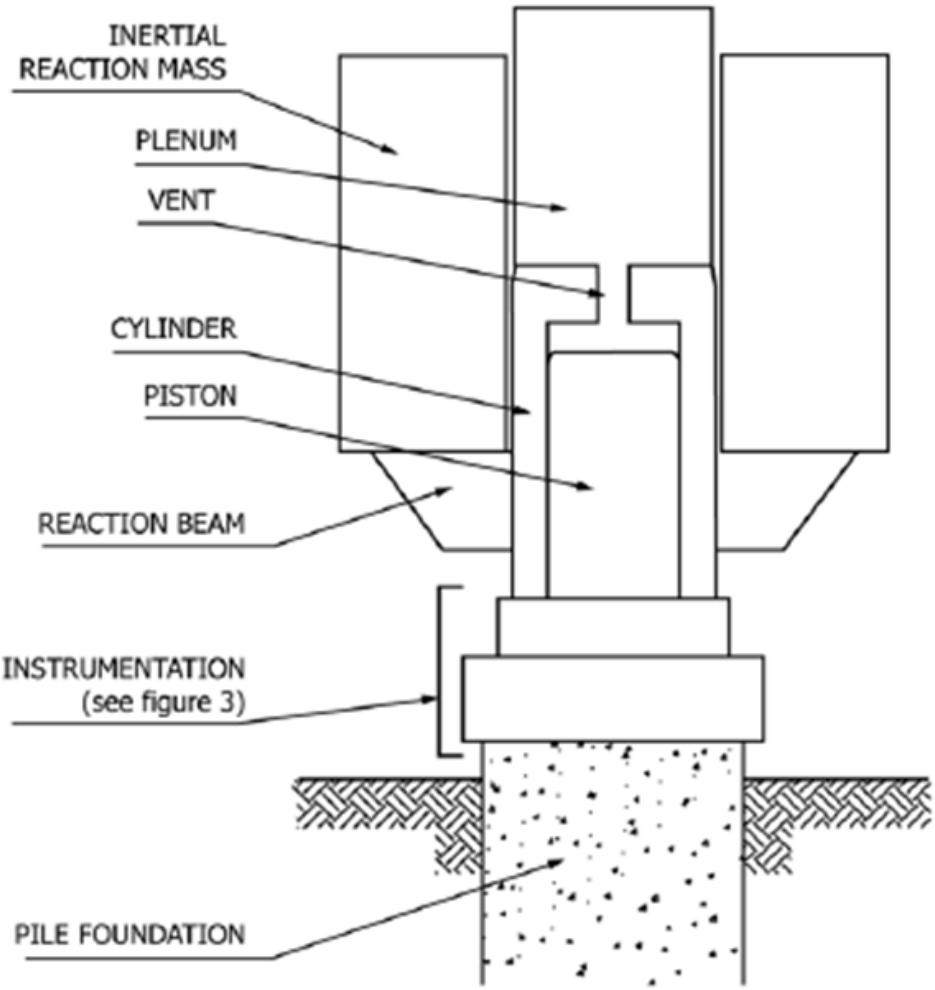

Figure 4.8. Combustion gas pressure test apparatus (Taken from ASTM D7383-2010).

4.3.2. Pseudo-Static Pile Load Test

In this type of load test a mass composed of concrete, steel or any other material is dropped from the required height to create the test load to act on pile. Springs or cushion materials are used to soften the impact of the mass on pile head. These materials should have sufficient capacity and strength to transfer load to pile. Same as in statnamic load testing, a load cell for measurement of load and a displacement transducer are placed on pile. When compared to dynamic load tests which also use a drop mass, this system creates loading pulse lasting in longer duration with the help of mechanical springs or cushions. Schematic sketch of test setup is provided in Figure 4.9 below.

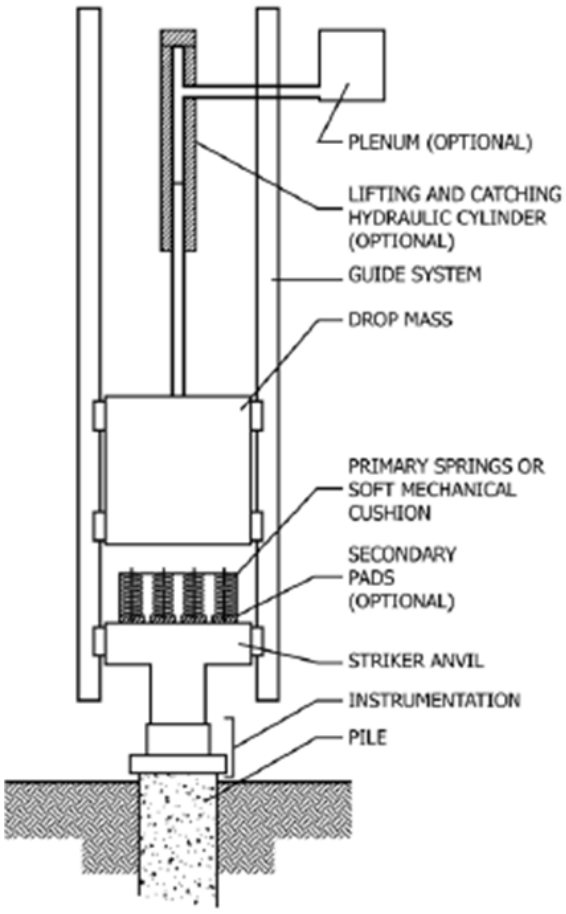

Figure 4.9. Cushioned drop mass test apparatus (Taken from ASTM D7383-2010).

5. STATIC LOAD TESTING BY OSTERBERG CELLS

5.1. History of Osterberg Cell Testing

Osterberg Cell testing takes its name from the person found the system who was Dr. Jorj Osterberg, emeritus professor at Northwestern University. He first used this load testing system in 1984 in an experimental bored pile to see whether the theory works or not. When he got reasonable results from the experiment, he worked for improving the system especially by refining the design of cells.

Haley Aldrich Inc. is the first company using this test methodology practically in 1987 with a steel driven pipe pile at a bridge project in Massachusetts. Osterberg cell having same diameter of 457mm with pile was placed at the bottom of pile. After an ultimate side shear of 1.26MN was reached, another test was conducted in same year by the same company in New York. This time a 610mm diameter steel pipe pile was tested with a 457mm diameter O-cell and 560mm top and bottom plates. An ultimate side shear of 4.0 MN was reached during testing (Schmertmann and Hayes, 1997).

Pile testing of bored piles with Osterberg Cell was first conducted in 1988 by Schmertman and Cropps Inc. within the scope of Port Orange Bridge Project supported by FHWA located in Florida. Test pile was failed under 2.28MN test load. After several years of experience O-cell has become popular and widespread around the world with its successful applications (Schmertmann and Hayes, 1997).

5.2. Instrumentation of O-Cell Testing

Osterberg Cell load test system consists of a specially designed hydraulic jack. At first year of this technology O-cell was being placed at the bottom of drilled hole, after a thin layer was created with concrete. There was a pipe having been connected to the top of O-cell extending to the ground level. This pipe worked for providing fluid pressure to O-cell which had been calibrated before. There was also another small

pipe passing through this main pipe and it was responsible for tracking the movement of bottom of O-cell from the ground level. This was like a telltale rod which is now used in developed testing setup of O-cell load test. When required strength is gained by concrete, test was initiated by giving pressure to the jacks through the pipe with oil or water. Then displacement of bottom of O-cell, top of O-cell and top of pile were recorded. In order to take readings from top of pile, a frame was established and gauges were placed in this frame. Figure 5.1 typically illustrates the scheme of setup. After test was performed successfully, readings were arranged as upward and downward movements and graphed with respect to load applied. These curves would be according to either ultimate side shear value or ultimate end bearing value whichever was reached before. If these piles were working piles then the part where O-cell had been placed could be grouted.

With the increasing demand in towers or other extreme structures requiring a strong foundation, this system had to be developed for larger diameter piles under higher loads. In order to make reinforcement installation easier, the pipe located at the center was replaced with special hoses for applying pressure and telltale rods for measuring displacements.

Today more powerful and better equipped testing system is used all over the world for bored and driven piles, barrettes, caissons, slurry walls, CFA or Auger Cast Piles. They can either be used for sacrificial piles or working piles. Moreover, in order to increase reliability of results and to get better understanding how the pile works in available complex soil conditions, multiple level of O-cells can be used. The depth of O-cell is determined according to the soil profile and testing program together with the geometry of pile. The point where O-cell is placed must be such that equal capacity can be satisfied above and below O-cell level to maximize the load applied to the pile. Therefore a calculation on pile shaft and bearing capacity is performed prior to testing for obtaining location of O-cell.

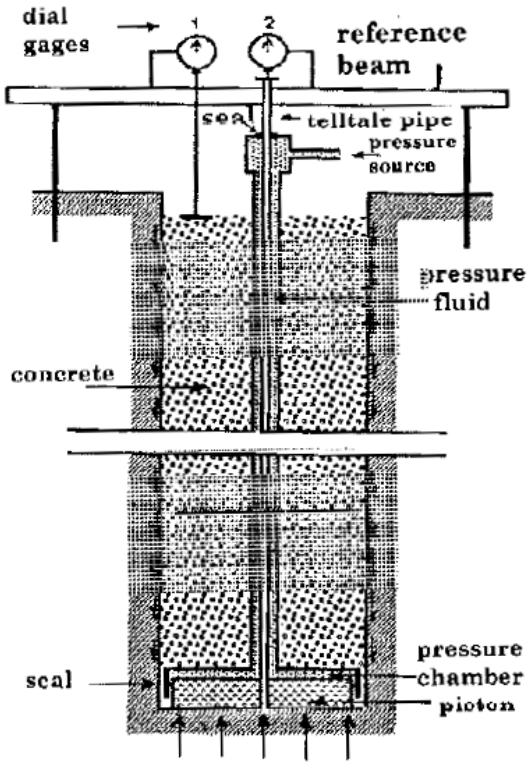

Figure 5.1. Modified O-cell arrangement (Osterberg, 1998).

Osterberg cells are placed during preparation of reinforcement cage together with other instruments and assemblies. Steel cages can be consisted of more than one segment due to pile length and/or choice of piing contractor on lifting equipment. O-cells are calibrated before they reach to the construction site by their manufacturer. In Figure 5.2 below there is a sample calibration certificate for O-cells.

Telltale casing and rod extensometers are placed on top of O-cell assembly extending to the top of pile in order to measure pile compression between O-cell and pile top point. Telltales are also used for measurement of pile toe movement (see Figure 5.3). They are located at pile toe and extend to pile top level and attached to Linear Vibrating Wire Displacement Transducer (see Figure 5.4).

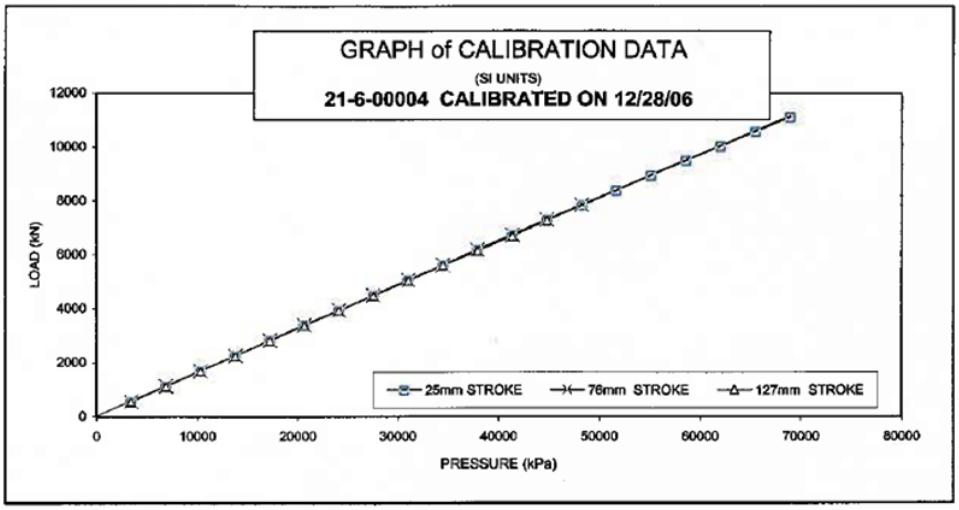

Figure 5.2. Sample calibration graph for an Osterberg load cell.

Actual pile toe movement is calculated as the measured toe movement minus top loading of pile. Top of pile movement is measured similar to the conventional load test by survey equipment like total station. A reference beam system which generally consists of 12 m long steel profile and is supported from one end fixed and other is free, is constructed on top of pile location to observe the most reliable pile top movement data. In addition to this measurements, automated digital survey equipment is used for monitoring reference beam.

Additionally, Linear Vibrating Wire Displacement Transducers are placed between top and bottom plates of O-cell in order to measure expansion of load cells during loading. Strain gauges are used for determination of unit shaft friction between previously determined soil layers and pile (see Figure 5.5). Number and location of strain gauges are important in order to estimate pile actual behavior. They should be located in each different layer and more than one in each level in order to check consistency of data and in order to be on the safe side if one of them fails or gets damaged.

Figure 5.3. Telltale casings and rods.

Figure 5.4. Linear vibrating wire displacement transducers (LVWDT).

Figure 5.5. Strain Gauges.

All internal measurement instruments are directly connected to computer gathering information per 30 or 60 seconds. Generally, in order to prevent residual strains on strain gauges quick load test is recommended.

Osterberg location on a pile with its bearing plates is given in Figure 5.6 below. Schematic sketch of developed O-cell instrumentation is presented below in Figure 5.7 for single level Osterberg pile load test. There are also load tests where multiple level of O-cells are used especially to investigate end bearing and shaft friction separately better than one level of O-cell.

Figure 5.6. Osterberg load cells together with upper and lower plates.

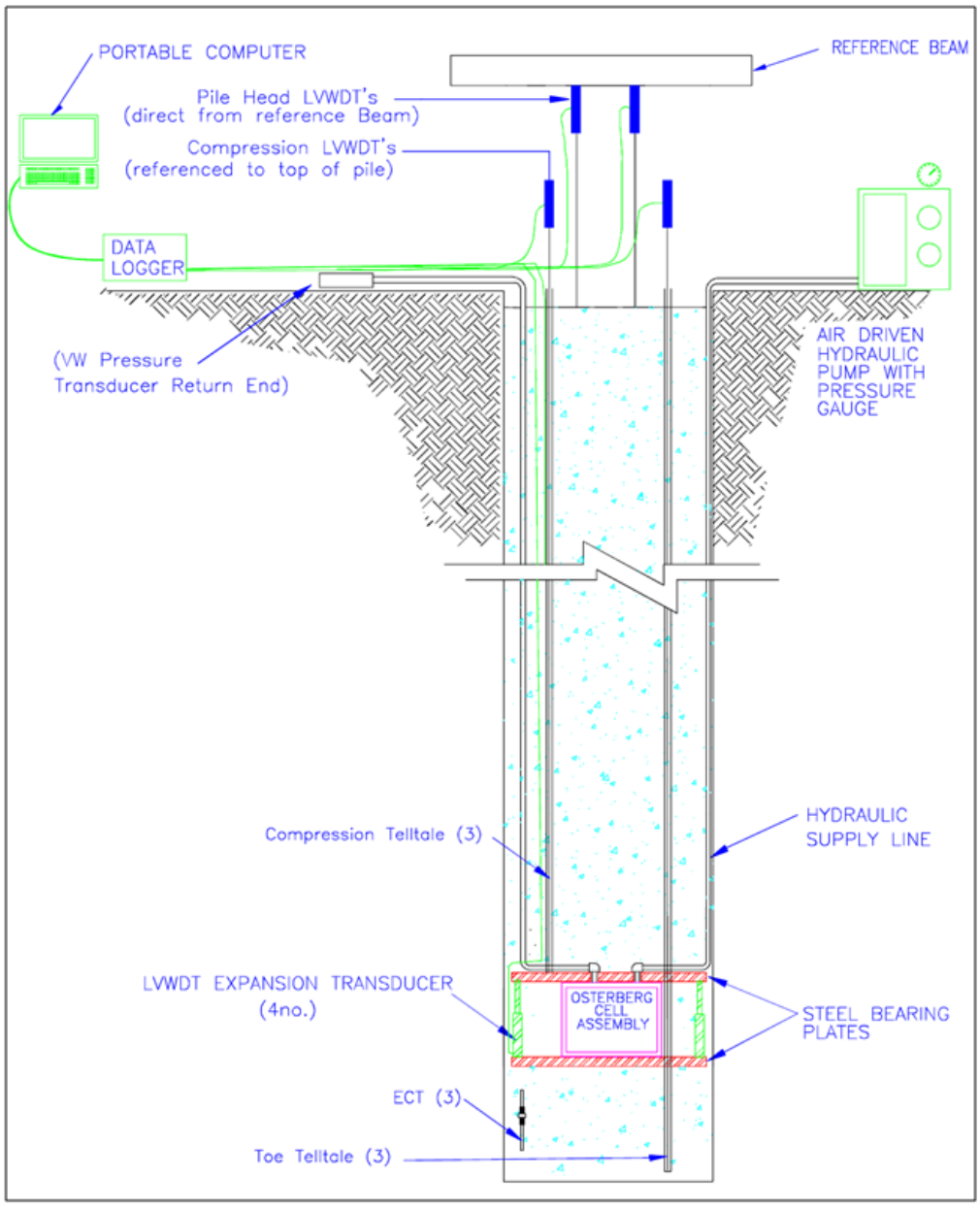

Figure 5.7. Schematic instrumentation for Osterberg load testing.

5.3. Analysis and Evaluation of O-Cell Test Results

After test is conducted results are obtained from the computer which all data stored. Data is evaluated to determine the designed pile is satisfactory to carry design load safely. In order to evaluate test results, a top-down curve is constructed by using parameters obtained during test.

Multiple methods may be used to generate a single load-settlement diagram regarding the measured results combination from a O-cell load test (OLT). The described method herein has been improved by Loadtest and is based on the sum of the resistances measured for the same displacement as well as an additional elastic shortening, which is not mobilized during the OLT, except which would occur when loading top-down. The technique has been evaluated independently of being a good estimate of the load movement curve for the foundation element when the load was applied to the top of the concrete. The method is valid equally for piles or barrette foundations.

The starting hypothesis is that the pile behaves like a rigid body, but containing the elastic compressions that are part of the motion data that were obtained from an O-cell test. With this assumption, a corresponding top-load test (TLT) is constructed.

When an O-cell, located at a distance above the bottom of the pile, the section of the pile below the O-cell is assumed to behave same when the entire pile is top-loaded. For conservative remaking of the top loaded settlement curve gross loads are changed over to net load to make allowance for the buoyant weight of the upper pile section. Then the upper net-load movement and lower load movement curves are constructed. Loads are added to each other making the same settlement. For example, a point which makes 3 mm movement to upward at 1000 ton and to downward 400 ton. Then this point is transformed to top-down rigid curve as 3mm displacement under 1400 tons. This is the construction of rigid top-down curve in which elasticity of pile is not taken into account. Second stage comes at this point as determining of elastic settlement of pile under top-loading.

Total elastic compression that is mobilized in the corresponding top load test would practically always go beyond that mobilized in an 0-cell test on the same pile. A TLT produces more top of pile movement then resulting in more mobilized skin friction. A precise solution of this non-linear load transfer behavior would necessitate utilizing fine element or finite difference methods using skin friction vs. vertical movement (t-z) curves to unite on a solution. Instead of applying such a complex analysis, the approximate solution described here is usually sufficient. Simplified equations for

modelling the elastic compressions occurring in the OLT are shown on the analysis given on Figure 5.8 whereas elastic compressions that occur in the equivalent TLT is presented in Figure 5.9. The desired additional elastic compression at the top of the TLT is obtained by subtracting the OLT from the TLT. The sum of the measured equivalent curve obtained from first stage is summed with the additional elastic compression to obtain the final, corrected equivalent load-settlement curve for the TLT on the same pile as the actual OLT. The initial solution for the additional elastic compression, gives an adequate and fairly conservative (higher) estimate of the additional compression versus more complicated load-transfer analyses.

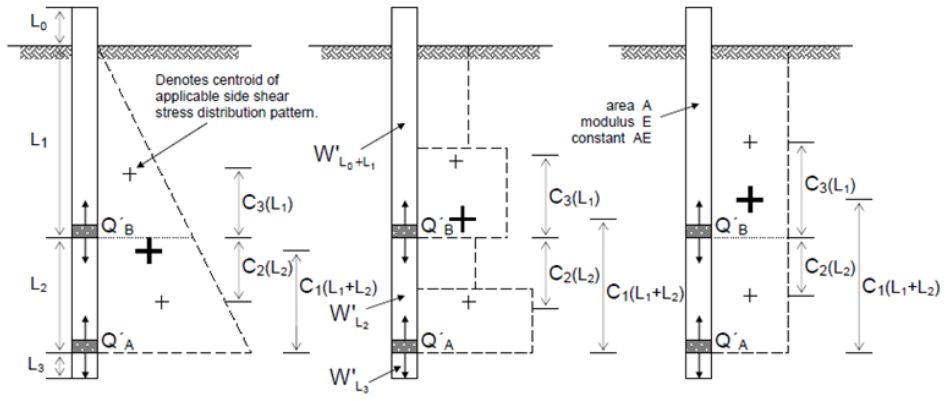

$C_1 = \frac{1}{3}$	Centroid Factor = C_1	$C_1 = \frac{1}{2}$
$\delta_{\uparrow(L_1+L_2)} = \frac{1}{3}\frac{Q'_{\uparrow A}(L_1+L_2)}{AE}$	$\delta_{\uparrow(L_1+L_2)} = C_1\frac{Q'_{\uparrow A}(L_1+L_2)}{AE}$	$\delta_{\uparrow(L_1+L_2)} = \frac{1}{2}\frac{Q'_{\uparrow A}(L_1+L_2)}{AE}$

Figure 5.8. Theoretical elastic compression in O-cell test.

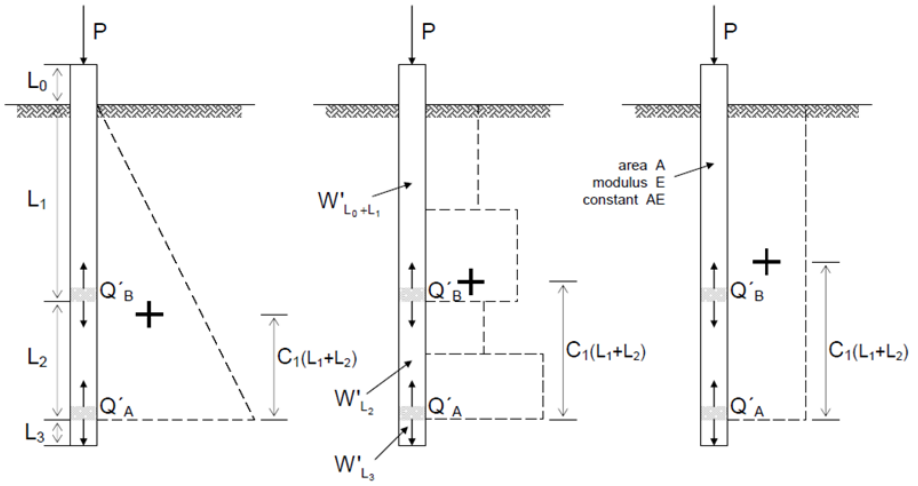

Top Loaded Test: $\delta_{TLT} = \delta_{\downarrow L_0} + \delta_{\downarrow L_1+L_2}$

$\delta_{\downarrow L_0} = \frac{PL_0}{AE}$	$\delta_{\downarrow L_0} = \frac{PL_0}{AE}$	$\delta_{\downarrow L_0} = \frac{PL_0}{AE}$
$C_1 = \frac{1}{3}$	Centroid Factor $= C_1$	$C_1 = \frac{1}{2}$
$\delta_{\downarrow L_1+L_2} = \frac{(Q'_{\downarrow A}+2P)}{3}\frac{(L_1+L_2)}{AE}$	$\delta_{\downarrow L_1+L_2} = \left[(C_1)Q'_{\downarrow A}+(1-C_1)P\right]\frac{(L_1+L_2)}{AE}$	$\delta_{\downarrow L_1+L_2} = \frac{(Q'_{\downarrow A}+P)}{2}\frac{(L_1+L_2)}{AE}$

Figure 5.9. Theoretical elastic compression in top-loaded test.

6. BACK-ANALYSIS OF OSTERBERG CELL LOAD TESTS

In order to investigate pile behavior during Osterberg Cell pile load test and its equivalent top-down loading analysis, pile tests were modeled in a finite element analysis software, Plaxis 2D (Plaxis 2D Manuals, 2017). Axisymmetric models were constructed by using solid elements for both soil and pile. Rigid interfaces were preferred for modelling soil pile interaction. Osterberg cells were placed to the exact location in pile load test. Loads were applied as line load by dividing load into pile cross sectional area. In order to distribute load uniformly through the pile, top and bottom plates of Osterberg Cell were also modelled.

Three load tests were back-calculated and analyzed within the scope of this thesis. These tests were performed in rock formation of Russia, Moscow City. Analysis started with the measured and reported soil parameters. Loading stages were simulated same with test data. Soil parameters were modified according to the load-displacement curves obtained during field Osterberg load test. After obtaining the best suited load-displacement curves, second arrangement came with the available strain gauge load measurements. By using strain gauge data shaft frictions were optimized. Analysis results are provided below.

6.1. Case Study 1

Test pile is socketed into limestone the sub-surface stratigraphy at the general location of the test pile is reported to consist of stiff clays underlain by limestone to depth. Diameter of test pile is 1200 mm and it is excavated from top level of 103.78 m to the tip elevation of 81.79 m under water table. The pile is started with a 1310 mm O.D. casing. A bucket was used for drilling and cleaning the pile. After cleaning the base, the reinforcing cage with attached O-cell assembly was inserted into the excavation and temporarily supported from the steel casing. Concrete was then delivered by tremie

through a 200 mm O.D. pipe into the base of the pile until the top of the concrete reached an elevation of +103.78 m.

The loading assembly consisted of two 540 mm O-cells, located 3.14 metres above the toe of pile. Calibration of O-cells was performed by an independent corporation up to 11.4 MN before they were delivered to site. Four Linear Vibrating Wire Displacements which were placed between lower and upper plates; two telltale casings and rods extending from the top of the O-cell assembly to top of concrete; one level of two sister bar vibrating wire strain gauges which were attached to the reinforcement cage below O-cell assembly were used for instrumentation.

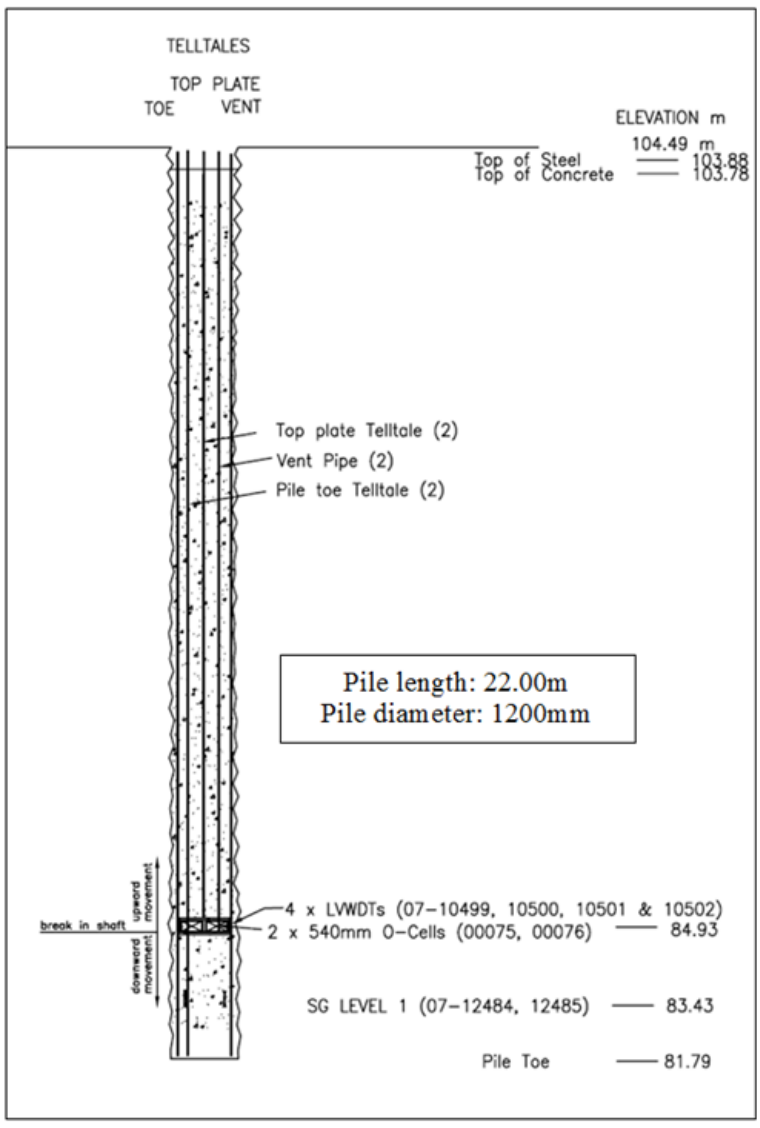

Figure 6.1. As built schematic section of instrumented test pile 1.

Load to O-cells were applied in 13 equal increments to 20100kN of bi-directional gross load. Unloading was then performed in four decrements and the test was concluded. Each successive load increment was maintained constant for 30 minutes while automatically maintaining the O-cell pressure constant. Loading stages are given below in Table 6.1.

Table 6.1. Loading stages and loads applied during testing of test pile 1.

Loading Stages	**Loads (MN)**	**Loads Applied to Plaxis (kPa)**
1L-1	1.61	1423.55
1L-2	3.19	2820.58
1L-3	4.52	3996.56
1L-4	6.3	5570.42
1L-5	7.63	6746.4
1L-6	9.42	8329.11
1L-7	11	9726.14
1L-8	12.76	11282.32
1L-9	14.55	12865.02
1L-10	16.1	14235.53
1L-11	17.88	15809.39
1L-12	19.22	16994.21
1L-13	20.11	17781.14

The maximum downward applied load was 20.1 MN which occurred at load interval 1L-13 where the average downward movement of the O-cell base was measured as 2.3 mm. The maximum upward applied net load to the upper skin friction was 19.77 MN which occurred at load interval 1L-13 where the average upward movement was calculated as 1.6 mm. Table 6.2 below shows the measured unit skin frictions for both upper and lower part of pile and unit end bearing under maximum load.

Table 6.2. Average net unit skin friction values under maximum load measured in field O-cell load test pile 1.

Load Transfer Zone	**Displacement***	**Net Mobilised Unit Side Shear****
Zero Shear to O-cell	↑ 1.73 mm	278 kPa
O-cell to Strain Gauge Level 1	↓ 1.99 mm	1303 kPa
*Average displacement of load transfer zone.		

According to constructed equivalent top down curve based on test results, test pile behavior has been analyzed for a combined skin friction and end bearing load of 41.9 MN. For a top loading of 20.0 MN, the adjusted test data indicated this pile would settle approximately 8.0 mm of which 7.3 mm is estimated elastic compression. For a top loading of 30.0 MN the adjusted test data indicate this pile would settle approximately 12.1 mm of which 10.8 mm is estimated elastic compression.

6.1.1. Modelling of O-cell Test for Case 1 with Plaxis

Before analyzing data closest soil profile is investigated and selected with appropriate soil parameters. Figure 6.2 below illustrates the soil profile and parameters provided by local authorities in their soil investigation report is presented below in Table 6.3.

Analyses has started with the parameters given in Table 6.3 and an axisymmetric model is formed changed accordingly until a good match between site measured and numerically measured load movement data is obtained. Analysis model constructed in Plaxis software is given in Table 6.3. Final parameters that obtained at the end of analysis are given below in Table 6.4.

Table 6.3. Soil parameters for test pile 1 reported in soil report.

Soil Unit	**Soil Definition**	**Modulus of Deformation E (MPa)**	**Unit Weight (kN/m^3)**	**Measured Cohesion (kPa)**	**Measured Internal Friction Angle (^{o})**
1	Hard Clay	44.0	22.00	103.0	29.0
2_B	Medium-strength Limestones	1500.0	23.00	700.0	45
3	Strong Limestone	2000.0	26.00	1000.0	52.0

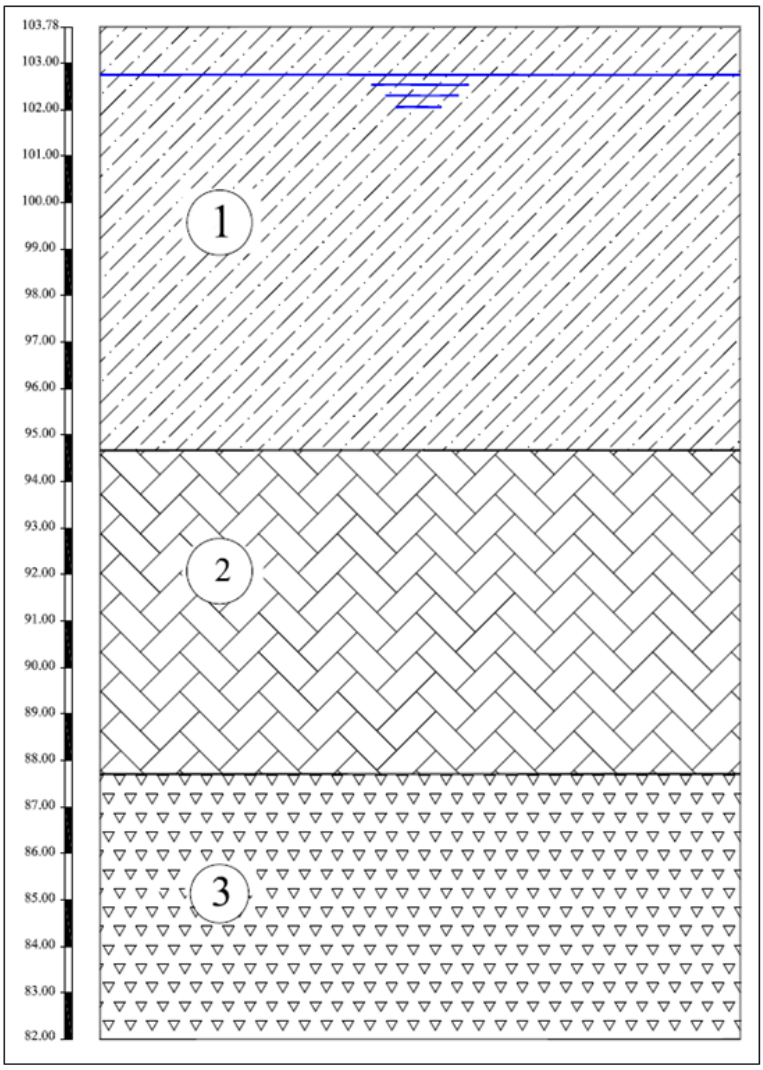

Figure 6.2. Soil profile of test location for test pile 1.

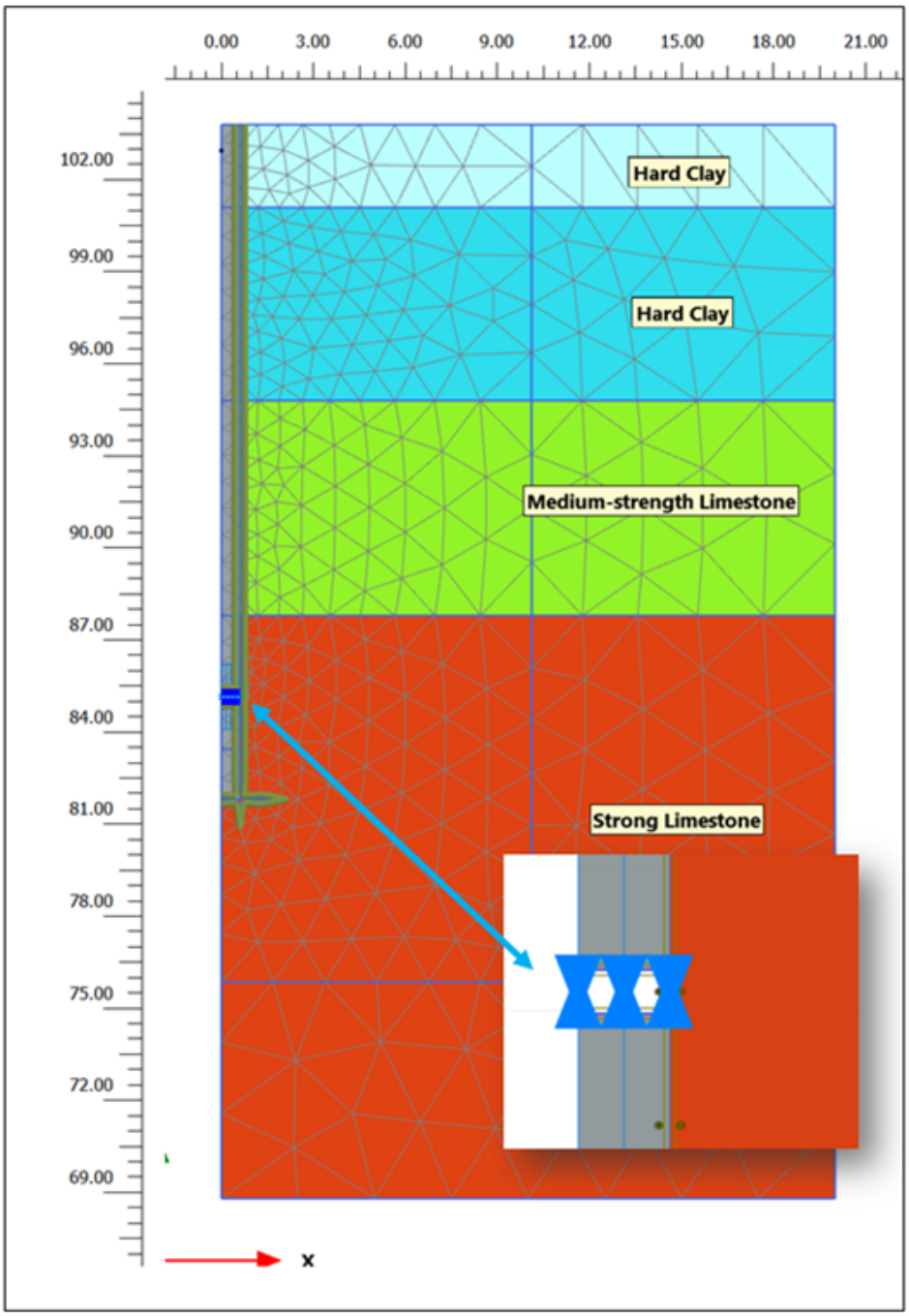

Figure 6.3. Model view of test pile 1.

Table 6.4. Soil parameters for test pile 1 found as a result of back analysis.

Soil Definition	**Hard Clay-Zero Shear**	**Hard Clay**	**Medium-strength Limestone**	**Strong Limestone**	**Concrete**
Soil Unit	1a	1	2	3	-
Material Model	Hardening Soil	Hardening Soil	Mohr-Coulomb	Mohr-Coulomb	Linear Elastic
Drainage Type	Drained	Drained	Drained	Drained	Non -porous
Modulus of Deformation E^{50}_{ref} (MPa)	40	40	-	-	-
power (m)	0.5	0.5	-	-	-
Modulus of Deformation E' (MPa)	-	-	2000	2500	35000
Poisson ratio υ'	-	-	0.2	0.2	0.2
Unit Weight (kN/m^3)	21.0	21.0	23.0	26.0	24.0
c' - Cohesion (kPa)	25	25	300	350	-
ϕ' - Internal Friction Angle (^{o})	30	30	40	42	-
ψ - Dilatancy Angle (^{o})	-	-	10	12	-
Interface	0.1	1.0	1.0	1.0	1.0

6.1.2. Results of Back Analysis for Case 1

As it is mentioned before, back analysis of field test is mainly conducted by optimizing parameters until a good and reasonable match is obtained with the measured and calculated load settlement behaviour of pile. When this match is achieved, strain gauge data are evaluated whether or not the analysis model satisfies the field-measured data. Actually for load settlement behaviour, the dominant parameter is the elasticity

modulus. When strain gauge data, hence the unit shaft friction values come into the stage, this time internal friction angle and cohesion values are calibrated so that it matches with field parameters. Figure 6.4 shows the comparison between measured and calculated load-settlement behaviour of pile generated during O-cell test. This part is the key element of analysis since it gives the calibrated soil parameters presented in Table 6.4 for further investigation of pile for top-down analysis.

After a good match is obtained regarding both load-movement curves and strain gauge data provided, top-down loading is modelled with the same parameters in the same model to observe the behavior of pile under actual loading application. Report provided by testing firm suggests an equivalent top-down curve, construction process of which is given in Chapter 5. This curve constructed by the test supervisors are compared with the one found in finite element analysis in Figure 6.5. By using calibrated soil parameters equivalent top-down curve is constructed by applying same load on top of pile. It is expected that a closest match should be obtained between this graph and calculated top-down curve.

After matching load-settlement graphs of both loading types, load-distribution graphs are obtained in order to see how the load is distributed along the shaft length of pile in two loading cases which are O-cell loading and top-down loading. During field O-cell testing, strain gauge reading s were recorded to obtain the shaft friction value of limestone layer. Strain gauge measurements which were transformed into load values are used to compare assumed distribution in load test report with the ones obtained in numerical analysis. Since the number and level of strain gauges are inadequate data obtained during this test only gives the immobilized shaft friction of limestone layer.

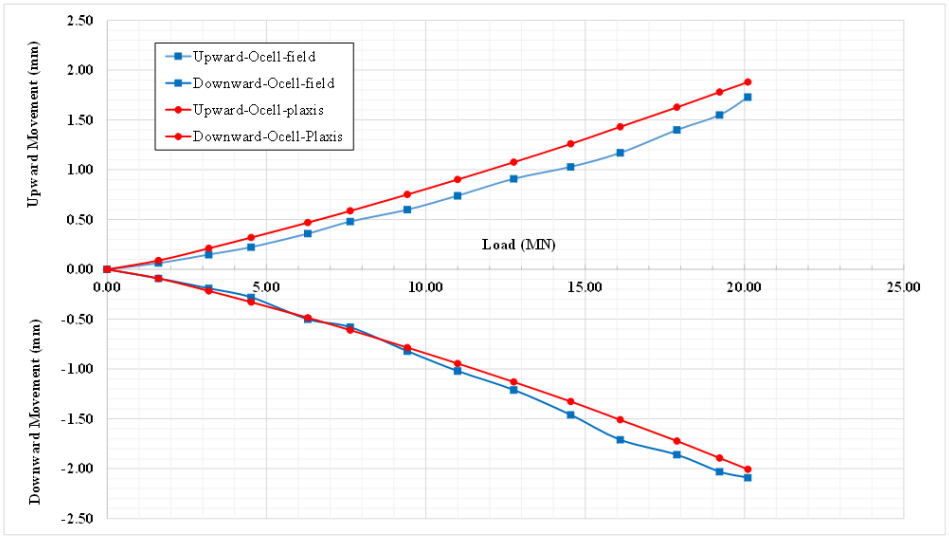

Figure 6.4. Measured and calculated load settlement curves for O-cell loading of test pile 1.

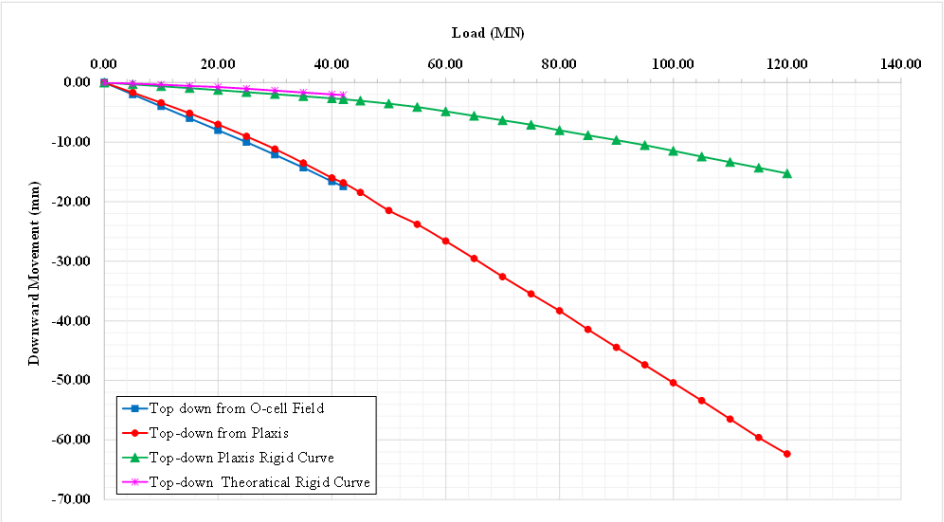

Figure 6.5. Measured and calculated load settlement curves for top-down loading of test pile 1.

Figure 6.6 and Figure 6.7 below illustrates load distribution behavior of pile in case of O-cell loading for both field measurements and numerical analysis and in case of top-down loading respectively. Pile load distribution curves are followed by analysis of unit shaft friction comparison for measured and numerically calculated O-cell loading and for top-down loading respectively in Figure 6.8 and Figure 6.9.

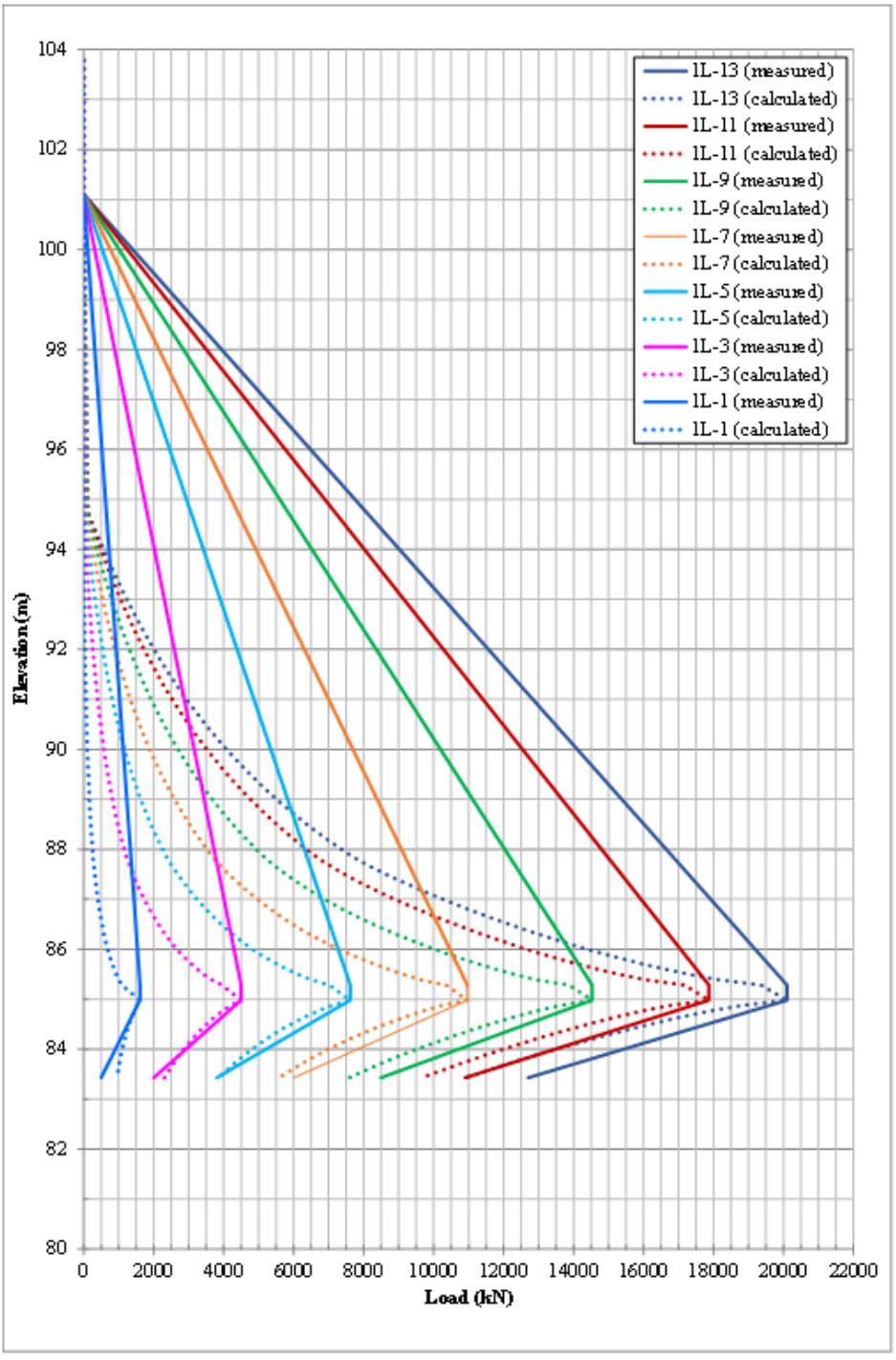

Figure 6.6. Comparison of load distribution curves for O-cell loading obtained from field measurements and numerical analysis of test pile 1.

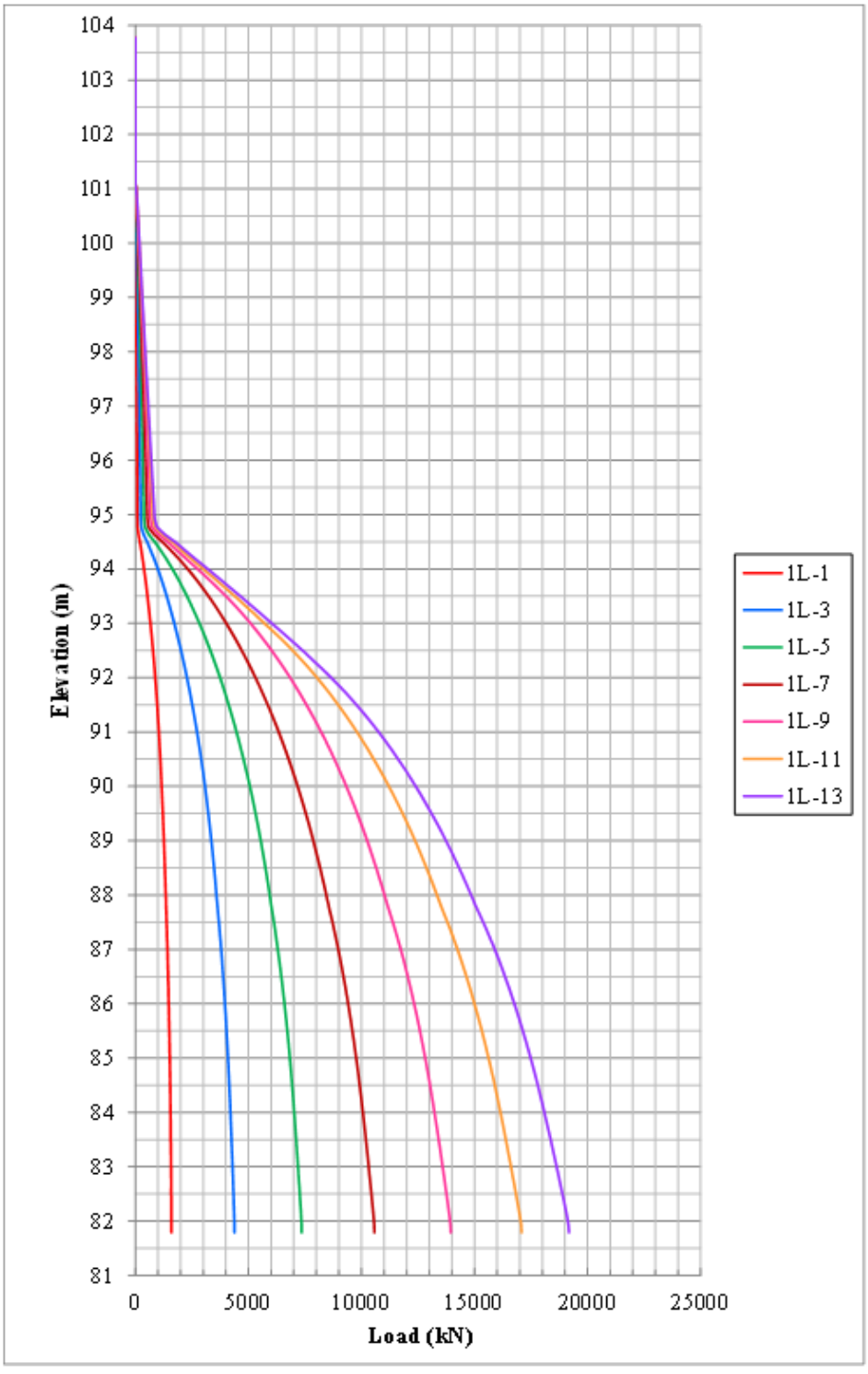

Figure 6.7. Load distribution curves for top-down loading obtained from numerical analysis of test pile 1.

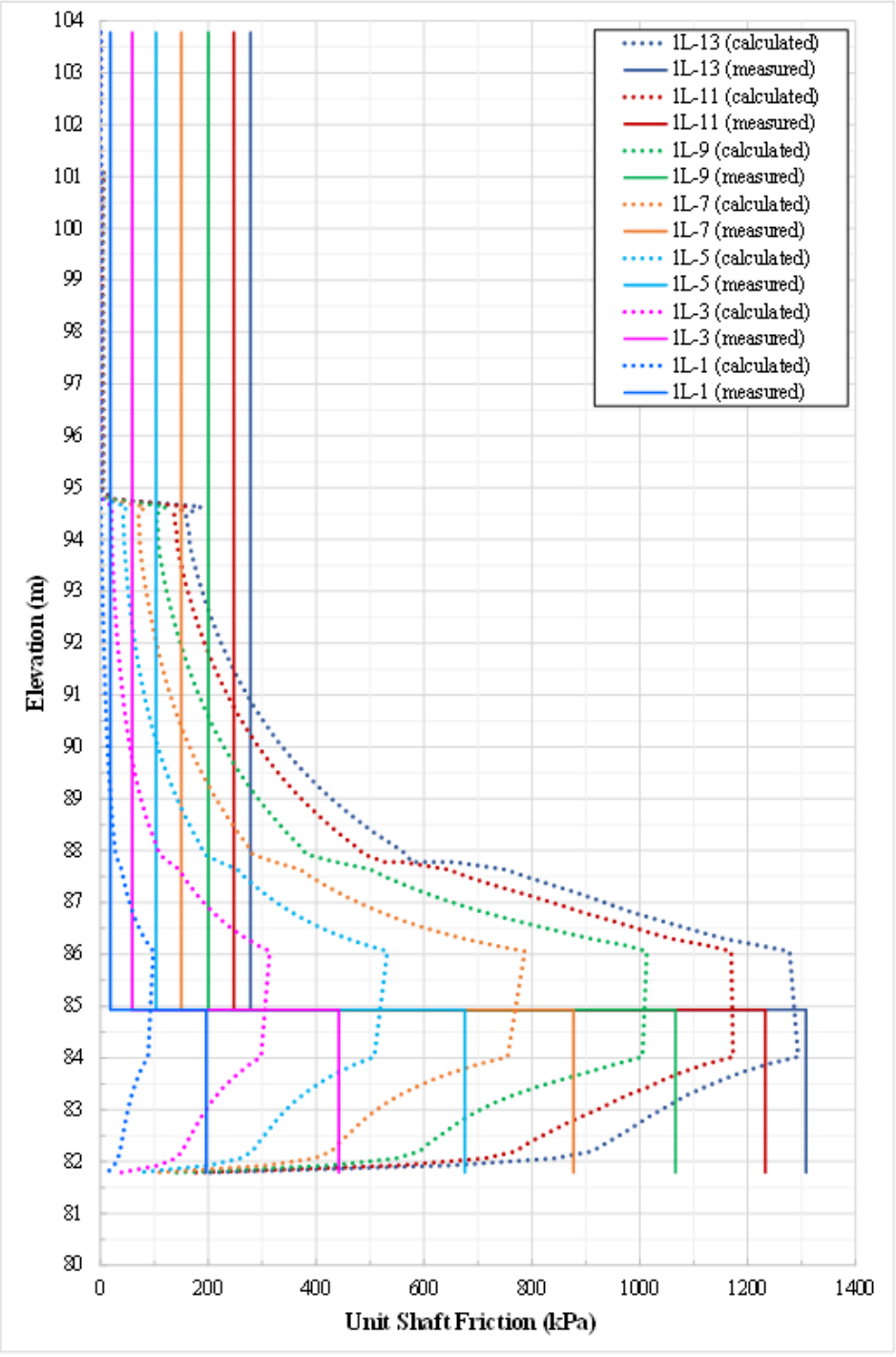

Figure 6.8. Comparison between measured and calculated unit skin friction values along length of test pile 1.

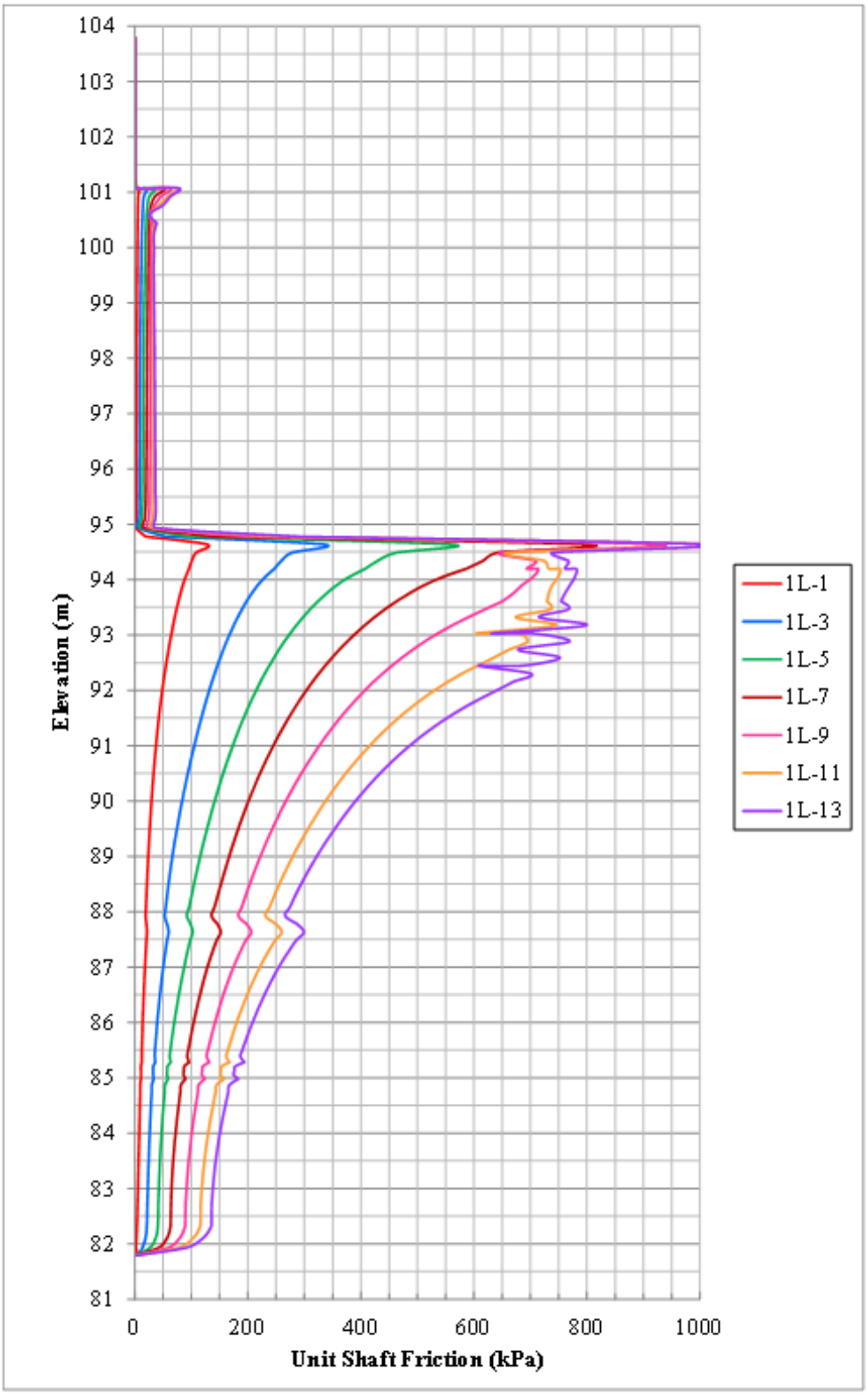

Figure 6.9. Distribution of unit skin friction values for top-down loading obtained from numerical analysis of test pile 1.

In Figure 6.6 it is observed that between O-cell level of 84.93m and pile zero shear level (which equals to bottom level of permanent steel pipe of 101.1) measured shaft load during testing is not true for determined pile load behavior. This is because of lack of strain gauge data between O-cell level and zero shear zone. Since there exists a strain gauge level under O-cell and value measured for this level is contributed to finite element analysis, measured and calculated data well suits to each other for this region. On the other hand, load distribution curves constructed for top-down loading which is shown on Figure 6.7 shows very similar load transfer mechanism for same load.

Further observations are conducted for unit shaft friction comparison between measured and calculated data. Since behavior of pile is modelled based on the data obtained from the maximum loading stage, values found in analysis are much similar to data obtained field test in higher loads. This behavior is clearly seen from Figure 6.8. After observing unit shaft friction distribution for O-cell testing, shaft friction distribution for top-down loading case is investigated and results are shown in Figure 6.9. When two figures are compared, it is observed that magnitude of maximum unit shaft frictions are close to each other but locations where they occur are different under same loads.

In addition to above explained findings, in the light of constructed pile load behavior and calibrated parameters t-z curves are generated for both top-loading and O-cell loading which are presented in Figure 6.10. Two levels are selected for investigation purpose above and below O-cell level. Upper part shows closer match between O-cell loading and top-down loading; whereas lower part shows more deformation under lower loads in O-cell loading. This is mainly due to location of O-cell which is closer to end of pile especially placed to see the shaft friction of only limestone formation. Figure 6.11 shows ultimate t-z curves for top-down loading. Blue curve represents ultimate capacity of skin friction capacity for weak limestone layer whereas green curve representing limestone layer under O-cell level do not show failure yet.

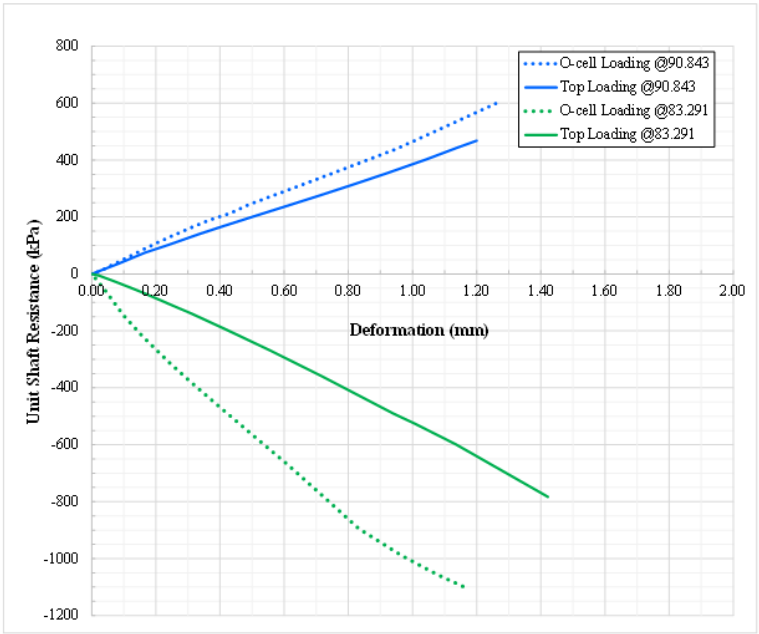

Figure 6.10. Comparison of calculated t-z curves for O-cell and top-down loading of test pile 1.

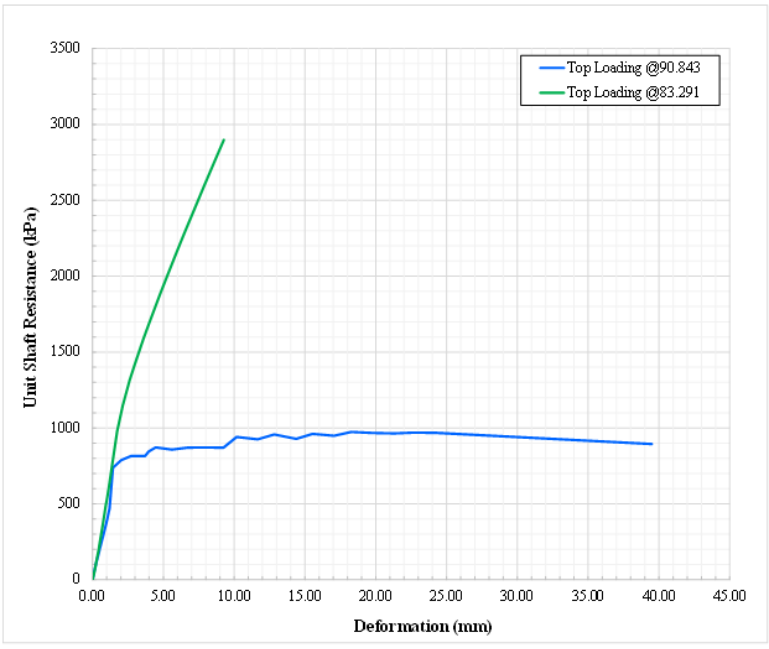

Figure 6.11. Calculated t-z curves for top-down loading of test pile 1.

In order to check t-z curves whether or not they are reasonable, piles were back-analyzed in Allpile software (Allpile Manual, 2015). Allpile is a software used for pile capacity calculation. In order to construct t-z curves load settlement behavior which is

given in Figure 6.12 below is also modelled in Allpile software by calibrating soil data based on parameters given in Table 6.3.

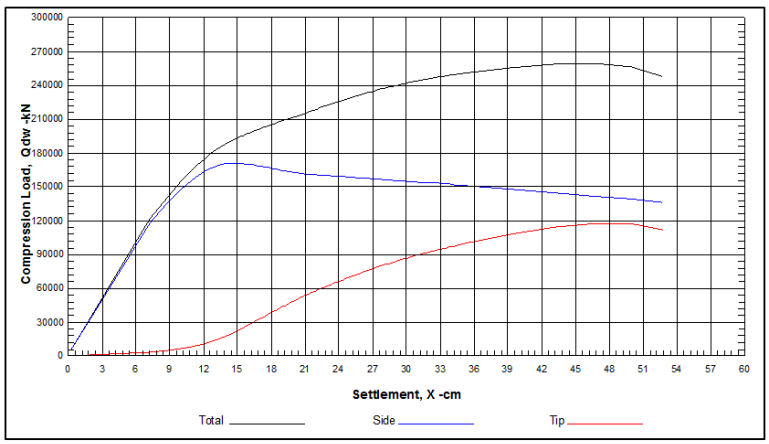

Figure 6.12. Calculated load-settlement behaviour for top-down loading of test pile 1 in Alpine software.

After match is obtained between measured load-settlement and calculated load-settlement behavior, t-z curves are constructed by using Allpile software in order to check the consistency of modelled t-z curves in Plaxis software for calibrated parameters. t-z curves constructed in Allpile is shown in Figure 6.13 below. t-z curves for weak substrata shows slightly higher values than measured with plaxis; on the other hand for strong limestone layer, calculated t-z behaviour are less than found in Plaxis analysis.

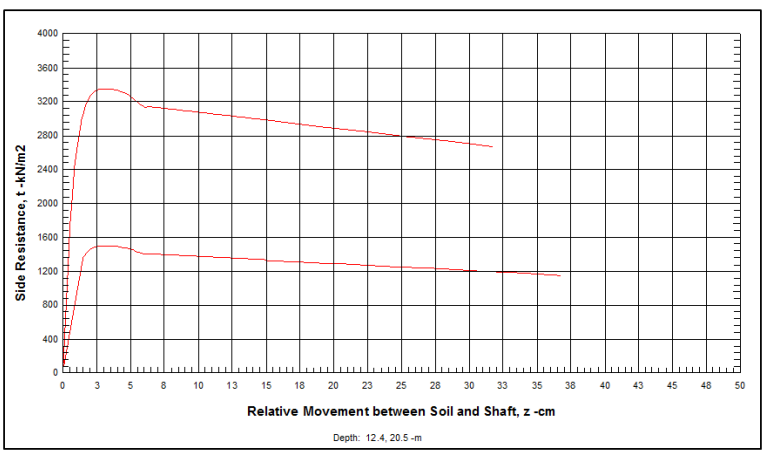

Figure 6.13. t-z curves from Allpile for verification top-down loading of test pile 1.

q-z curves are also evaluated both for top loading and O-cell loading in Figure 6.14. Observed behaviour are compared both for each other and for field measured data and results. Actually there is not a specific data obtained for q-z evaluation. This data is obtained by interpretation of toe telltale readings with respect to transferred end bearing load. Transferred end bearing load is calculated for each loading stage, by obtaining measured unit skin friction value between O-cell level and strain gauge level and using it for lower part (below O-cell part) shaft friction load and subtracting it from the applied load. It is important to note that unit skin friction value and thus the end bearing value is closely related with the strain gauge data. If any creep in soil during testing or tension forces occurred during concrete curing is observed these values may change misleading values. Therefore, using more than one level of strain gauges may show more accurate results.

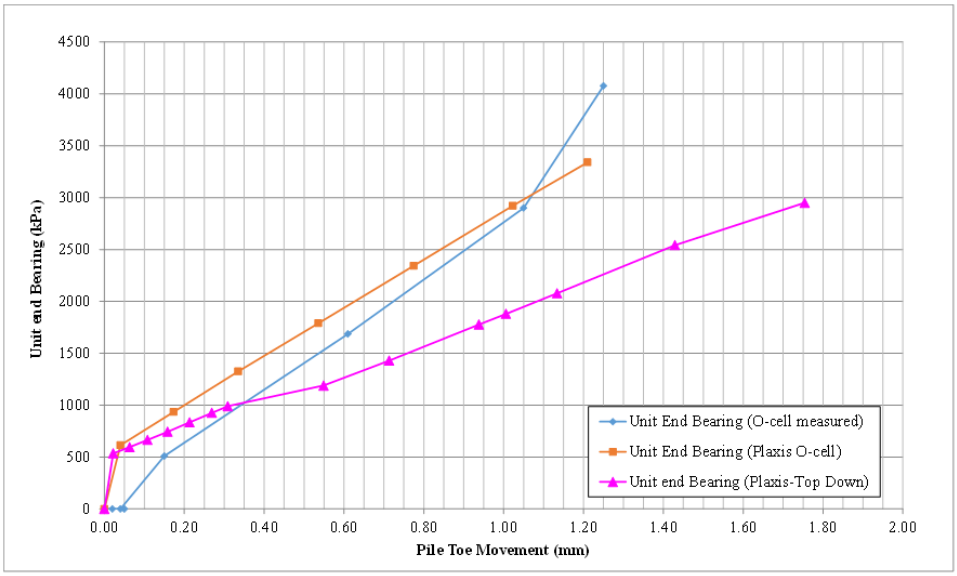

Figure 6.14. Measured and calculated q-z curves for test pile 1.

6.2. Case Study 2

Test pile is socketed into limestone. The sub-surface stratigraphy at the general location of the test pile is reported to consist of sands and stiff clay. Below these strata, limestone was encountered. Diameter of test pile is 1200 mm and it is excavated from top level of 130.45 m to the tip elevation of 103.8 m under water table. The pile was

started with a 1305 mm O.D. casing. After cleaning the base, the reinforcing cage with attached O-cell assembly was inserted into the excavation and temporarily supported from the steel casing. Concrete was then delivered by tremie through a 250 mm O.D. pipe into the base of the pile until the top of the concrete reached an elevation of +129.90 m

The loading assembly consisted of two 540 mm O-cells, located 0.59 meters above the toe of pile which is very close to end of pile. Calibration of O-cells was performed by an independent corporation up to 11.1 MN before they were delivered to site.

Three Linear Vibrating Wire Displacements which were placed between lower and upper plates of O-cell; two telltale casings and rods extending from the top of the O-cell assembly to top of concrete; two level of two sister bar vibrating wire strain gauges which were attached to the reinforcement cage below and above of O-cell assembly were used for instrumentation.

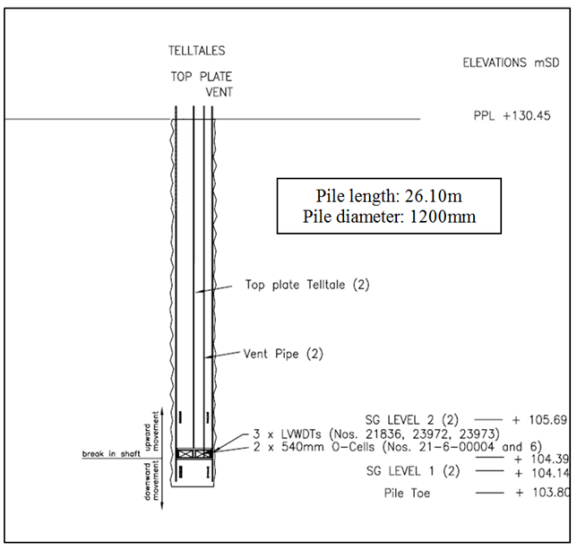

Figure 6.15. As built schematic section of instrumented test pile 2.

Load to O-cells were applied in 8 equal increments to 14330kN of bi-directional gross load. Unloading was then performed in four decrements and the test was concluded. Each successive load increment was maintained constant for 30 minutes while automatically maintaining the O-cell pressure constant. Loading stages are given below

in Table 6.5.

Table 6.5. Loading stages and loads applied during testing of test pile 2.

Loading Stages	**Loads (MN)**	**Loads Applied to Plaxis (kPa)**
1L-1	1.83	1618.08
1L-2	3.62	3200.78
1L-3	5.4	4774.65
1L-4	7.19	6357.36
1L-5	8.97	7931.22
1L-6	10.76	9513.93
1L-7	12.54	11087.79
1L-8	14.33	12670.5

The maximum downward applied load was 14.33 MN which occurred at load interval 1L-8 where the average downward movement of the O-cell base was measured as 44.2 mm. The maximum upward applied net load to the upper skin friction was 13.79 MN which occurred at load interval 1L-8 where the average upward movement was calculated as 2.4 mm. Table 6.6 below shows the measured unit skin frictions for both upper and lower part of pile and unit end bearing under maximum load.

Table 6.6. Average net unit skin friction values under maximum load measured in field O-cell load test pile 2.

Load Transfer Zone	**Displacement***	**Net Mobilised Unit Side Shear****
Zero Shear to Strain Gauge Level 2	↑ 1.08 mm	108 kPa
Zero Shear to O-cell	↑ 2.29 mm	802 kPa
O-cell to Strain Gauge Level 1	↓ 44.14 mm	6309*** kPa
*Average displacement of load transfer zone.		
** Applied upward load is the net load which is equal to buoyant weight of upper segment of pile.		
*** Misleading value		

According to constructed equivalent top down curve based on test results, test pile behavior has been analyzed for a combined skin friction and end bearing load of 26.0 MN. For a top loading of 16.0 MN, the adjusted test data indicated this pile would settle approximately 10.2 mm of which 7.5 mm is estimated elastic compression. For a top loading of 24.0 MN the adjusted test data indicate this pile would settle approximately 18.4 mm of which 11.4 mm is estimated elastic compression.

6.2.1. Modelling of O-cell Test for Case 2 with Plaxis

Before analyzing data closest soil profile is investigated and selected with appropriate soil parameters. Figure 6.16 below illustrates the soil profile and parameters provided by local authorities in their soil investigation report is presented below in Table 6.7.

Table 6.7. Soil parameters for test pile 2 reported in soil report.

Soil Unit	**Soil Definition**	**Modulus of Deformation E (MPa)**	**Unit Weight (kN/m^3)**	**Measured Cohesion (kPa)**	**Measured Internal Friction Angle (^{o})**
1	Medium dense sand	30.0	18.0	1.0	33.0
2	Hard clay	20.0	18.0	45.0	25.0
3	Stiff clay with marl	70.0	20.0	45.0	17.0
4	Limestone and dolomite with clay	400.0	22.0	300.0	20.0
5	Dense dolomite	550.0	23.0	400.0	22.0

Analyses has started with the parameters given in Table 6.7 and an axisymmetric model is formed changed accordingly until a good match between site measured and numerically measured load movement data is obtained. Analysis model constructed in Plaxis software (Plaxis 2D Manuals, 2017) is given in Figure 6.17. Final parameters that obtained at the end of analysis are given below in Table 6.8.

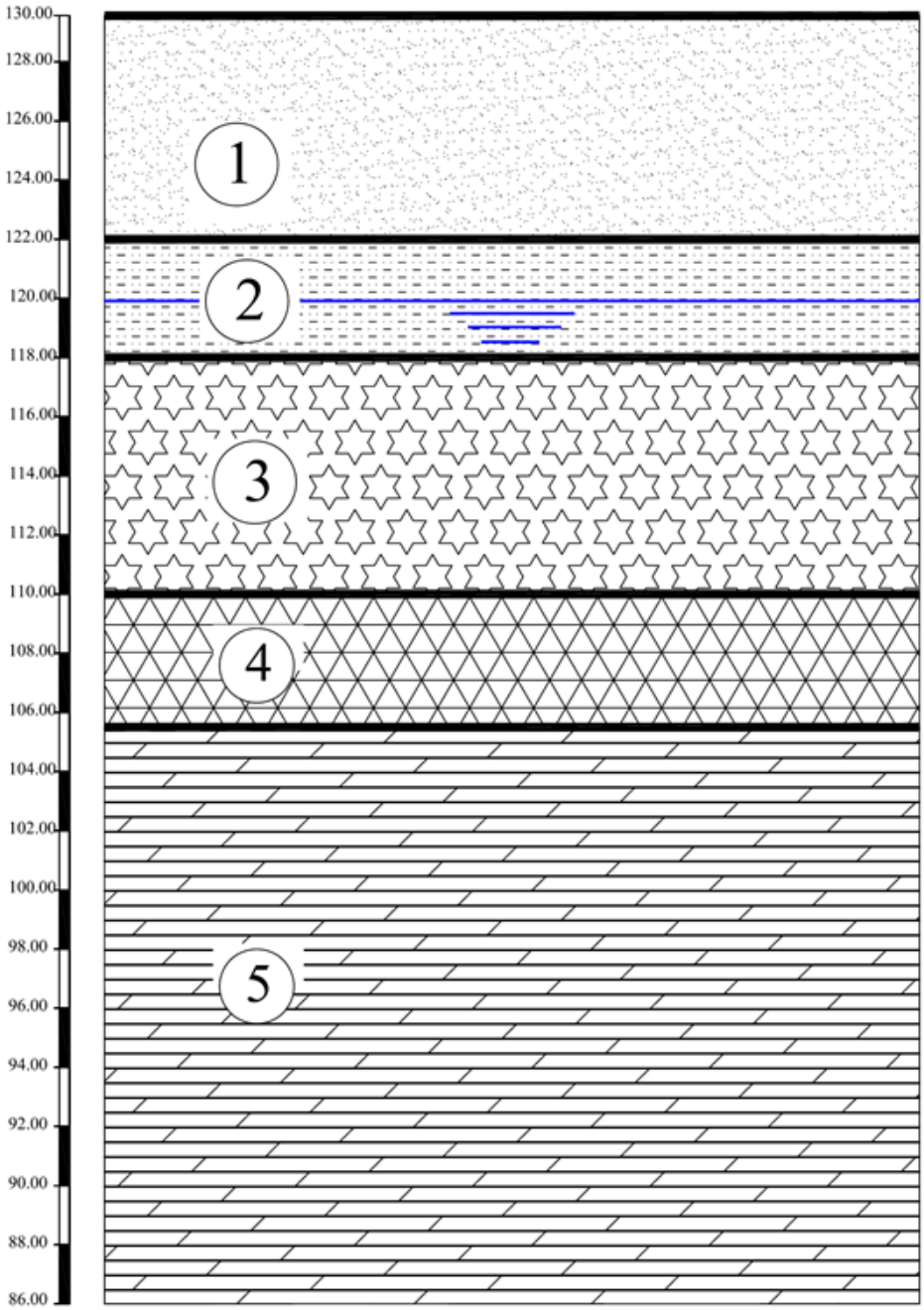

Figure 6.16. Soil profile of test location for test pile 2.

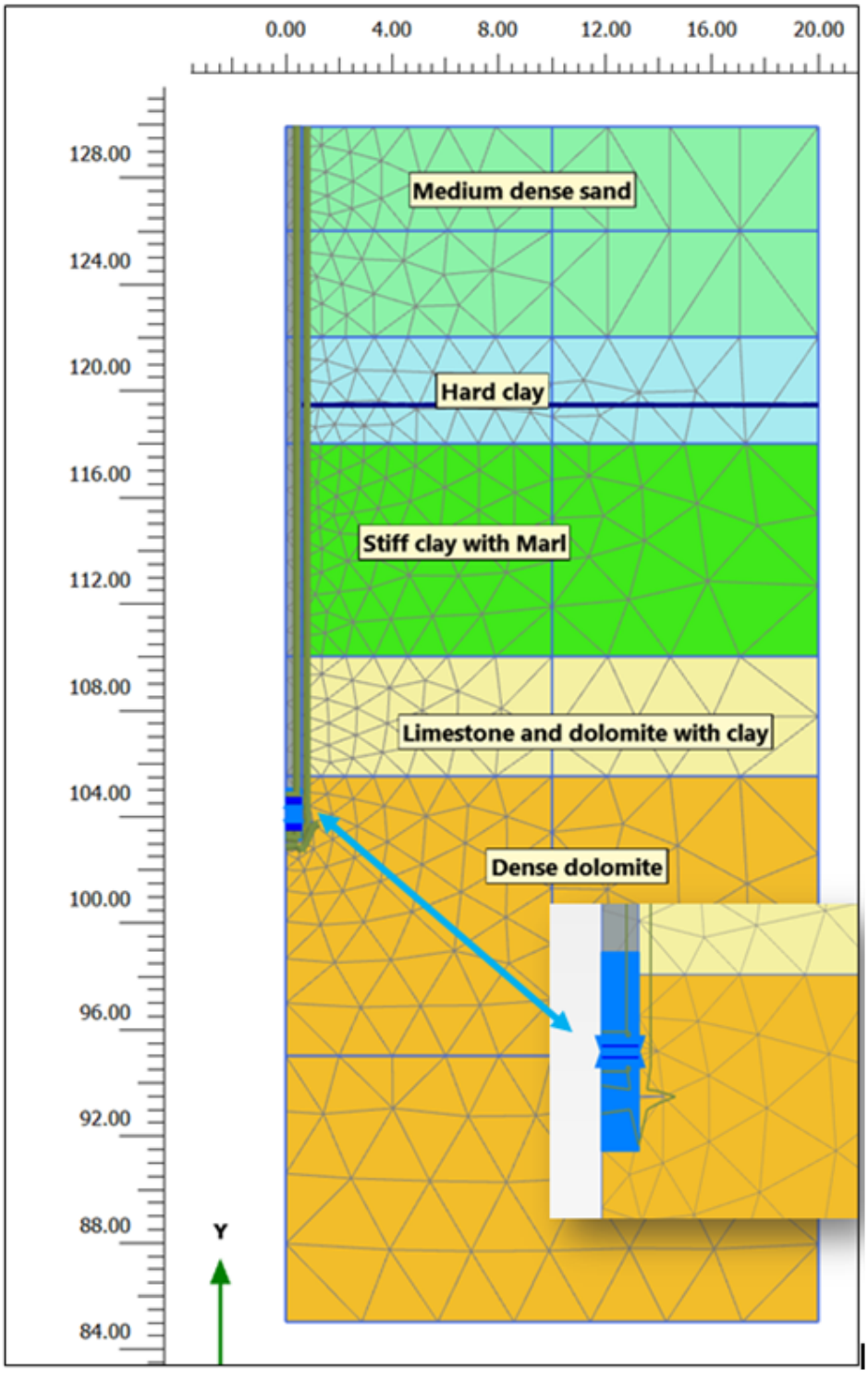

Figure 6.17. Model view of test pile 2.

Table 6.8. Soil parameters for test pile 2 found as a result of back analysis.

Soil Definition	**Medium dense sand**	**Hard clay**	**Stiff clay with marl**	**Limestone and dolomite with clay**	**Dense dolomite**	**Concrete**
Soil Unit	1	2	3	4	5	-
Material Model	Hardening Soil	Hardening Soil	Mohr-Coulomb	Mohr-Coulomb	Mohr-Coulomb	Linear Elastic
Drainage Type	Drained	Drained	Drained	Drained	Drained	Non-porous
Unit Weight (kN/m^3)	18.0	18.0	20.0	22.0	23.0	24.0
Modulus of Deformation E^{50}_{ref} (MPa)	30	40	-		-	-
power (m)	0.5	1	-		-	-
Modulus of Deformation E' (MPa)	-	-	300	450	400	35000
Poisson ratio υ'	-	-	0.20	0.20	0.20	0.20
c' - Cohesion (kPa)	1.0	15.0	100.0	250.0	80.0	-
ϕ' - Internal Friction Angle (^{o})	35	27	27	40	40	-
ψ - Dilatancy Angle (psi)	5	-	10	10	10	-
Interface	1	1	1	1	1	1

6.2.2. Results of Back Analysis for Case 2

As it is mentioned before, back analysis of field test is mainly conducted by optimizing parameters until a good and reasonable match is obtained with the measured and calculated load settlement behaviour of pile. When this match is achieved, strain gauge data are evaluated whether or not the analysis model satisfies the field-measured data. Actually for load settlement behaviour, the dominant parameter is the elasticity modulus. When strain gauge data, hence the unit shaft friction values come into the stage, this time internal friction angle and cohesion values are calibrated so that it matches with field parameters. Figure 6.18 shows the comparison between measured and calculated load-settlement behaviour of pile generated during O-cell test. This part is the key element of analysis since it gives the calibrated soil parameters presented in Table 6.8 for further investigation of pile for top-down analysis.

After a good match is obtained regarding both load-movement curves and two no's of strain gauge data provided, top-down loading is modelled with the same parameters in the same model to observe the behavior of pile under actual loading application.

Report provided by testing firm suggests an equivalent top-down curve, construction process of which is given in Chapter 5. This curve constructed by the test supervisors are compared with the one found in finite element analysis in Figure 6.19. By using calibrated soil parameters equivalent top-down curve is constructed by applying same load on top of pile. It is expected that a closest match should be obtained between this graph and calculated top-down curve.

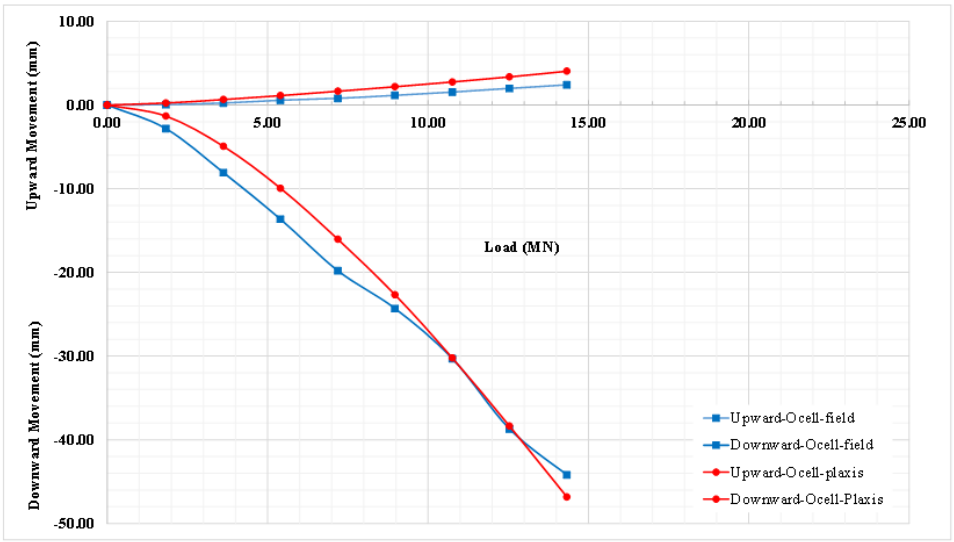

Figure 6.18. Measured and calculated load settlement curves for O-cell loading test pile 2.

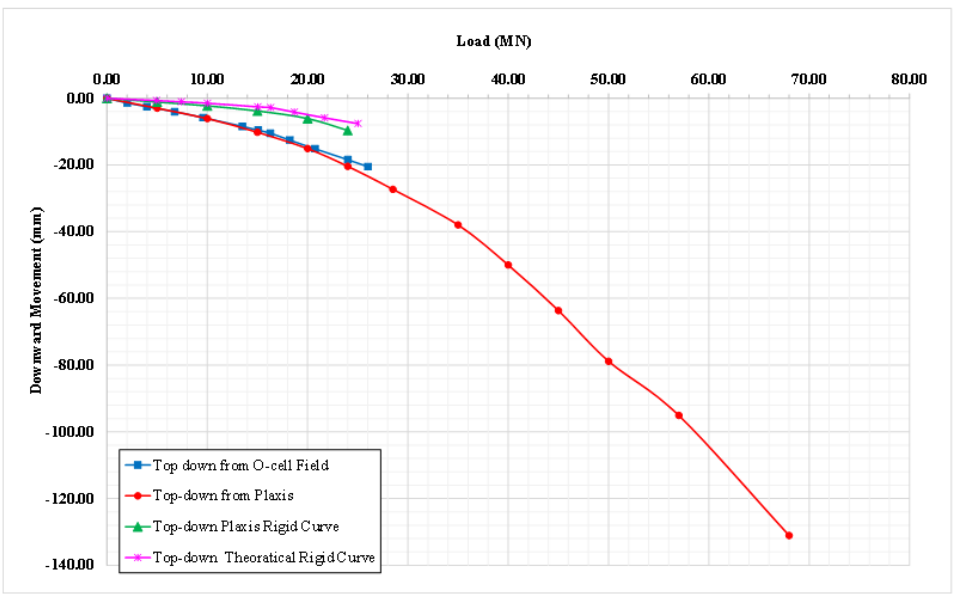

Figure 6.19. Measured and calculated load settlement curves for top-down loading.

After matching load-settlement graphs of both loading types, load-distribution graphs are obtained in order to see how the load is distributed along the shaft length of pile in two loading cases which are O-cell loading and top-down loading. During field O-cell testing, strain gauge reading s were recorded to obtain the shaft friction value of limestone and dolomite layers. Strain gauge measurements which were transformed into load values are used to compare assumed distribution in load test report with the ones obtained in numerical analysis. Since the number and level of strain gauges are inadequate data obtained during this test only gives the shaft friction of limestone layer.

Figure 6.20 and Figure 6.21 below illustrates load distribution behavior of pile in case of O-cell loading for both field measurements and numerical analysis and in case of top-down loading respectively. Pile load distribution curves are followed by analysis of unit shaft friction comparison for measured and numerically calculated O-cell loading and for top-down loading respectively in Figure 6.22 and Figure 6.23.

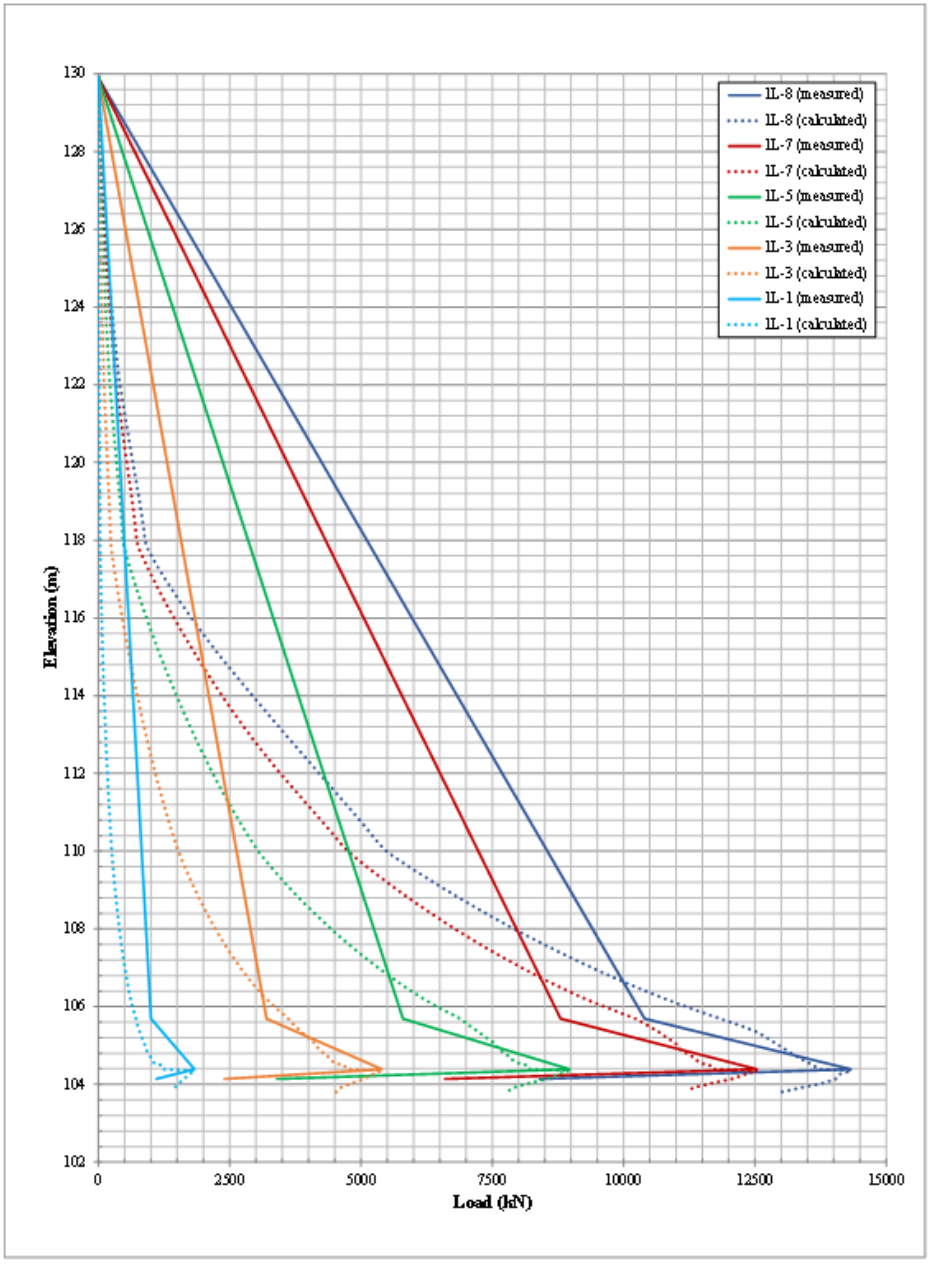

Figure 6.20. Comparison of load distribution curves for O-cell loading obtained from field measurements and numerical analysis of test pile 2.

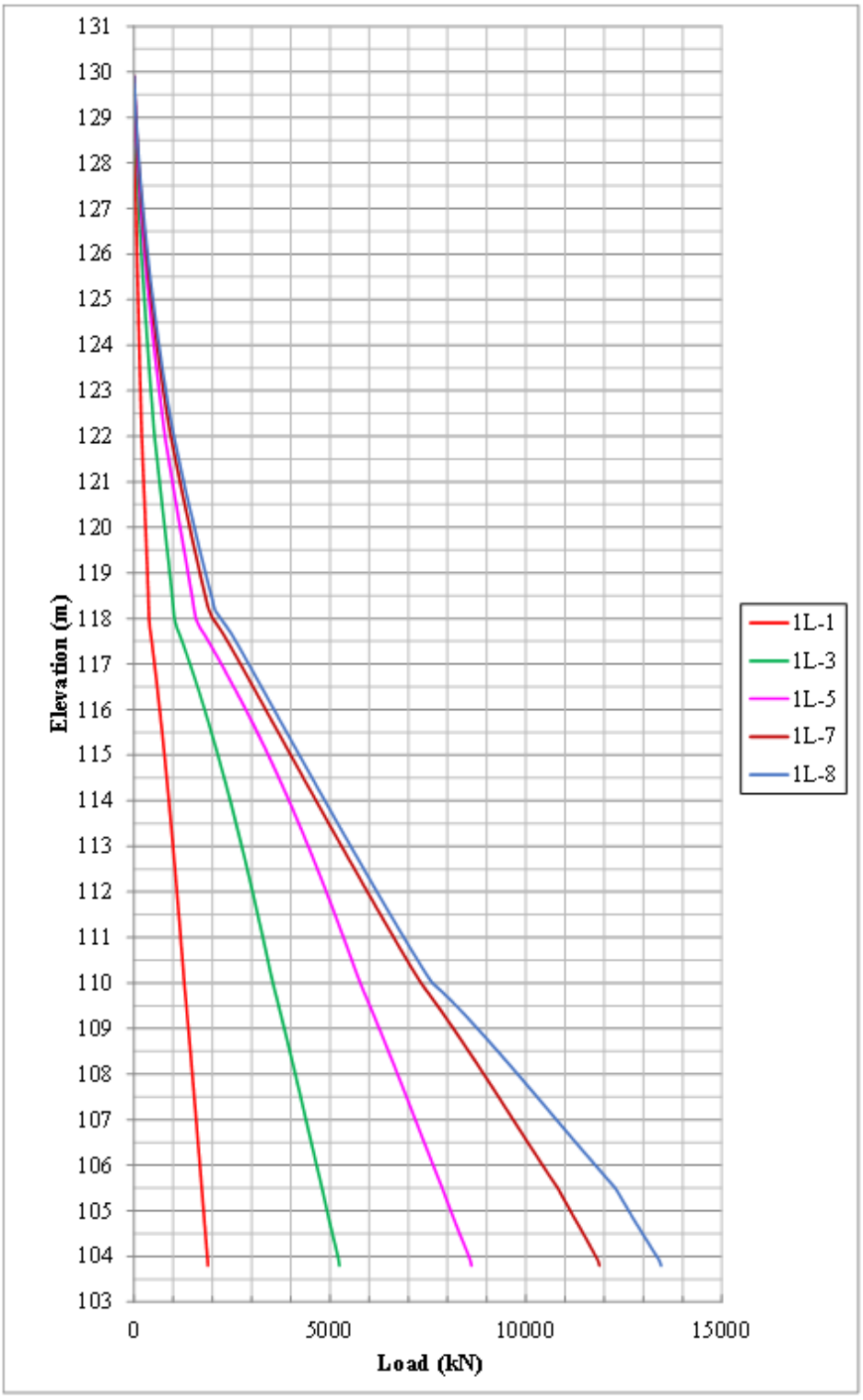

Figure 6.21. Load distribution curves for top-down loading obtained from numerical analysis of test pile 2.

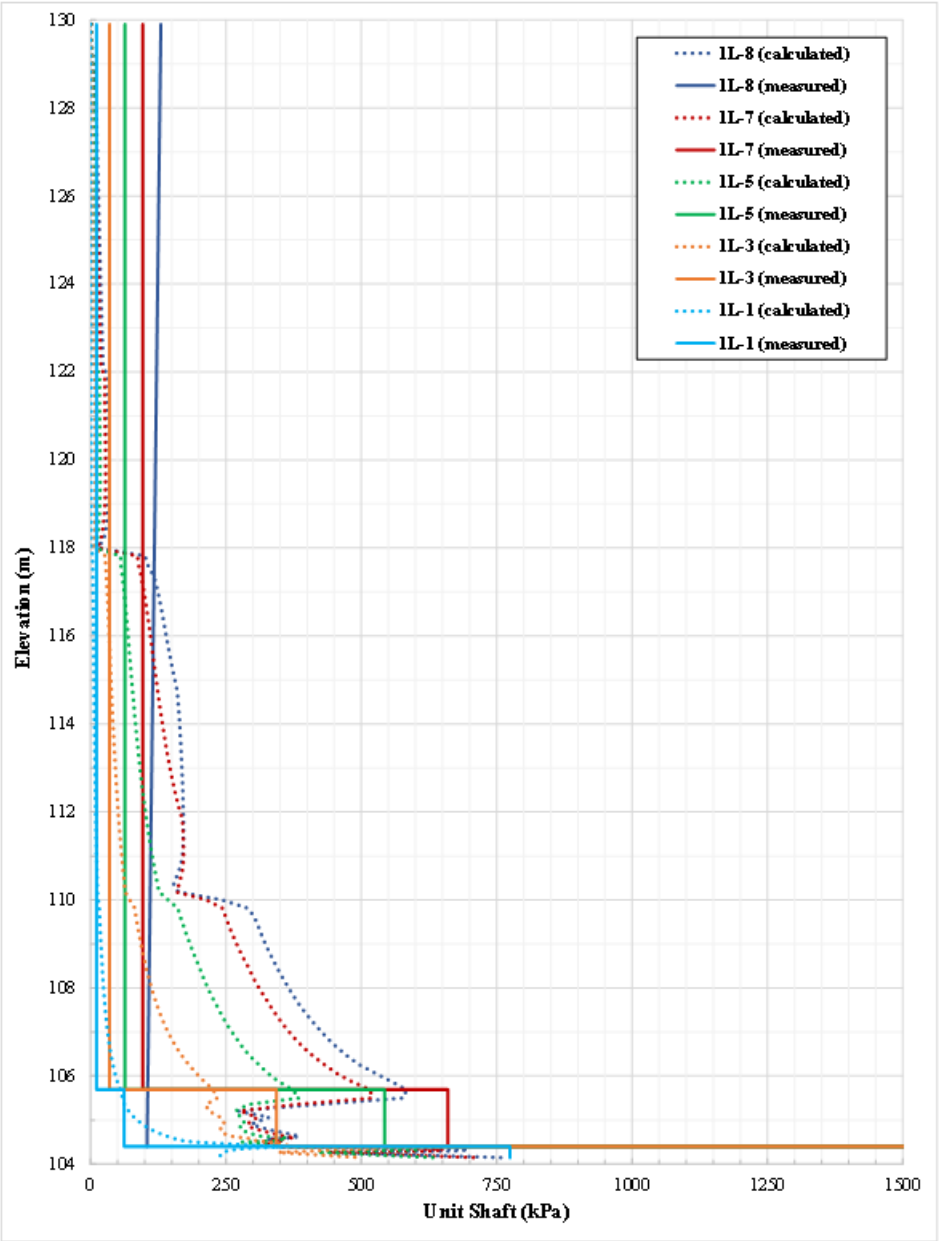

Figure 6.22. Comparison between measured and calculated unit skin friction values along length of test pile 2.

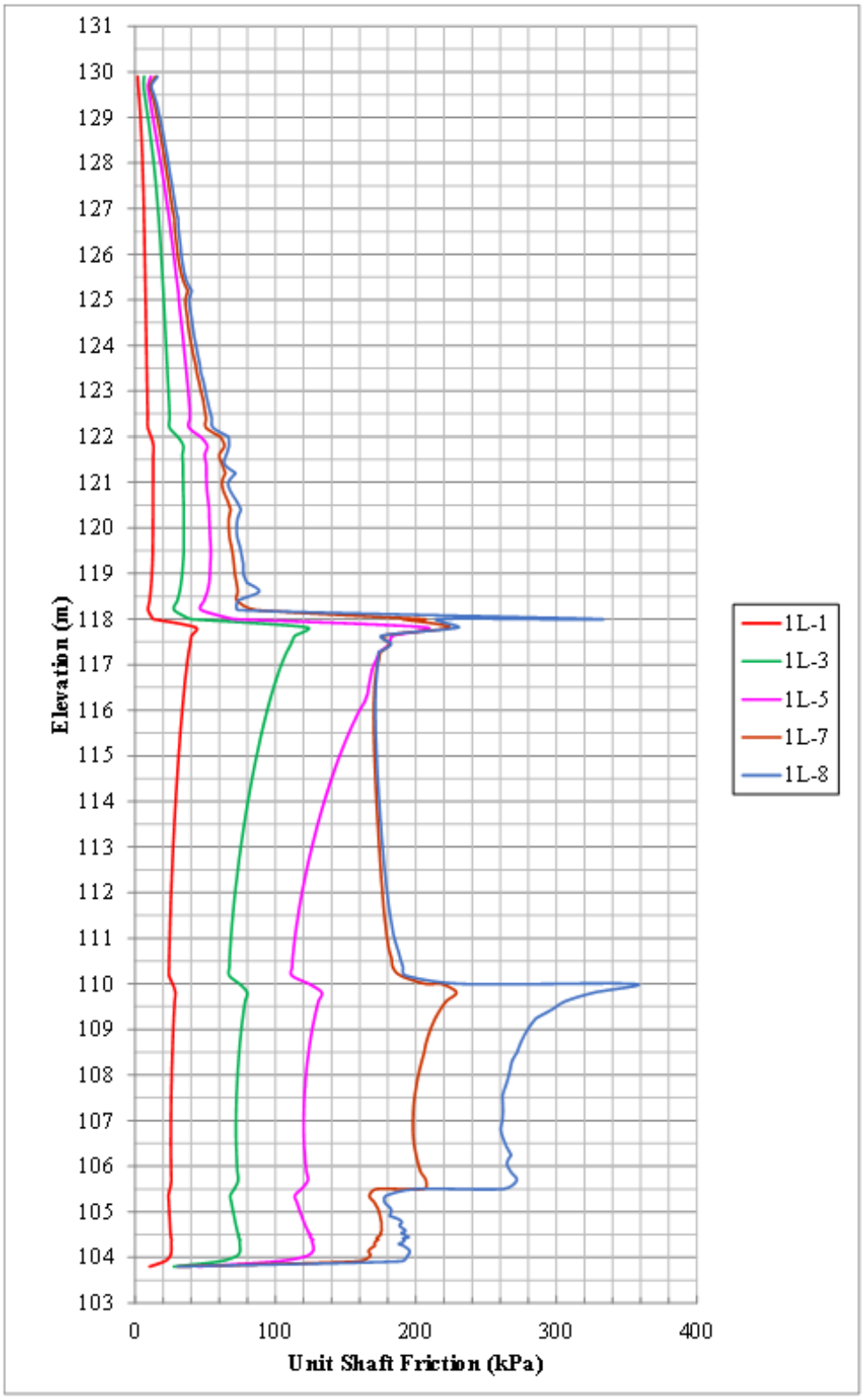

Figure 6.23. Distribution of unit skin friction values for top-down loading obtained from numerical analysis of test pile 2.

In Figure 6.20 it is observed that between O-cell level of 104.39 m and pile top level of 129.90m measured shaft load during testing is not true for determined pile load behavior. This is because of the fact that there is only one level of strain gauge data between O-cell level and top level and close to O-cell level. For the upper pile segment of 24.20m this level of strain gauge is inadequate to observe its behavior. Moreover, there exists one level of strain gauge under O-cell; however it is too close to O-cell level. When data is observed together with analyzed data it is clearly seen that it is too high than the value it should be. Hence it is not contributed to finite element analysis. On the other hand, load distribution curves constructed for top-down loading which is shown on Figure 6.21 shows very similar load transfer mechanism for same load.

Further observations are conducted for unit shaft friction comparison between measured and calculated data. Since strain gauge data under O-cell level is misleading and measured too high in field test, therefore shaft friction values found in analysis shows difference from the measured ones. This behavior is clearly seen from Figure 6.22. After observing unit shaft friction distribution for O-cell testing, shaft friction distribution for top-down loading case is investigated and results are shown in Figure 6.23. When two figures are compared, it is observed that magnitude of maximum unit shaft frictions are close to each other but locations where they occur are different under same loads.

In addition to above explained findings, in the light of constructed pile load behavior and calibrated parameters t-z curves are generated for both top-loading and O-cell loading which are presented in Figure 6.24. Two levels are selected for investigation purpose above and below O-cell level. Upper part shows closer match between O-cell loading and top-down loading; whereas lower part shows more deformation under lower loads in O-cell loading. This is mainly due to location of O-cell which is closer to end of pile especially placed to see the shaft friction of only limestone formation. Figure 6.25 shows ultimate t-z curves for top-down loading. Blue curve represents ultimate capacity of skin friction capacity for weak limestone layer whereas green curve representing limestone layer under O-cell level do not show failure yet.

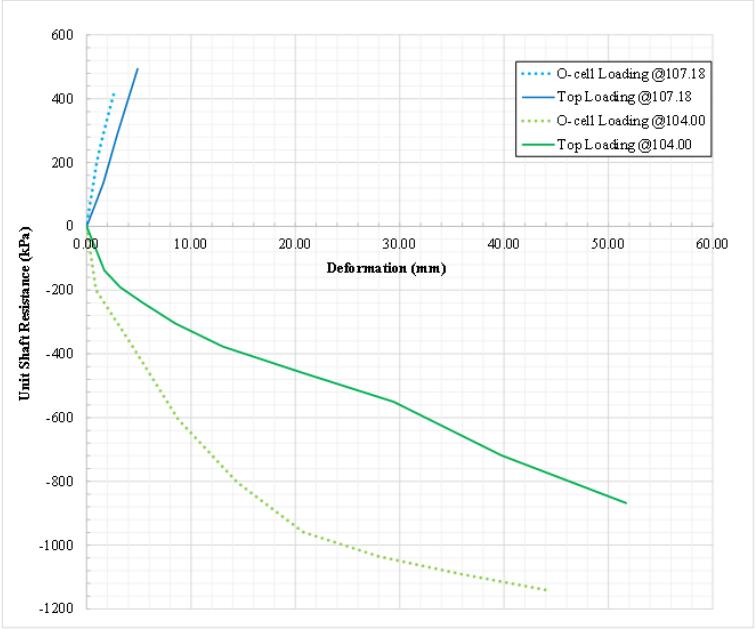

Figure 6.24. Comparison of calculated t-z curves for O-cell and top-down loading of test pile 2.

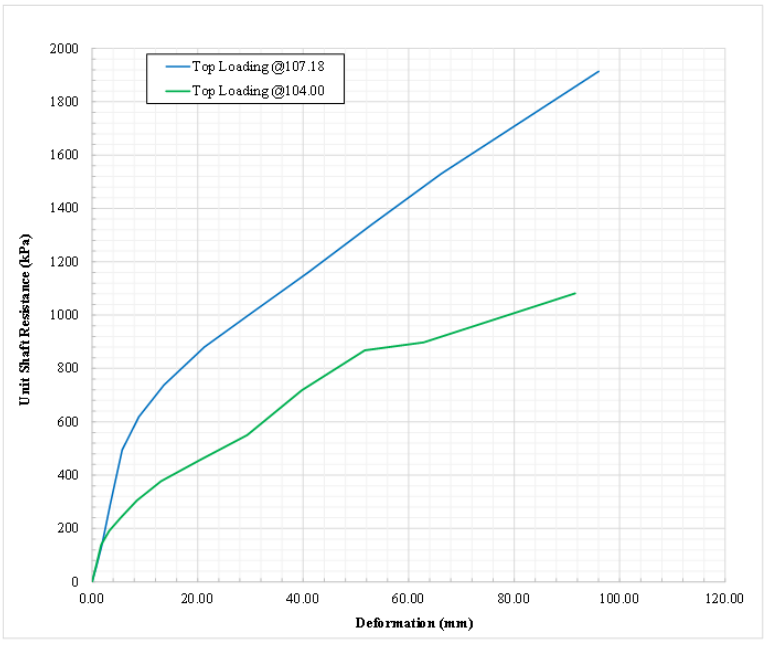

Figure 6.25. Calculated t-z curves for top-down loading of test pile 2.

In order to check t-z curves whether or not they are reasonable, piles were back-analyzed in Allpile software (Allpile Manual, 2015). In order to construct t-z curves load settlement behavior which is given in Figure 6.26 below is also modelled in Allpile

software by calibrating soil data based on parameters given in Table 6.7.

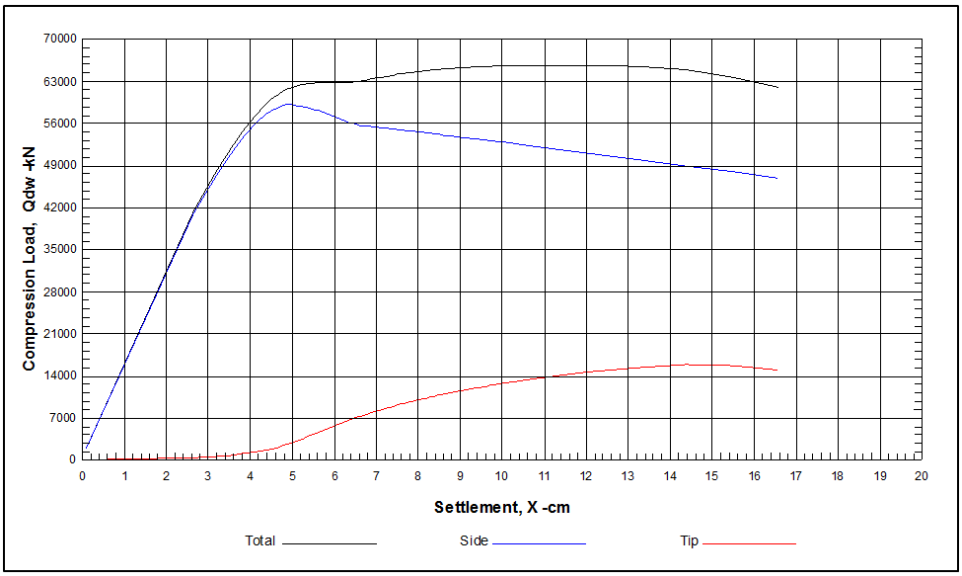

Figure 6.26. Calculated load-settlement behaviour for top-down loading in Allpile software for test pile 2.

After match is obtained between measured load-settlement and calculated load-settlement behavior, t-z curves are constructed by using Allpile software in order to check the consistency of modelled t-z curves in Plaxis software for calibrated parameters. t-z curves constructed in Allpile is shown in Figure 6.27 below. They show very similar behavior to the one constructed with the analysis performed via Plaxis.

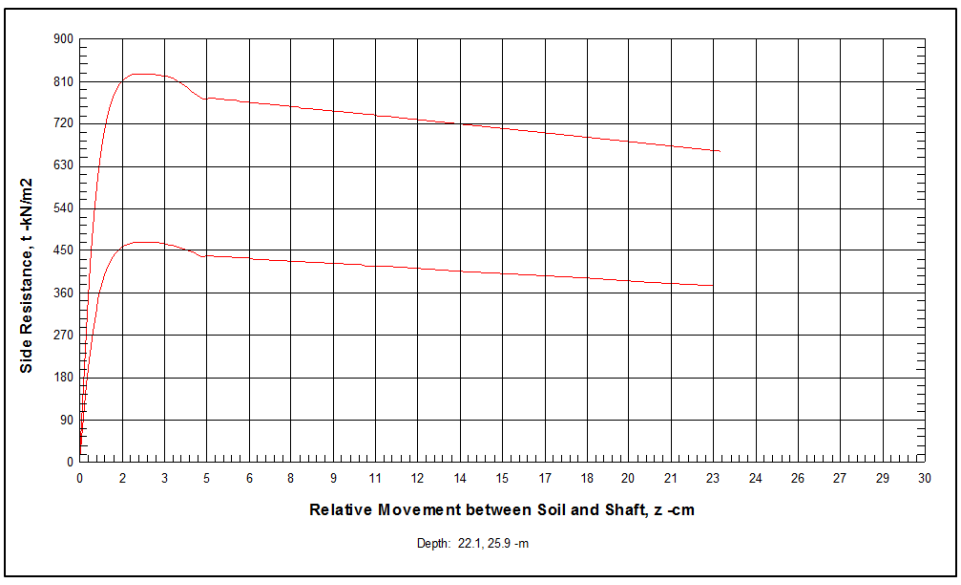

Figure 6.27. t-z curves from Allpile for verification top-down loading of test pile 2.

q-z curves are also evaluated both for top loading and O-cell loading in Figure 6.28. Observed behaviour are compared both for each other and for field measured data and results. In this test pile no telltale is placed at the bottom of pile because O-cell level is only 0.5m above pile toe. In other words, O-cell is placed to see the pile tip behaviour in dolomite-limestone formation. Therefore, downward applied O-cell load and downward movement of pile is directly taken into account for measured q-z behaviour. Results show nearly perfect match between measured and calculated O-cell q-z behaviour. However top-loading case shows a little bit different behaviour like in first test pile 1. In top-loading it gives more tip deformation under same unit end bearing.

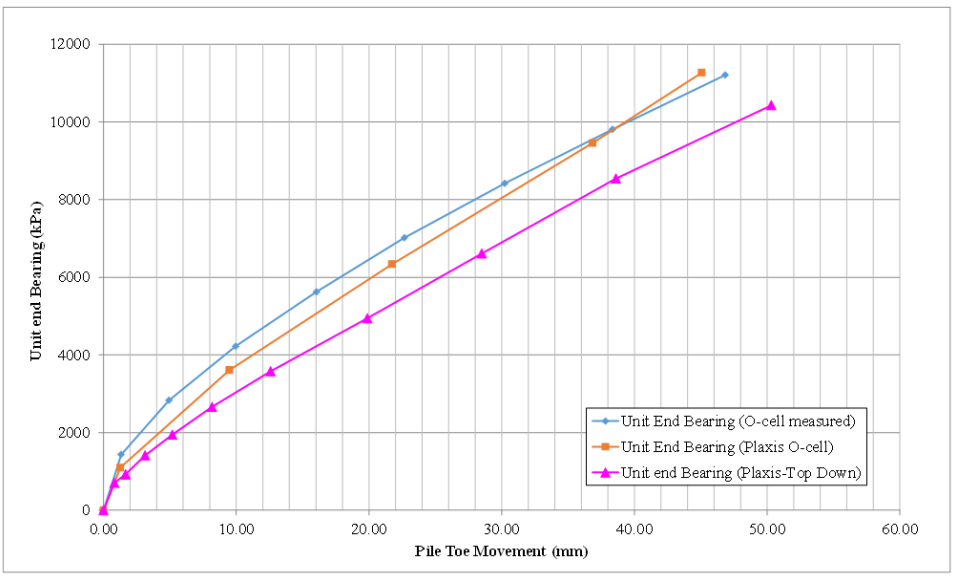

Figure 6.28. Measured and calculated q-z curves for test pile 2.

6.3. Case Study 3

Test pile is socketed into limestone. The sub-surface stratigraphy at the general location of the test pile is reported to consist of marly hard clay underlain by limestone was encountered. Diameter of test pile is 1500 mm and it is excavated from top level of 116.0 m to the tip elevation of 93.56 m under water table. The pile was started with a 1600 mm O.D. casing. After cleaning the base, the reinforcing cage with attached O-cell assembly was inserted into the excavation and temporarily supported from the

steel casing. Concrete was then delivered by tremie through a 250 mm O.D. pipe into the base of the pile until the top of the concrete reached an elevation of +116.0 m

The loading assembly consisted of three 610 mm O-cells, located 3.94 metres above the toe of pile. Calibration of O-cells was performed by an independent corporation up to 13.60 MN before they were delivered to site. Three upper compression telltale casings and rods extending from the top of the O-cell assembly to top of concrete, three pile toe displacement telltale casings and rods extending from the bottom of the reinforcing cage to the ground level, three embedded compression telltale casings and rods located below O-cell assembly, four Linear Vibrating Wire Displacement Transducer which were placed between lower and upper plates of O-cell, seven levels of four sister bar vibrating wire strain gauges which were attached to the reinforcement cage below and above of O-cell assembly were used for instrumentation.

Load to O-cells were applied in 14 equal increments to 56010 kN of bi-directional gross load. Unloading was then performed in four decrements and the test was concluded. Each successive load increment was maintained constant for 30 minutes while automatically maintaining the O-cell pressure constant. Loading stages are given below in Table 6.9.

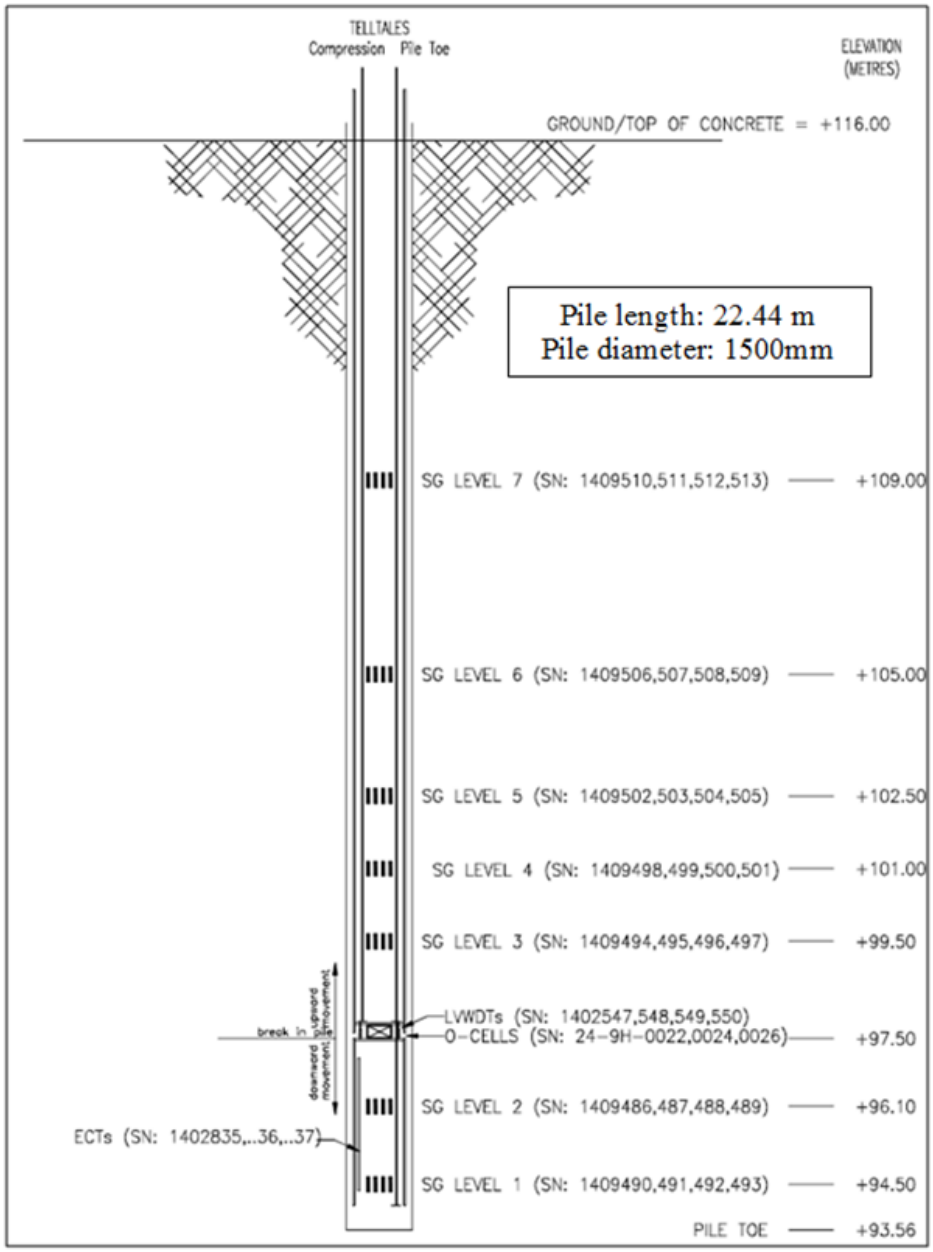

Figure 6.29. As built schematic section of instrumented test pile 3.

Table 6.9. Loading stages and loads applied during testing for test pile 3.

Loading Stages	**Loads (MN)**	**Loads Applied to Plaxis (kPa)**
1L-1	4.06	2297.49
1L-2	8.02	4538.39
1L-3	12.03	6807.59
1L-4	16.08	9099.42
1L-5	20.04	11340.32
1L-6	24.05	13609.52
1L-7	28.05	15873.05
1L-8	32.06	18142.25
1L-9	36.02	20383.15
1L-10	40.03	22652.35
1L-11	44.08	24944.18
1L-12	47.98	27151.13
1L-13	52.01	29431.64
1L-14	56.01	31695.18

The maximum downward applied load was 56.01 MN which occurred at load interval 1L-14 where the average downward movement of the O-cell base was measured as 9.89 mm. The maximum upward applied net load to the upper skin friction was 55.54 MN which occurred at load interval 1L-14 where the average upward movement was calculated as 44.73 mm. Table 6.10 below shows the measured unit skin frictions for both upper and lower part of pile and unit end bearing under maximum load.

Table 6.10. Average net unit skin friction values under maximum load measured in field O-cell load test pile 3.

Load Transfer Zone	**Displacement***	**Net Mobilised Unit Side Shear**
Zero Shear to Strain Gauge Level 7	↑ 28.7 mm	366 kPa
Strain Gauge Level 7 to Strain Gauge Level 6	↑ 30.9 mm	908 kPa
Strain Gauge Level 6 to Strain Gauge Level 5	↑ 33.9 mm	454 kPa
Strain Gauge Level 5 to Strain Gauge Level 4	↑ 36.5 mm	1925 kPa
Strain Gauge Level 4 to Strain Gauge Level 3	↑ 39.1 mm	327 kPa
Strain Gauge Level 3 to O-cell	↑ 42.6 mm	446kPa
O-cell to Strain Gauge Level 2	↓ 9.8 mm	5386 kPa
Strain Gauge Level 2 to Strain Gauge Level 1	↓ 9.3 mm	1544 kPa
* Average displacement of load transfer zone.		

According to constructed equivalent top down curve based on test results, test pile behavior has been analyzed for a combined skin friction and end bearing load of 56.01 MN. For a top loading of 27.0 MN, the adjusted test data indicated this pile would settle approximately 10.1 mm. For a top loading of 40.50 MN the adjusted test data indicate this pile would settle approximately 15.3 mm.

6.3.1. Modelling of O-cell Test for Case 3 with Plaxis

Before analyzing data closest soil profile is selected with appropriate soil parameters. Figure 6.30 below illustrates the soil profile and parameters provided by local authorities in their soil investigation report is presented below in Table 6.11.

Table 6.11. Soil parameters for test pile 3 reported in soil reports.

Soil Unit	**Soil Definition**	**Modulus of Deformation E (MPa)**	**Unit Weight (kN/m^3)**	**Measured Cohesion (kPa)**	**Measured Internal Friction Angle (^{o})**
1	Dolomitic limestone	440	21	2370	47
2	Marly clay	280	20	1700	36
3	Solid clay	340	20	810	30
4	Weak limestone	810	22	2360	37
5	Limestone	930	24	6040	50

Analyses has started with the parameters given in Table 6.11 and an axisymmetric model is formed changed accordingly until a good match between site measured and numerically measured load movement data is obtained. Analysis model constructed in Plaxis software (Plaxis 2D Manuals, 2017) is given in Figure 6.31. Final parameters that obtained at the end of analysis are given below in Table 6.12.

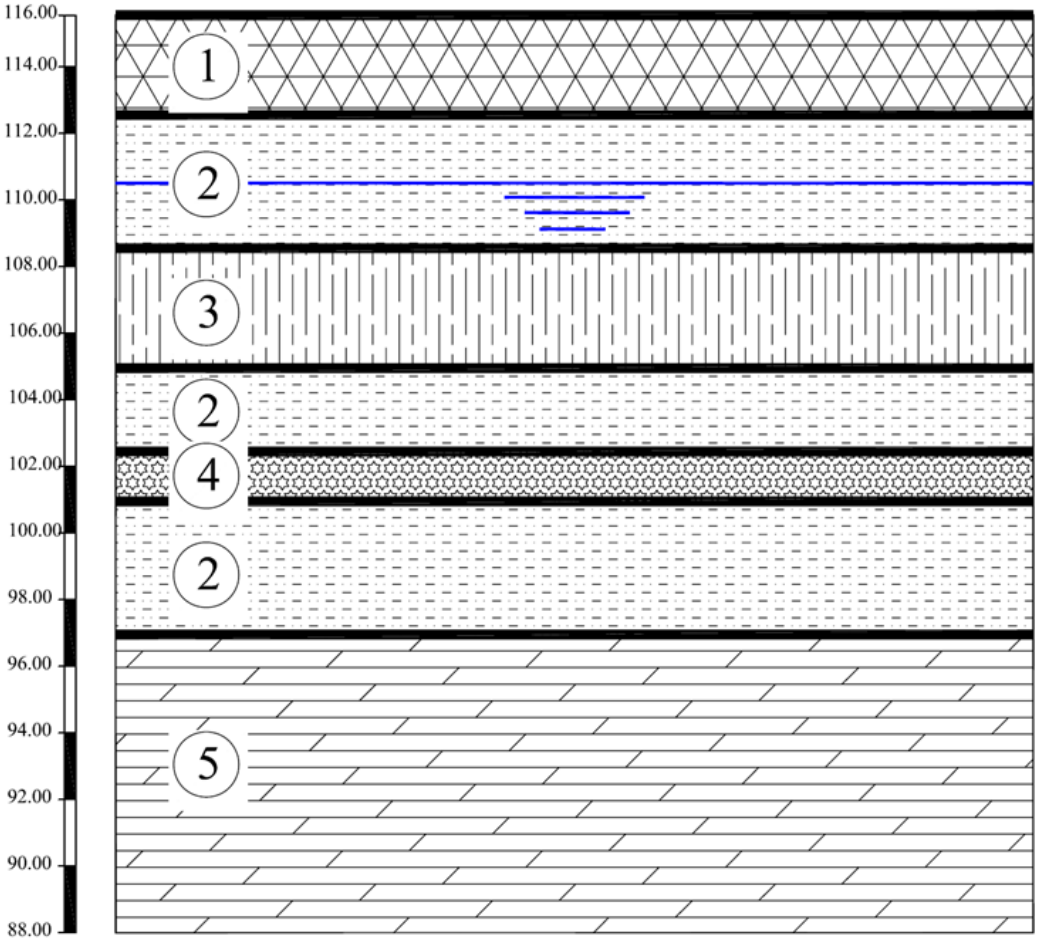

Figure 6.30. Soil profile of test location for test pile 3.

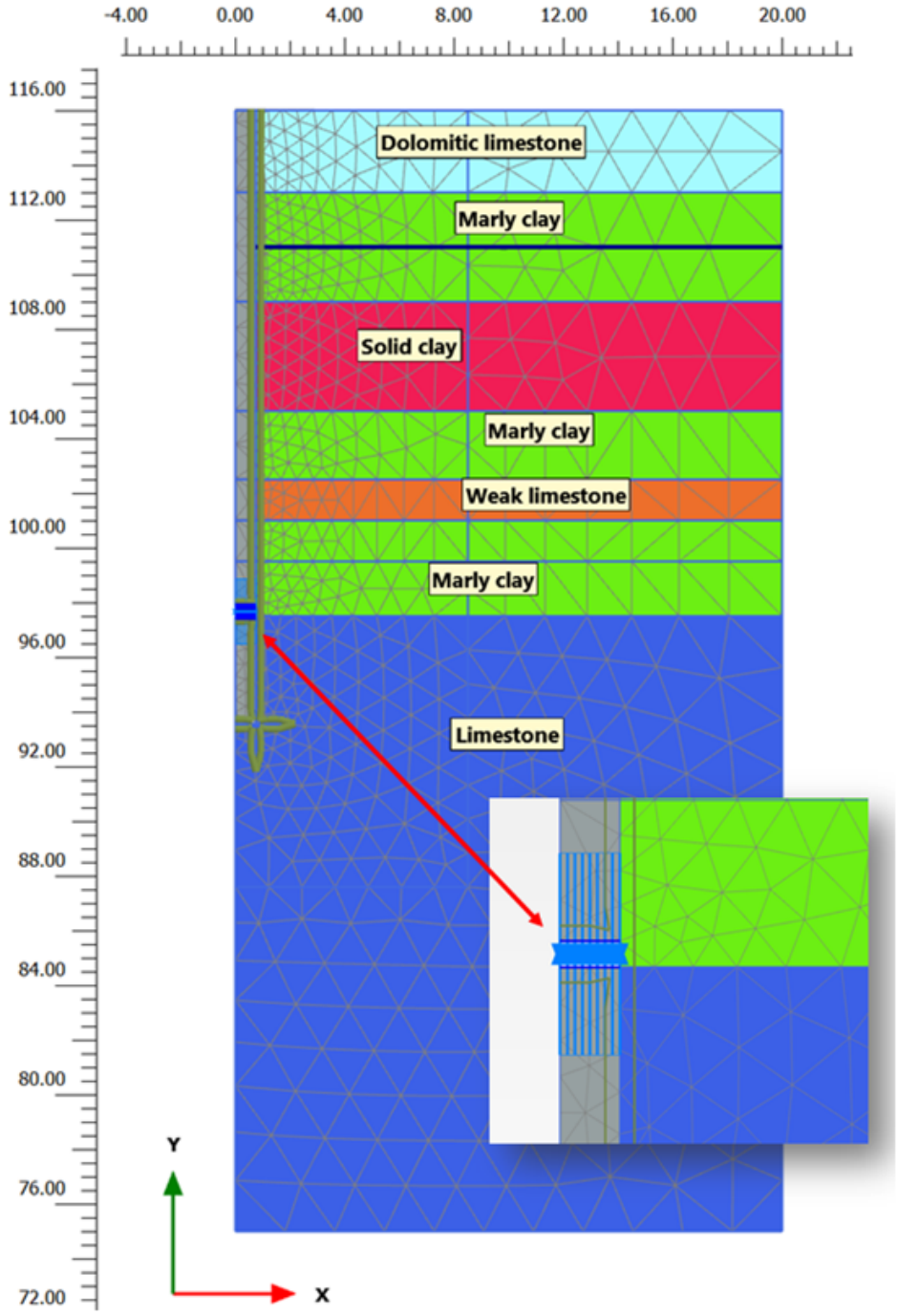

Figure 6.31. Model view of test pile 3.

Table 6.12. Soil parameters for test pile 3 found as a result of back analysis.

Soil Definition	**Dolomitic limestone**	**Marly clay**	**Solid clay**	**Weak limestone**	**Limestone**	**Concrete**
Soil Unit	1	2	3	4	5	-
Material Model	Mohr-Coulomb	Mohr-Coulomb	Mohr-Coulomb	Mohr-Coulomb	Mohr-Coulomb	Linear Elastic
Drainage Type	Drained	Drained	Drained	Drained	Drained	Non-porous
Unit Weight (kN/m^3)	21.0	19.0	19.0	22.0	24.0	24.0
Modulus of Deformation E' (MPa)	400	250	350	1000	1600	30000
Poisson ratio υ'	0.2	0.25	0.25	0.20	0.20	0.15
c' - Cohesion (kPa)	350.0	200.0	300.0	350.0	450.0	-
ϕ' - Internal Friction Angle (^{o})	40.0	32.0	35.0	40.0	52.0	-
ψ - Dilatancy Angle (psi)	10.0	2.0	5.0	10.0	12	-
Interface	1.0	1.0	1.0	1.0	1.0	1.0

6.3.2. 6.3.2. Results of Back Analysis for Case 3

Back analysis of field test is mainly conducted by optimizing parameters until a good and reasonable match is obtained with the measured and calculated load settlement behaviour of pile. When this match is achieved, strain gauge data are evaluated whether or not the analysis model satisfies the field-measured data. Actually for load settlement behaviour, the dominant parameter is the elasticity modulus. When strain gauge data, hence the unit shaft friction values come into the stage, this time internal friction angle and cohesion values are calibrated so that it matches with field parameters. Figure 6.32 shows the comparison between measured and calculated load-settlement behaviour of pile generated during O-cell test. This part is the key element of analysis since it gives the calibrated soil parameters presented in Table 6.12 for further investigation of pile for top-down analysis.

After a good match is obtained regarding both load-movement curves and strain

gauge data provided, top-down loading is modelled with the same parameters in the same model to observe the behavior of pile under actual loading application. Report provided by testing firm suggests an equivalent top-down curve, construction process of which is given in Chapter 5. This curve constructed by the test supervisors are compared with the one found in finite element analysis in Figure 6.33. By using calibrated soil parameters equivalent top-down curve is constructed by applying same load on top of pile. It is expected that a closest match should be obtained between this graph and calculated top-down curve. However this time top-down load-movement behavior obtained from Plaxis analysis and field measured data do not exhibit a close match; although load-movement curves obtained from both field and analysis for O-cell loading well suit with each other. This may be evaluated as misinterpretation of elastic behavior of constructed top-down curve.

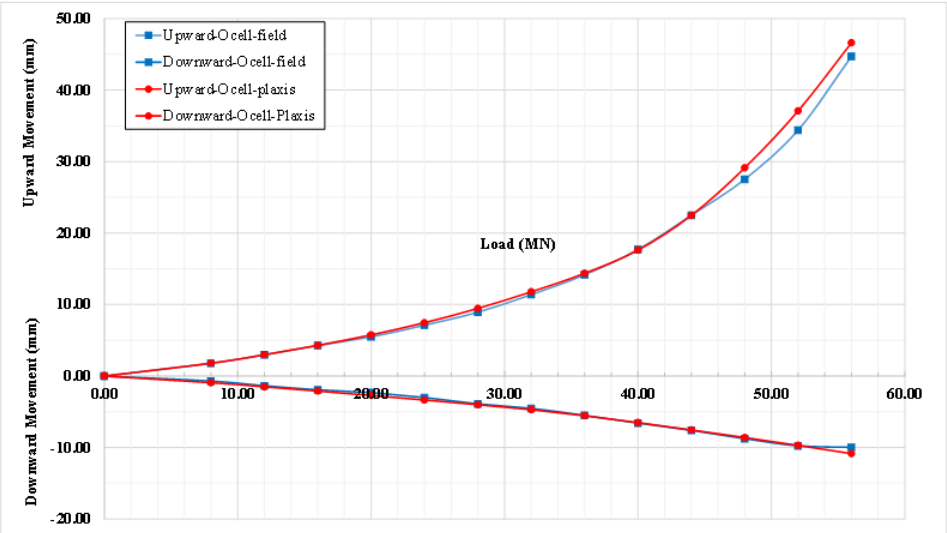

Figure 6.32. Measured and calculated load settlement curves for O-cell loading.

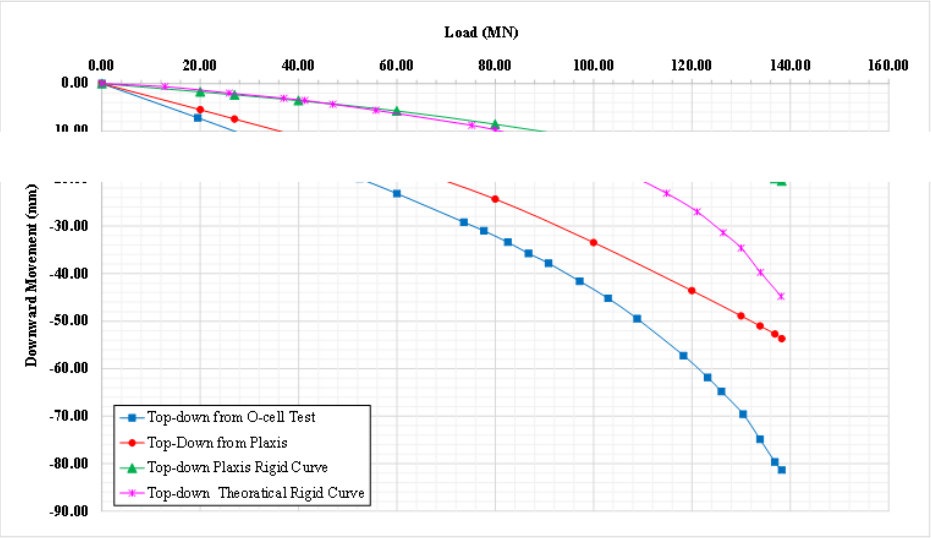

Figure 6.33. Measured and calculated load settlement curves for top-down loading.

After matching load-settlement graphs of both loading types, load-distribution graphs are obtained in order to see how the load is distributed along the shaft length of pile in two loading cases which are O-cell loading and top-down loading. During field O-cell testing, strain gauge reading s were recorded to obtain the shaft friction value of soil layers. Strain gauge measurements which were transformed into load values are used to compare assumed distribution in load test report with the ones obtained in numerical analysis. Since the number and level of strain gauges are adequate, data obtained during this test gives a good estimation of shaft friction in all soil layers encountered in this region.

Figure 6.34 and Figure 6.35 below illustrates load distribution behavior of pile in case of O-cell loading for both field measurements and numerical analysis and in case of top-down loading respectively. Pile load distribution curves are followed by analysis of unit shaft friction comparison for measured and numerically calculated O-cell loading and for top-down loading respectively in Figure 6.36 and Figure 6.37.

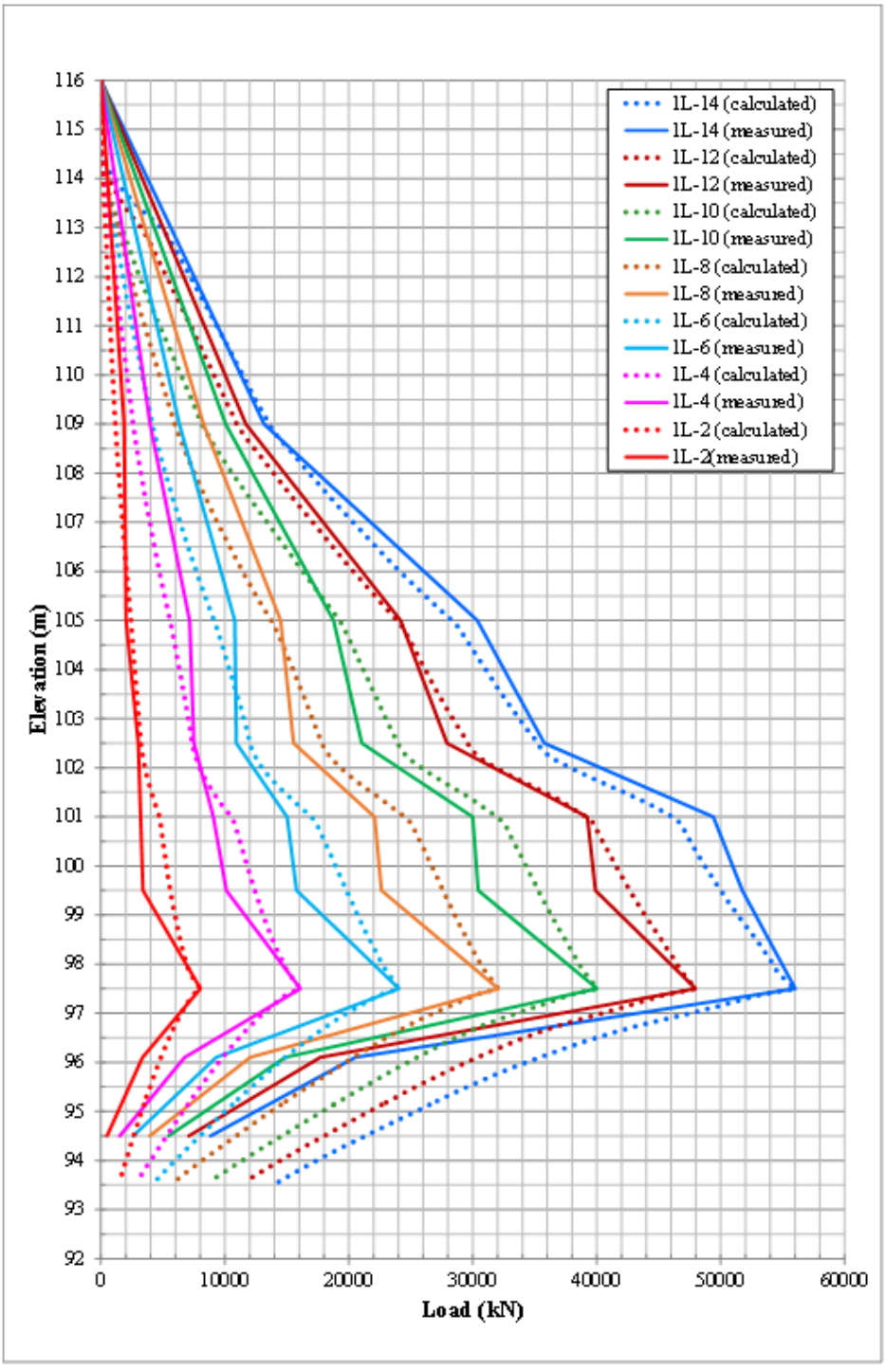

Figure 6.34. Comparison of load distribution curves for O-cell loading obtained from field measurements and numerical analysis of test pile 3.

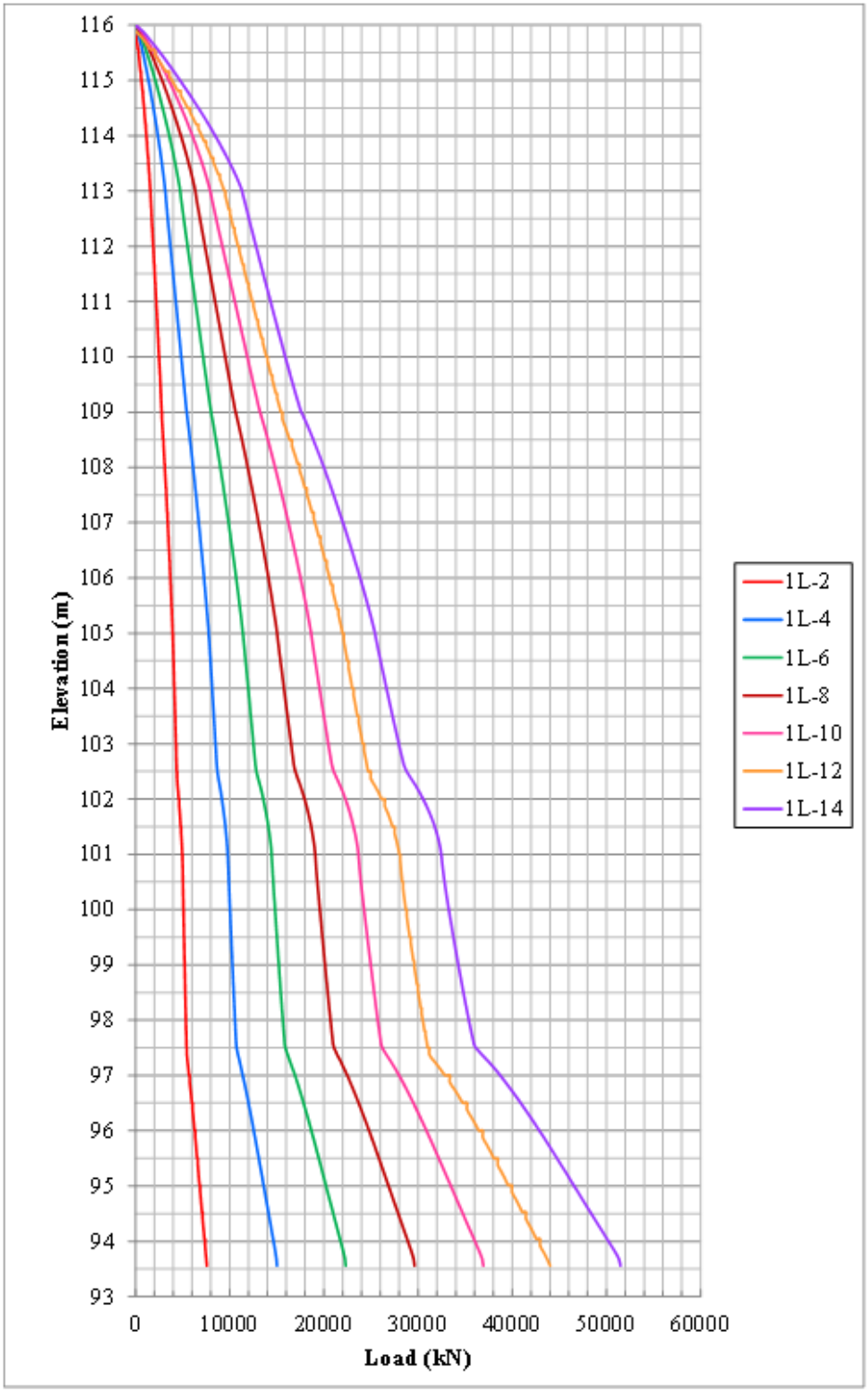

Figure 6.35. Load distribution curves for top-down loading obtained from numerical analysis of test pile 3.

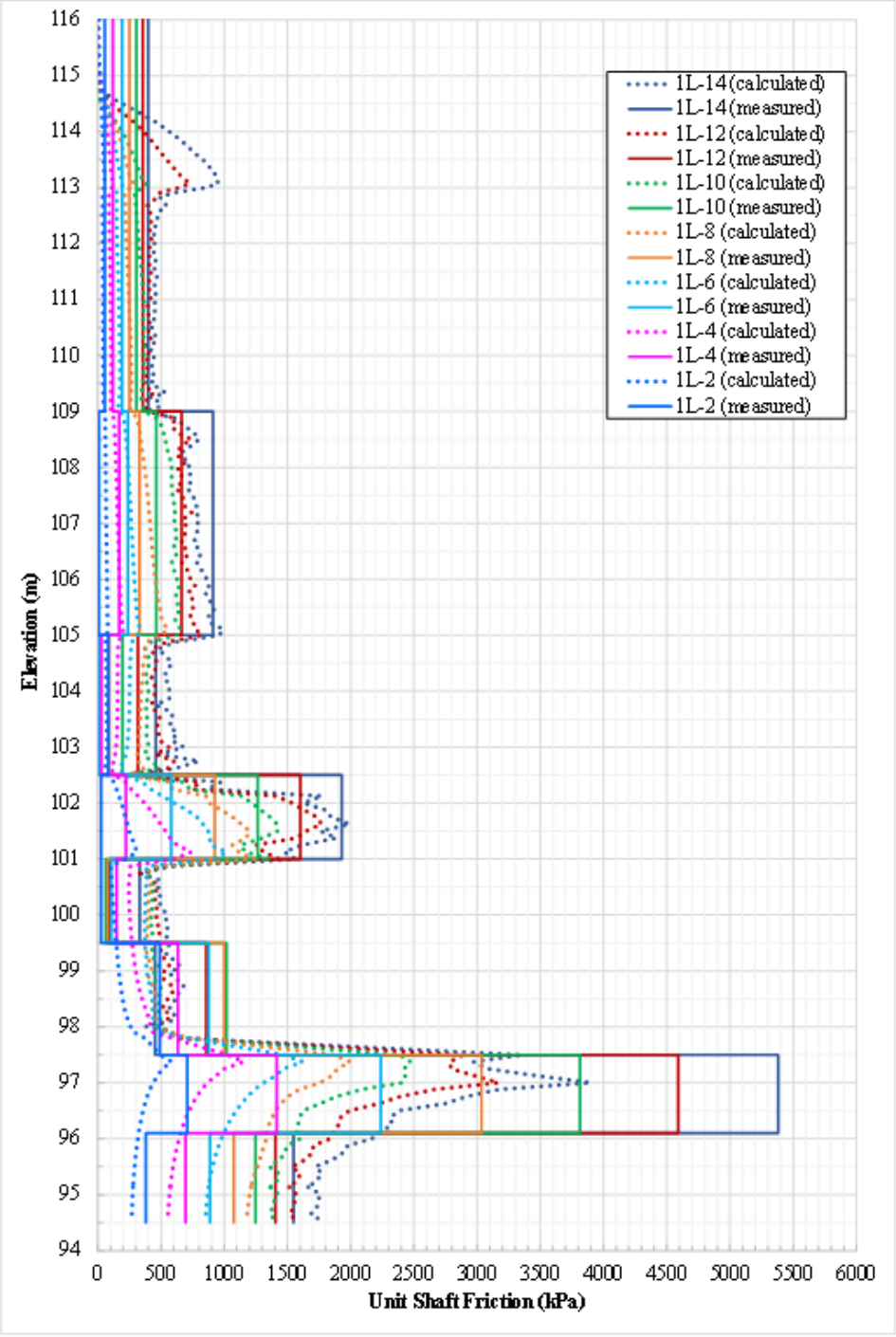

Figure 6.36. Comparison between measured and calculated unit skin friction values along length of test pile 3.

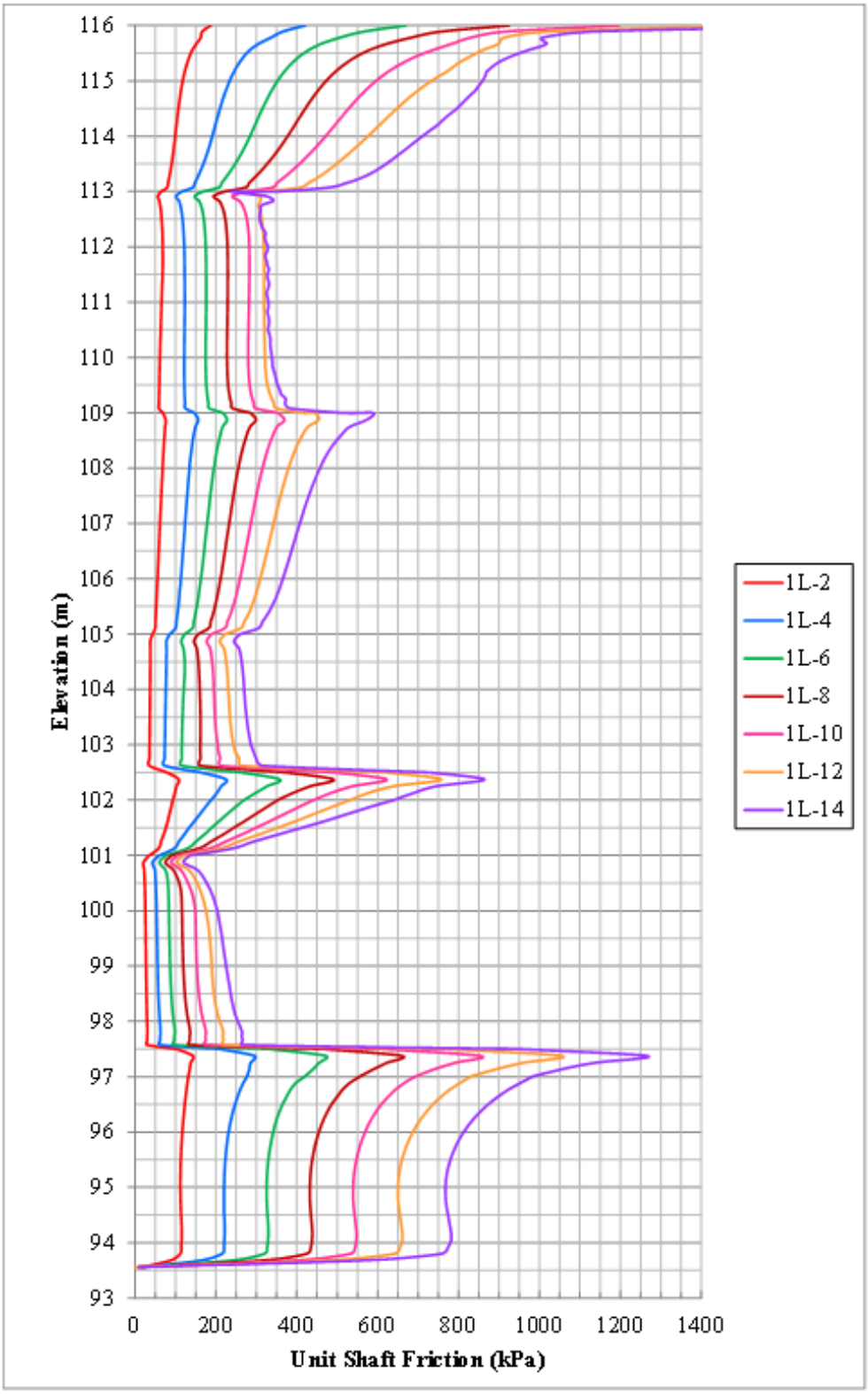

Figure 6.37. Distribution of unit skin friction values for top-down loading obtained from numerical analysis of test pile 3.

It is clearly observed from Figure 6.34 that when adequate number of strain gauge data is available pile load distribution behavior is very well modelled with the help of measured shaft load during testing. There exist five number of strain gauges located on top of O-cell level, each of which gives valuable information on how the load is transferred to different soil layers. Below O-cell level there are two strain gauges, one of which is close to O-cell level and gives misleading values for unit shaft friction under O-cell. This can be seen from Figure 6.34 either. All these seven train gauges are contributed to finite element analysis to get a close match between measured and calculated data. On the other hand, load distribution curves constructed for top-down loading which is shown on Figure 6.35 shows similar load transfer mechanism for same load.

Further observations are conducted for unit shaft friction comparison between measured and calculated data. Since behavior of pile is modelled based on the data obtained from the strain gauges, soil parameters are calibrated so that values found in field test can be obtained in finite element analysis. However Figure 6.36 shows that measured data just under the O-cell is not like what has been calculated. Measured shaft friction is found too high. Bearing in mind the best fitted load settlement curves and load distribution curves, it is seen that value obtained from strain gauge level 2 is misleading. If this part of loading is omitted from the results, from Figure 6.37, it is observed that magnitude of maximum unit shaft frictions are close to each other but locations where they occur are different under same loads.

In addition to above explained findings, in the light of constructed pile load behavior and calibrated parameters t-z curves are generated for both top-loading and O-cell loading which are presented in Figure 6.38. This time three levels are selected for investigation purpose above and below O-cell level. Upper part shows closer match between O-cell loading and top-down loading; whereas lower part shows more deformation under lower loads in O-cell loading. This is mainly due to location of O-cell which is closer to end of pile especially placed to see the shaft friction of only limestone formation. Figure 6.39 shows ultimate t-z curves for top-down loading.

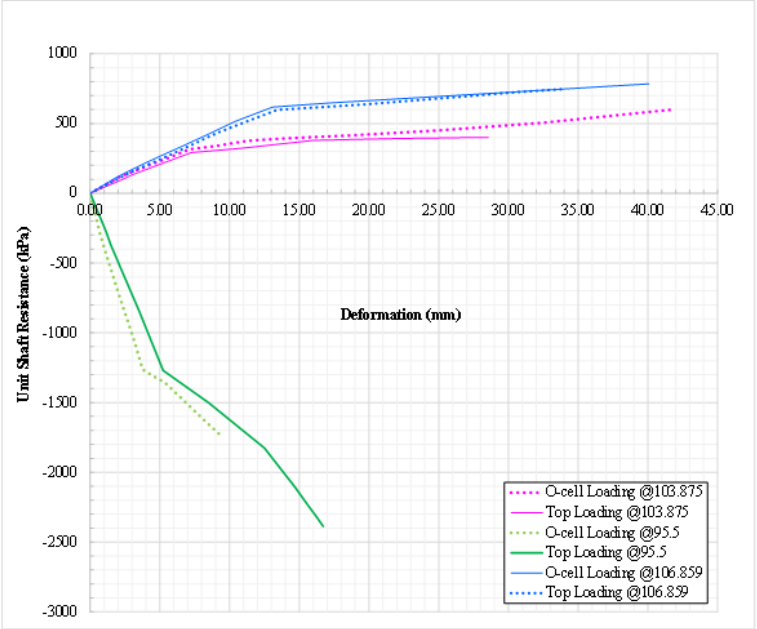

Figure 6.38. Comparison of calculated t-z curves for O-cell and top-down loading of test pile 3.

In order to check t-z curves whether or not they are reasonable, piles were back-analyzed in Allpile software. In order to construct t-z curves load settlement behavior which is given in Figure 6.39 below is also modelled in Allpile software by calibrating soil data based on parameters given in Table 6.11.

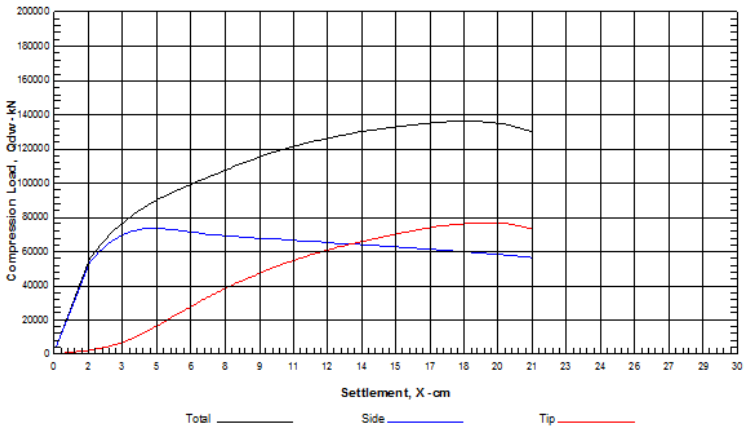

Figure 6.39. Calculated load-settlement behaviour for top-down loading of test pile 3 in Allpile software.

After match is obtained between measured load-settlement and calculated load-settlement behavior, t-z curves are constructed by using Allpile software (Allpile Manual, 2015) in order to check the consistency of modelled t-z curves in Plaxis software for calibrated parameters. t-z curves constructed in Allpile is shown in Figure 6.40 below. t-z curves are well suited to the calculated t-z behaviour found in Plaxis analysis.

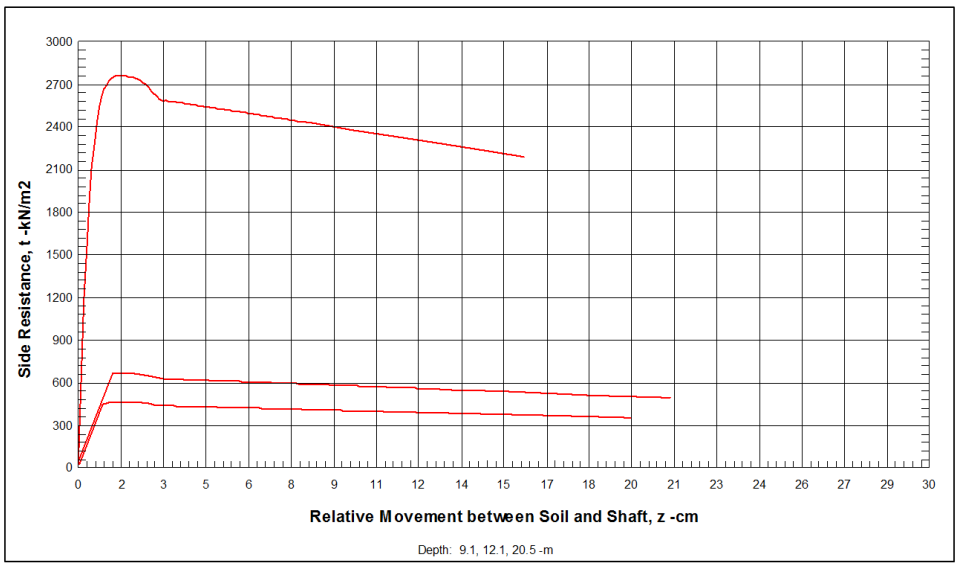

Figure 6.40. t-z curves from Allpile verification in top-down loading of test pile 3.

q-z curves are also evaluated both for top loading and O-cell loading in Figure 6.41. Observed behaviour are compared both for each other and for field measured data and results. This data is obtained by interpretation of toe telltale readings with respect to transferred end bearing load. Transferred end bearing load is calculated for each loading stage, by obtaining measured unit skin friction value between O-cell level and strain gauge level and using it for lower part (below O-cell part) shaft friction load and subtracting it from the applied load. Since data obtained in strain gauge level 2 is found misleading as a result of this analysis, unit end bearing calculated by evaluating O-cell field test results are not suited to the calculated data. Owing to the fact that value obtained in strain gauge level 2 is too high, it is found that no load is transferred into the end of pile. Reason may be that the location of strain gauge being close to O-cell level or creep in soil during testing or tension forces occurred during concrete curing. Additionally, top-loading case shows a little bit different behaviour like in first test pile 1. In top-loading it gives more tip deformation under same unit end bearing.

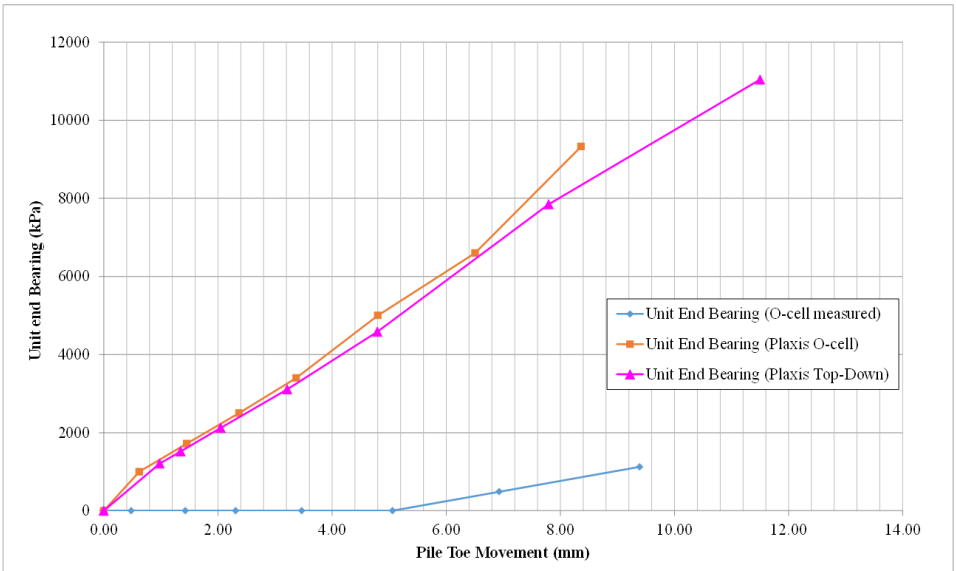

Figure 6.41. Measured and calculated q-z curves for test pile 3.

7. INTERPRETATION OF LOAD TEST RESULTS

There are several methods for interpretation of pile load test results in order to determine ultimate pile capacity. During load test of piles settlement readings are recorded with respect to time and applied load. Failure of a pile is determined when plunging or settlement occurs suddenly under applied load. Some of these methods; depending mainly on local or international standards, looks for limitations of pile head displacement, displacement ratio etc. Methods using limit of displacements for different countries are provided below:

(i) Limitation of total head displacement of pile
- 25.4 mm (Netherlands, New York)
- 10% of Diameter of Pile Tip (United Kingdom)
- Elastic Displacement of Pile + B/30 where B is equal to pile diameter (Canada)

(ii) Limitation of plastic displacement of pile
- 6.4 mm (New York State, Louisana)
- 12.7 mm (Boston)

(iii) Limitation of plastic displacement over elastic displacement
- 1.5 (Denmark)

(iv) Limitation for ratio of displacement per load
- Total ; 0.25 mm / ton (California, Chicago)
- Increment; 0.75 mm / ton (Ohio)
- Total; 1.27 mm / ton (Raymond Int.)

(v) Limitation for ratio of plastic displacement per load
- Total; 0.25 mm / ton (New York City)
- Increment; 0.08 mm / ton (Raymond Int.)

In addition to above explained limit of displacements, following methods are used to determine ultimate capacity of pile from load tests (Prakash and Sharma, 1990):

(i) Davisson's method (1972)

(ii) Chin's method (1970, 1971)
(iii) De Beer's method (1967) or De Beer and Wallays' method (1972)
(iv) Brinch Hansen's 90 percent criterion (1963)
(v) Brinch Hansen's 80 percent criterion (1963)
(vi) Mazurkiewicz's method (1972)
(vii) Fuller and Hoy's method (1970)
(viii) Butler and Hoy's method (1977)
(ix) Vander Veen's method (1953)

These methods are looked through for further investigation of analysed cases in order to determine failure load. Among above given methods Davisson's method, Chin's method, De Beer's method, Brinch Hansen's 80 percent criterion method are studied. However, De Beer and Brinch Hansen methods do not converge for s solution. Therefore only Davisson and Chin method are selected for further investigation for analysed cases.

Before studying these failure methods ultimate loads for three cases are presented below. Analysis is performed according to load settlement behaviour of pile in Allpile software as also indicated in Chapter 6. Ultimate capacity of pile is estimated by using same soil parameters which give the same load-settlement and t-z curves in Chapter 6.

7.1. Davisson's Method

This is the widely used method which was suggested by Davisson in 1972. In this method, pile is assumed as a free standing column. First of all load-movement curve is obtained. Then elastic movement of pile in each loading stage is calculated by using Equation 7.1 below. In this formula Q is equal to applied load, L is the pile length and A is the cross sectional area of pile, E is the elasticity modulus of pile.

After obtaining elastic settlement of pile then a curve is constructed by using

Equation 7.2 where D is the diameter of pile (Prakash and Sharma, 1990).

$$s_e = \frac{QL}{AE} \tag{7.1}$$

$$s = s_e + 4mm + D/120 \tag{7.2}$$

By using above given equations three analysis cases are examined to determine ultimate failure load. In Figure 7.1 Davisson method is applied to test pile 1. It is observed that Davisson line does not intersect the load-settlement curve. Therefore any failure load cannot be determined. On the other hand, as it can be seen from Figure 7.2 and Figure 7.3, plunging occurs on load-settlement curves and method converges for a solution for test pile 2 and 3. The ultimate failure load for test pile 2 is found as 37 MN whereas it is found as 133 MN for test pile 3.

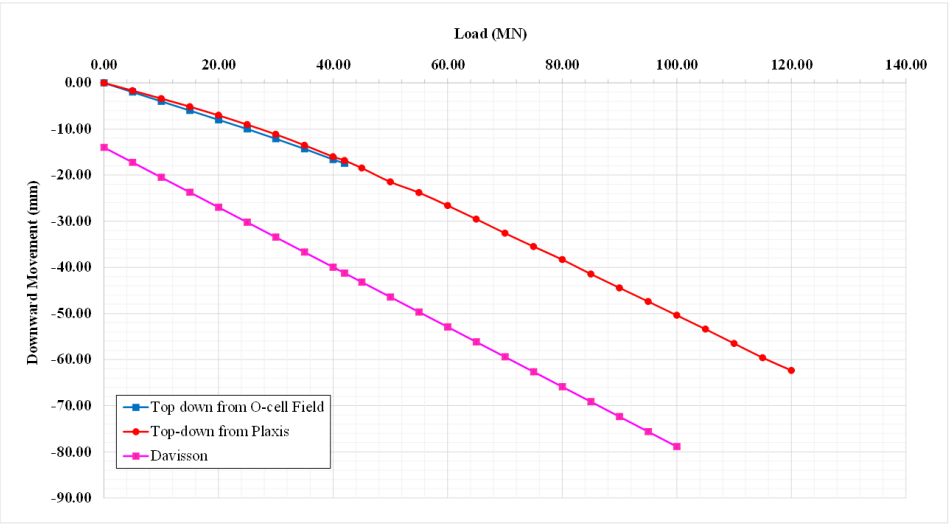

Figure 7.1. Davisson method for test pile 1.

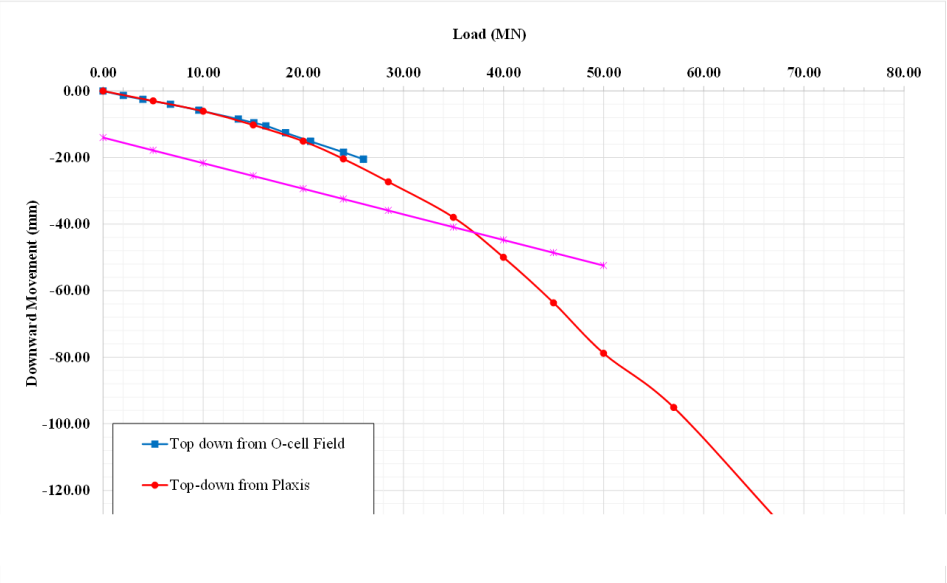

Figure 7.2. Davisson method for test pile 2.

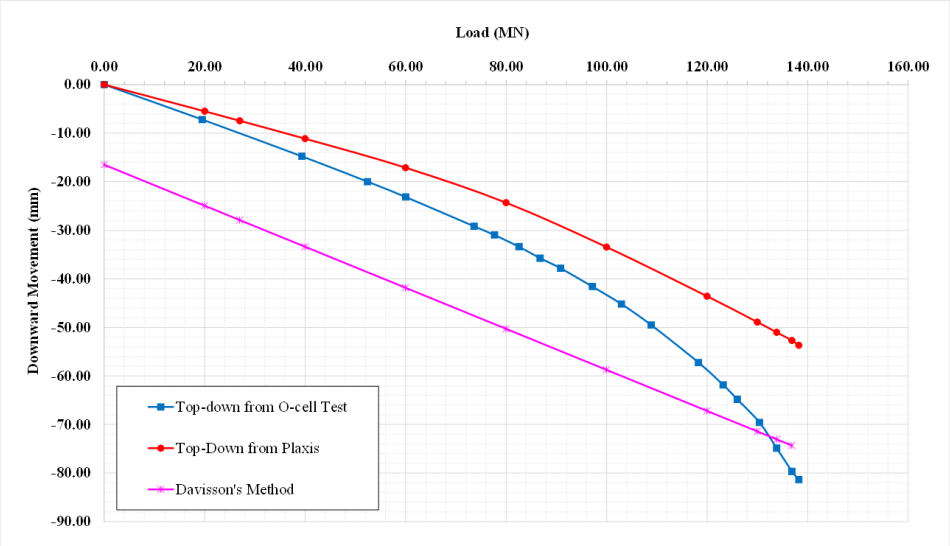

Figure 7.3. Davisson method for test pile 3.

7.2. Chin's method (1970)

Chin's method is another widely used load test interpretation method. It is constructed by obtaining the ratio by dividing settlement to applied load. Then this value is plotted against settlements. When the curve is plotted, slope of last part straight portion is determined. Then the ultimate load is found by dividing slope of

this line to 1 as given in equation 7.3 where C1 is the slope of line (Prakash and Sharma, 1990):

$$Q_{ult} = \frac{1}{C_1} \tag{7.3}$$

- or test pile 1, C1 is found as 2E-06 and Q_{ult} is found as 500 MN from Figure 7.4.
- For test pile 2, C1 is found as 7E-06 and Q_{ult} is found as 143 MN from Figure 7.5.
- For test pile 3, C1 is found as 4E-06 and Q_{ult} is found as 250 MN from Figure 7.6.

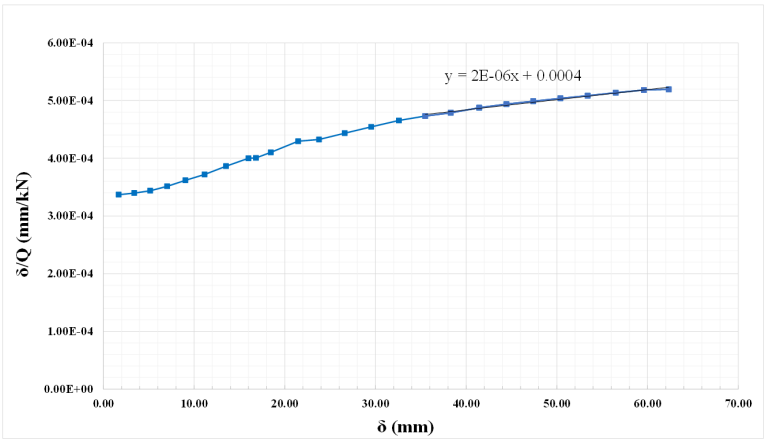

Figure 7.4. Chin's method for test pile 1.

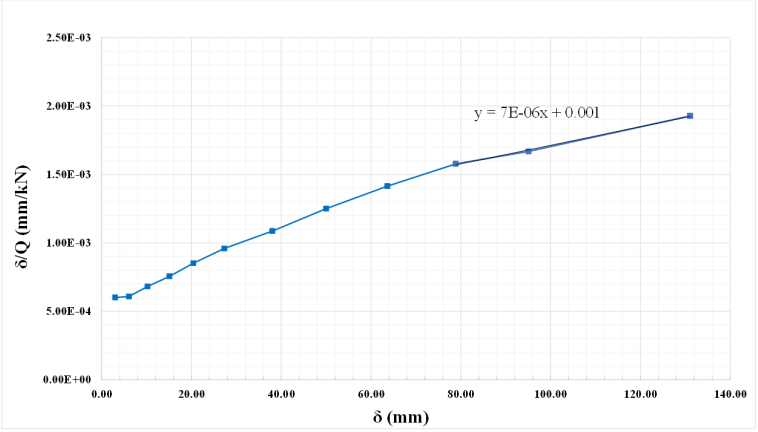

Figure 7.5. Chin's method for test pile 2.

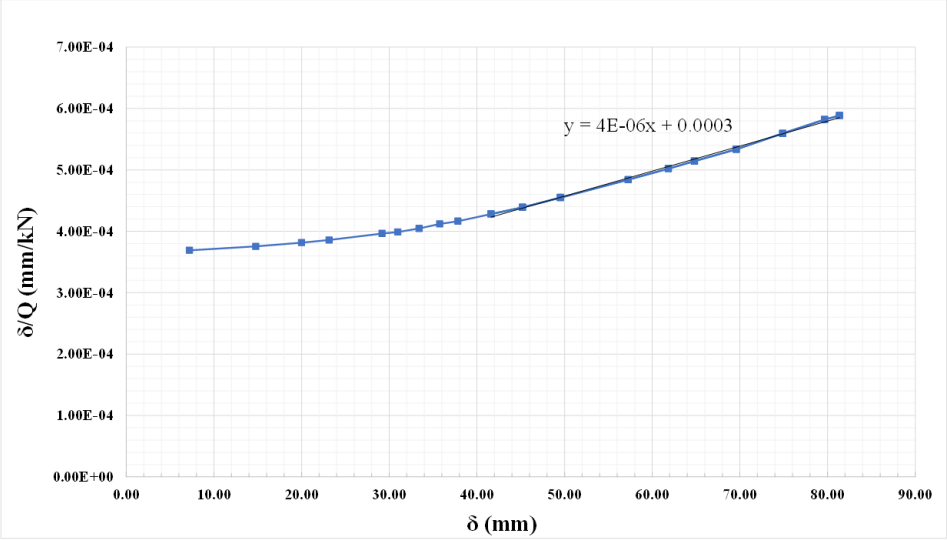

Figure 7.6. Chin's method for test pile 3.

7.3. Pile Load Capacity Calculation by Using Allpile

Pile load capacities are calculated by using Allpile software using Drilled Shaft Method.(Allpile Manual, 2015) Load-settlement curves and t-z curves are given in Chapter 6. For all three cases, compression capacity vs pile length is given below in Figure 7.7, Figure 7.8 and Figure 7.9 respectively.

- For test pile 1 whose length is 22.0 m, ultimate compression load capacity of pile is found as 210 MN
- For test pile 2 whose length is 26.1 m, ultimate compression load capacity of pile is found as 65 MN
- For test pile 3 whose length is 22.44 m, ultimate compression load capacity of pile is found as 136 MN

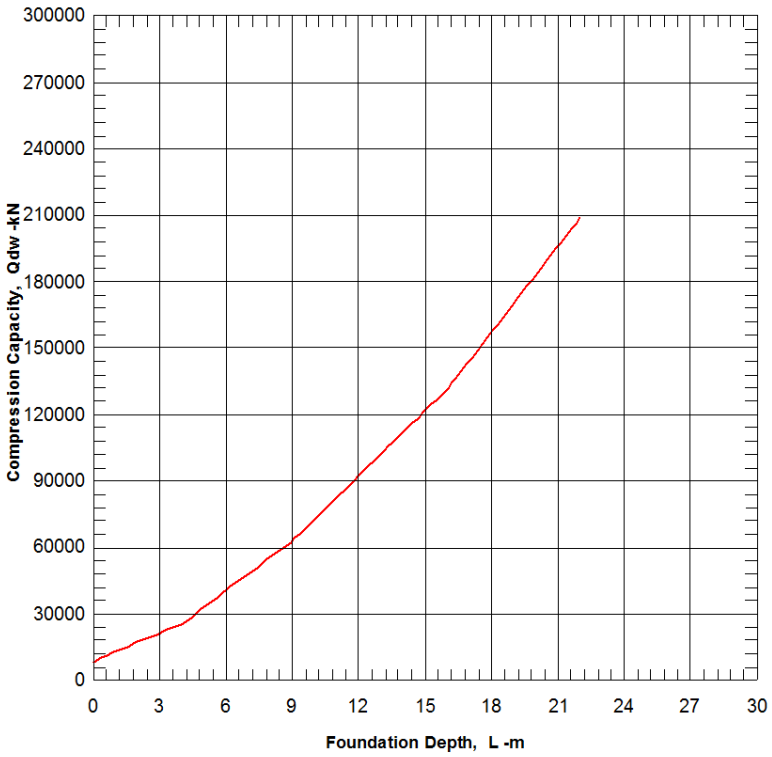

Figure 7.7. Ultimate compression load capacity vs pile length for test pile 1.

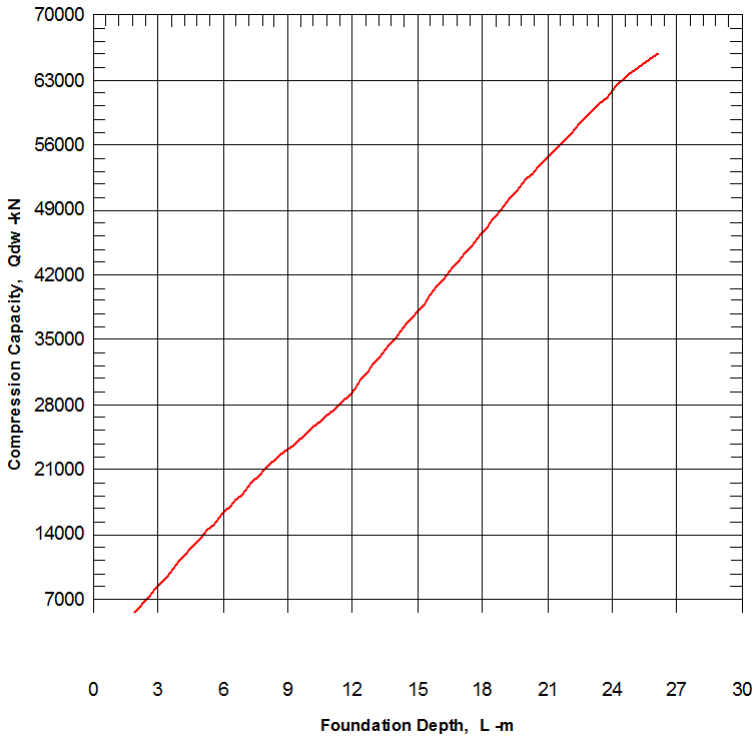

Figure 7.8. Ultimate compression load capacity vs pile length for test pile 2.

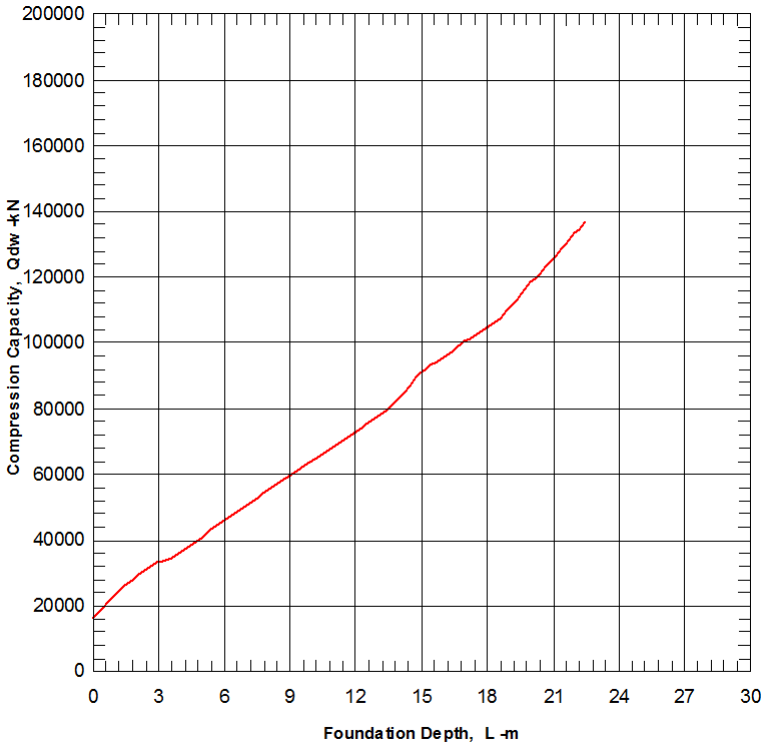

Figure 7.9. Ultimate compression load capacity vs pile length for test pile 3.

8. CONCLUSION

In the scope of this thesis three different static load tests performed with bi-directional testing method of Osterberg Cell are back-analyzed using Finite Element approach. Piles on which load test were applied are all rock socketed piles with large diameters.

Back analysis of field test is mainly conducted by optimizing parameters until a good and reasonable match is obtained between field-measured and finite element calculated load settlement behaviour of pile. After obtaining a good match, the parameters are calibrated according to available strain gauge data.

It is seen in the analysis that if the settlement of pile at the end of the test is too small; in other words pile is tested under much smaller load than its capacity, then the parameters obtained from the back-analysis can be found higher than in reality. However if pile exhibits large settlements under the applied load then, parameters calibrated especially for deformed part are found lower than what is taken during design. This behaviour is observed by interpreting soil parameters given before the analysis and after analysis in Chapter 6 for all three piles.

As a result of the analyses, it is also observed that the pile bearing capacity and pile behaviour could not be predicted correctly when the applied test load is much smaller than the bearing capacity of pile.

Level and number of strain gauge data is very important to investigate actual load distribution behaviour of pile. If there exists inadequate data like in test pile 1 and test pile 2, one can get misleading unit shaft friction values based on only O-cell load and zero friction assumption as it can also be seen from the comparison of load distribution graphs of test pile 1 and test pile 2 presented in Chapter 6. On the other hand, load distribution graph of test pile 3 obtained by back-analysis closely matched the data obtained from O-cell testing, since number of strain gauge data is adequate.

Another point related with strain gauges comes into stage at test pile 2. Location of strain gauge located only 0.25m under O-cell level causes a misinterpretation of test data. It gives nearly two times higher unit shaft resistance than analysed value. Thus, both load distribution curves and unit shaft friction comparison curves do not fit for this test pile. However, observation of this situation shows that by positioning O-cell to nearly the end of the pile gives very close and accurate unit end bearing. From this point on, it can be said that among all three piles test pile 2 shows the most matching end-bearing movement behaviour. By analysing this data, one can conclude that using multilevel O-cells in static pile load tests especially performed in rock socketed piles will be the best solution to obtain real and most reasonable pile behaviour.

After performing a well instrumented test pile, one can construct the t-z curves by back-analysis of field test using especially strain gauge values. Within the scope of this thesis, obtained t-z curves are checked with software by obtaining same load-settlement behaviour and compared with the ones found from Plaxis Finite Element analyses. They are nearly similar to each other. t-z curves are found to be closer to each other for top-loading and O-cell loading if it is far from the location of O-cell and above it. For the points below O-cell level and close to pile tip, settlement obtained for O-cell loading is found to be lower than the same load applied on top of pile.

Furthermore, when O-cell loading and top-down loading is compared according to unit shaft friction values obtained from analysis, it is observed that magnitude of maximum unit shaft frictions are close to each other but locations where they occur are different under same loads. Therefore construction of t-z curves is important to understand behavior of pile in actual design case which is top-loading.

For test pile 3; although load distribution curves obtained by field tests and finite element analysis and load settlement curves for O-cell loading both in field and analysis are closely matched with each other, theoretically constructed top down curve is observed not to match with numerically calculated top-down curve. There can be two reasons for this behaviour. It can be either because of cleaning of pile base may not be performed well during construction or wrong estimation of pile elastic

behaviour. When the data in Figure 6.33 is investigated, it can be seen that up to 80 MN of test load rigid load-settlement curves are suited with each other; however when elastic load-settlement curves come into the stage, compatibility between field measured and numerically calculated load-settlement behaviour is observed to be broken. This actually shows that elastic calculation approach explained in Chapter 5 remains too conservative for this test pile. It can be concluded that additional elastic settlement analysis should be done especially for larger diameter piles.

In all measured and calculated load-settlement and load-distribution curve comparison, it is observed that for higher loads difference between calculated and measured behaviour becomes smaller. This is mainly because all parameters are obtained under ultimate loading phase in analysis models.

In Chapter 6, pile load test interpretation methods are evaluated for all three cases together with compression load capacities evaluated with the software Allpile. Four ultimate load capacity interpretation methods are studied and for the cases investigated only two was found as suitable due to the nature of load-settlement curve.

As a result of load test interpretation data, Davisson method does not converge for a solution because settlement found in load test is too small and there is no information where data plunges. This lack of knowledge also appears in Chin's method by observing a failure load of 500 MN which is too high when compared to 210MN of calculated data. For test pile 2 and 3, results in both methods found an estimated value but Chin method is observed to give much higher than the Davisson method and calculated value with Allpile. As it is clearly observed from the test results, best fit is observed for test pile 3 between Davisson and Calculated Allpile methods. This explicitly shows that Davisson method is better estimator than Chin's method and the more the pile is instrumented and well recorded; the better estimation of pile capacity is.

REFERENCES

Bowles, J.E., "Foundation Anlaysis and Design", *McGraw-Hill*, 5^{th} Edition, Singapore, 1997.

Bui, T.Y., Y. Li, S.A. Tan and C.F. Leung, "Back Analysis of O-cell Pile Load Test Using FEM", *Millpress Science*, Proc. of 16^{th} ICSMGE, Osaka, September 12-16, 2005.

Civiltech Softwares, *Allpile Manual*, 2015.

Collin, J.G., "Timber Pile Design and Construction Manual", *Timber Piling Council American Wood Preservers Institute*, USA, 2002.

Fellenius, B.H., and S.S. Tan, "Analysis of Bi-directional Cell Tests for Icon Condominiums, Singapore", *Proceedings of the 9^{th} International Conference on Testing and Design Methods for Deep Foundations*, Vol. 1, pp. 725-733, September 18-20, 2012.

Fellenius, B.H. A. Altae, R. Kulesza, J. Hayes, "O-cell Testing and FE Analysis of 28m deep Barrette in Manila, Philippines", *Journal of Geotechnical and Geoenvironmental Engineering*, July, 1999.

Fleming, K., A. Weltman, M. Randolph, K. Elson, "Piling Engineering", *Taylor and Francis*, Newyork, USA, 3rd edition, 2009.

Keller, F., "The Lake Dwellings of Switzerland and Other Parts of Europe", *Longsmans Green and Co.*, London, United Kingdom, 1866.

Limas, V.V. and P.P. Rahardjo, "Comparative Study of Large Diameter Bored Pile Under Conventional Static Load Test and Bi-directional Load Test", *Malaysian Journal of Civil Engineering*, Vol. 27, No. 1, pp. 1-18, 2015.

Osterberg J.O., "The Osterberg Load Test Mehod for Drilled Shafts and Driven Piles-The first Ten Years", *Proceedings of the 7th International Conference on Piling and Deep Foundations*, Vienna, Austria, June 1998.

Osterberg, J.O., "What has Been Learned About Drilled Shafts from the Osterberg Load Test", *Deep Foundations Institute Annual Meeting*, Dearborn, Michigan, October, 1999.

Plaxis Company, *Plaxis 2D Manuals*, 2017.

Prakash, S. and H.D. Sharma, "Pile Foundations in Engineering Practice", *John Wiley and Sons*, Inc., USA, 1990.

Rajapakse, R., "Pile Design for Structural and Geotechnical Engineers", *Butterworth-Heinemann*, United Kingdom, 2008.

Schmertmann, J.H., J.A. Hayes, "The Osterberg Cell and Bored Pile Testing - A Symbiosis", *The Third International Geotechnical Engineering Conference*, Cairo, Egypt, January 5-8, 1997.

Seol, H. and S. Jeong, "Load-settlement behavior of rock-socketed drilled shafts using Osterberg-Cell tests", *Computers and Geotechnics*, Elsevier, 2009.

Tomlinson, M. and J. Woodward, "Pile Design and Construction Practice", *Taylor and Francis*, Newyork, USA, 5th edition, 2007.